ADSORPTION OF REACTIVE RED DYE USING ORGANO-MONTMORILLONITE

PARIWAT NAMDUANG

A THESIS SUBMITTED IN PARTIAL FULLFILLMENT OF THE REQUIREMENTS FOR THE DEGREE OF MASTER OF ENGINEERING MAJOR IN ENVIRONMENTAL ENGINEERING

FACULTY OF ENGINEERING

UBONRATCHATHANI UNIVERSITY

ACADEMIC YEAR 2014

UBON RATCHATHANI UNIVERSITY

THESIS APPROVAL

MASTER OF ENGINEERING

IN ENVIRONMENTAL ENGINEERING FACULTY OF ENGINEERING

TITLE ADSORPTION OF REACTIVE RED DYE USING ORGANO-MONTMORILLONITE

AUTHOR MR. PARIWAT NAMDUANG

EXAMINATION COMMITTEE

DR. ATTHAPHON MANEEDAENG	CHAIRPERSON
ASST. PROF. DR. CHAKKRIT UMPUCH	MEMBER
ASST. PROF. DR. KARNIKA RATANAPONGLEKA	MEMBER

ADVISOR

.....

(ASST. PROF. DR. CHAKKRIT UMPUCH)

.....

(ASSOC. PROF. DR. KULACHATE PIANTONG)

DEAN, FACULTY OF ENGINEERING

.....

(ASSOC. PROF. DR. ARIYAPORN PONGRAT)

VICE PRESIDENT FOR ACADEMIC AFFAIRS

ACADEMIC YEAR 2014

ACKNOWLEDGMENTS

The author would like to thank Asst. Prof. Dr. Chakkrit Umpuch Department of Chemical Engineering, Faculty of Engineering, Ubon Ratchathani University for his guidance and critical evaluation of the performed work. His guidance has helped the author locate and articulate purpose, value and meaning in being an engineer and researcher. He has taught the author not to be afraid to take a stand and assisted the author to deconstruct the thinking and reconstruct thoughts and action in the complex area of chemical and environmental engineering. His in put, particularly regarding the oral and written presentations of the research results to the research community, was also very helpful and instructive.

Thanks also go to the committees, Dr. Atthaphon Maneedaeng School of Chemical Engineering, Faculty of Engineering, Suranaree University of Technology and Asst.Prof.Dr. Karnika Ratanapongleka Department of Chemical Engineering, Faculty of Engineering, Ubon Ratchathani University for theirinvaluable support. The author would like to thank Asst .Porf. Dr Sompop Sanongraj and all of the members of Department of Chemical Engineering, Faculty of Engineering Ubon Ratchathani University for making the work environment pleasant and friendly. The author would like to thank Ubon Ratchathani University for the financial support. The author wishes to express his appreciation and thanks to Mr. Bob Tremaynefor correcting language and proofreading this thesis.

The author dedicates this thesis to his father (Molton), mother (Nittaya), brother and of course, to his family (Namduang and Jarupath), whose inspiration and encouragement was a constant support to the author.

Pariwat Namduang

Researcher

บทคัดย่อ

เรื่อง : การดูดซับสีรีแอคทีฟเรด โดยใช้ออร์กาโนมอนต์มอริลโลไนต์

ผู้วิจัย : ปริวัชร นามด้วง

ชื่อปริญญา : วิศวกรรมศาสตรมหาบัณฑิต

สาขาวิชา : วิศวกรรมสิ่งแวดล้อม

อาจารย์ที่ปรึกษา : ผู้ช่วยศาสตราจารย์ ดร. จักรกฤษณ์ อัมพุช

ศัพท์สำคัญ : ออร์กาโนมอนต์มอริลโลไนต์, การดูดซับ, สีรีแอคทีฟเรด 120, การแทรกสอด

งานวิจัยนี้ศึกษาการเตรียมแร่ดินออร์กาโนมอนต์มอริลโลไนต์ (OMMT) แร่ดินมอนต์มอริลโลไนต์ดัดแปรด้วยไคโตซาน (CTS/MMT) และแร่ดินออร์กาโนมอนต์มอริลโลไนต์ดัดแปรด้วยไคโตซาน (CTS/OMMT) เพื่อใช้เป็นตัวดูดซับในการกำจัดสีรีแอคทีฟเรด 120 (RR120) จากสารละลายสีสังเคราะห์ คุณลักษณะของตัวดูดซับถูกวิเคราะห์ด้วยเครื่อง FTIR Autosorb SEM และ XRD ผลการวิเคราะห์แสดงหลักฐานการแทรกสอดของสารดัดแปรเข้าไปในโครงร่างของแร่ดินมอนต์มอริลโลไนต์ (MMT) เช่น การปรากฏขึ้นของหมู่แอลคิล การเพิ่มขึ้นของขนาดรูพรุนจำเพาะ และการขยายตัวของช่องว่างภายในแร่ดิน แร่ดิน OMMT มีเปอร์เซ็นต์การกำจัดสีย้อมสูงสุด ดั้งนั้นจึงถูกเลือกใช้เป็นตัวดูดซับในการทดลองต่อไป การดูดซับสี RR120 ด้วย OMMT ถูกศึกษาในการทดลองแบบกะและหอบรรจุ ปัจจัยที่ศึกษาในการทดลองแบบกะ ได้แก่ เวลาสัมผัส ความเข้มข้นสีเริ่มต้น pH เริ่มต้น และอุณหภูมิ ผลการทดลองแสดงให้เห็นว่าการดูดซับของสี RR120 เกิดขึ้นอย่างรวดเร็วในช่วงแรก และเข้าสู่สมดุลที่เวลา 360 นาที ปริมาณการดูดซับเพิ่มขึ้นตามความเข้มข้นสีเริ่มต้นและอุณหภูมิ แต่ลดลงเล็กน้อยเมื่อ pH เริ่มต้นมีค่าเพิ่มขึ้น ปริมาณการดูดซับของ RR120 เพิ่มขึ้นตามอุณหภูมิที่เพิ่มขึ้น ชี้ให้เห็นถึงกระบวนการดูดความร้อน ข้อมูลด้านจลนพลศาสตร์สามารถอธิบายได้โดยแบบจำลองปฏิกิริยาอันดับ 2 เทียม และข้อมูล ณ จุดสมดุลสอดคล้องกับไอโซเทอมแลงเมียร์ โดยมีปริมาณการดูดซับแบบชั้นเดียวสูงสุด คือ 265.00 mg/g ที่ 65°C ปัจจัยที่ศึกษาในหอบรรจุ ได้แก่ ความเข้มข้นสีเริ่มต้น อัตราการไหล และ ความสูงเบด พบว่า สภาวะที่เหมาะสมอยู่ที่ ความเข้มข้นสีเริ่มต้น 100 mg/L อัตราการไหล 1.4 mL/min และ ความสูงเบด 80 mm ผลการทดลองถูกนำไปหาความสัมพันธ์กับแบบจำลองของโทมัส อดัมส์-โบฮาร์ต และยุน-เนลสัน จากผลการทดลองเหล่านี้แสดงให้เห็นว่า แร่ดิน OMMT สามารถใช้เป็นตัวดูดซับที่มีประสิทธิภาพในการกำจัดสี RR120 จากสารละลายได้

ABSTRACT

TITLE : ADSORTPING OF REACTIVE RED DYE USING ORGANO-MONTMORILLONITE
AUTHOR : PARIWAT NAMDUANG
DEGREE : MASTER OF ENGINEERING
MAJOR : ENVIRONMENTAL ENGINEERING
ADVISOR : ASST. PROF.CHAKKRITUMPUCH, Ph.D.
KEYWORDS : ORGANO-MONTMORILLONITE, ADSORPTION, REACTIVE RED 120, INTERCALATION

In this present work, organo montmorillonites (OMMT), chitosan modified montmorillonite (CTS/MMT), and chitosan modified organo montmorillonite (CTS/OMMT) clays were prepared as adsorbents for removing Reactive Red 120 (RR120) dye from synthesized aqueous solution. The characteristics of those adsorbents were analyzed by the FTIR, the autosorb, SEM, and XRD techniques. The analytical results show some evidence of intercalation of modified agents into montmorillonite (MMT) such as presenting of alkyl group, increasing of specific pore size, and basal spacing. The highest percent dye removal was obtained by using the OMMT. Thus it was selected for further experiments. The adsorption of RR120 onto OMMT was investigated in a batch and a fixed bed column. The factors affecting in batch tests such as contact time, initial dye concentration, initial pH, and temperature were investigated. The result revealed that adsorption of RR120 was initially rapid and reached equilibrium at 360 minutes. The adsorption capacity increased with the initial dye concentration and temperature but decreased slightly with initial pH. The uptake of RR120 increased with temperatures indicating an endothermic process. Kinetics data were well described by the pseudo-second order model. The equilibrium data were better fitted by the Langmuir isotherm providing maximum monolayer adsorption capacity of 265.00 mg/g at 65°C. In fixed bed column, influences of initial concentration, flow rate, and bed height were studied. The optimum condition was obtained under 100 mg/L inlet concentration, 1.4 mL/min flow rate, and 80 cm bed height. Thomas, Adams-Bohart, and Yoon-Nelson models were fitted with

experimental data. These results suggested that the OMMT can be used as an effective adsorbent for removing RR120 from aqueous solutions.

CONTENTS

CONTENTS (CONTINUE)

LIST OF TABLES

LIST OF TABLES (CONTINUE)

LIST OF FIGURES

LIST OF FIGURES (CONTINUE)

LIST OF FIGURES (CONTINUE)

LIST OF APPREVIATIONS

V	= the suspension volume (L)
M	= the mass of adsorbent (g)
C_1	= the concentration of stock solution, 1000 mg/L
C_2	= the concentration of wanted diluted solution (mg/L)
V_1	= the volume of stock solution that has to be used (mL)
V_2	= the volume of desired diluted solution (mL).
C_0	= initial dye concentration or the influent RR120 concentration (mg/L)
C_e	= equilibrium dye concentration (mg/L)
q_e	= the amount of dye adsorbed at equilibrium (mg/g)
q_m	= a constant related to maximum adsorption capacity (mg/g)
b	= Langmuir constant related to energy of adsorption (L/mg)
R_L	= equilibrium parameter for characterize Langmuir isotherm
K_f	= the adsorption capacity of Freundlich isotherm (mg/g)
n	= the adsorption intensity, Freundlich isotherm
q_t	= the amount of dye adsorbed at time t (mg/g)
k_1	= the pseudo-first-order adsorption rate constant (min^{-1})
k_2	= the pseudo-second-order adsorption rate constant (g/mg/min)
R^2	= the regression coefficient
t	= time (min)
t_b	= time ofBreak-through (min)
E_a	= the Arrhenius activation energy of adsorption(kJ/mol)
A	= the Arrhenius factor
R	= the gas constant which is equal to 8.314 J/mol/K
T	= the system temperature (K)
$\Delta G°$	= Gibbs free energy change (kJ/mol)

LIST OF APPREVIATIONS (CONTINUE)

$\Delta H°$	= standard enthalpy (kJ/mol)
$\Delta S°$	= standard entropy (J/mol)
K_0	= the equilibrium constant (L/mg)
k_T	= the Thomas rate constant(mL/min/mg)
q_0	= the equilibrium RR120 uptake per g of the adsorbent (mg/g)
C_t	= the effluent concentration at time t (mg/L)
w	= the mass of adsorbent (g)
v	= the flow rate (mL/min)
K	= the kinetic constant (L/mg.min)
F	= the linear velocity(cm/min)
Z	= the bed height of column(cm)
N	= the saturation concentration(mg/L)
k_{YN}	= the rate velocity constant(L/min)
τ	= the time in required for 50% adsorbate breakthrough(min)
RR120	= Reactive red 120 dye
MMT	= Montmorillonite clay
CTS	= Chitosan
CTAB	= Cetyltrimethylammonium bromide
TTAB	= Tetradexyltrimethylammonium bromide
CTS/MMT	= Montmorillonite clay modified by chitosan
CTAB/MMT	= Montmorillonite modified by cetyltrimethylammonium bromide
TTAB/MMT	= Montmorillonite modified by tetradexyltrimethylammonium bromide
OMMT	= Montmorillonite clay modified by cationic surfactants (CTAB or TTAB)

LIST OF APPREVIATIONS (CONTINUE)

CTS/OMMT	=	Montmorillonite clay modified by cationic surfactants (CTAB or TTAB) and then further modified with chitosan

CHAPTER 1
INTRODUCTION

1.1 Background and rationales

Reactive dyes are most commonly used in textile industry because of their good fastness properties and ease applications. However, by using conventional dyeing method, 50-90 % of dye deposited in dyeing materials and another 10-50 % left into water body which becomes wastewater and directly discharged to the natural supports without any treatments (Al-Degs et al., 2008). The release of colored water into the natural stream causes harmful to the aquatic lives, for example, reduction of photosynthetic activity due to reducing light penetration and also toxicity due to the presence of aromatics, metals, chlorides, etc., in the dyes (Bayramoğlu and Yakup Arıca, 2007).

Among the several methods for dyes removal from wastewater such as coagulation and flocculation, membrane separation, oxidation, electro-coagulation and adsorption, adsorption has been found to be an effective and economical method (Asok Adak, 2005). It is an accumulation of dye molecules on a surface of solid, which is known as adsorbent. Activated carbon is a well-known natural materials based adsorbent which is used in many applications such as dyes and heavy metal adsorption, and air pollutant removal, etc. However, the preparation of activated carbon consumes a lot of heat and it has low reutilization. This results in high cost of activated carbon. Hence, development of new low cost adsorbents becomes more interesting. These low-cost alternative adsorbents could be classified into (a) natural materials such as wood, peat, coal, clay etc. (b) industrial/agricultural wastes or by-products such as slag, sludge, fly ash, bagasse fly ash, red mud etc. and (c) synthesized products (Gupta and Suhas, 2009).

Surfactant modified adsorbent is an interesting method for enhancing the pollutant adsorption capacity, the surface property of the adsorbent alters from hydrophilic to hydrophobic. The method of changing is consequent of the adsorption of ionic surfactants on the charged surface. The ionic surfactant molecules will form

bilayer structures when their concentration reaches a certain amount. This structure is called "admicelle", and has ability to solubilize the organic molecules into the three dimension structures. The process is called "adsolubilization" (Asok Adak, 2005).

Recently, natural clay such as montmorillonite (MMT) has been accepted as one of the low-cost adsorbents for the removal of dyes from wastewater(Q. Wang et al., 2012). In Thailand, MMT is very cheap and is commercially produced. MMT, a member of the smectite group, is a 2:1 clay, meaning that it has 2 tetrahedral sheets sandwiching a central octahedral sheet. MMT swells with the addition of water due to water penetrating the interlayer molecular spaces and concomitant adsorption. Expandable layered silicate is an important characteristic to enhance adsorption. MMT has high cation exchange capacity (CEC), it has highly negative charge on the surface providing good property for cationic surfactant modification. From our preliminary study, the adsorption capacity of MMT to Reactive Red 120 (RR120) is very low (<5%) due to the repulsive interaction between the negatively fixed charge on the MMT surface and the RR120 anions. After the modification, organo montmorillonite (OMMT) has much higher the RR120 uptake than that of precursor. Several studies have also been reported that the surfactant modified clays (organo-clays) were successfully in dyes removal such as adsorption of Congo red by using cationic surfactant-modified MMT and very high adsorption capacity (229 mg/g) was reported (L. Wang and Wang, 2007), and also another cationic surfactant-modified clay using for the adsorption of an acid dye (Orange II) had been observed very high adsorption capacity (868.1 mg/g) as well (Zhu and Ma, 2008). Hence, OMMT could have high affinity for reactive dye such as Reactive Red 120 (RR120) due to electrostatic interactions and hydrophobic interaction. The electrostatic interactions occur between dye anions and the positive charges on the external surface of admicelle coating on the MMT. The hydrophobic interaction takes place between hydrophobic part of the dye and long chain inside admicelle of surfactant coating on the MMT surface.

Chitosan (CTS), a polysaccharide composed mainly of β-(1,4)-linked 2-deoxy-2-amino-D-glucopyranose units, is second most abundance natural polymer next to cellulose and it has many interesting properties such as hydrophilicity, biocompatibility, biodegradability and multiple functional groups which make it becomes an interesting material in water treatment applications, especially dye

removal. Many novel CTS modified adsorbents had been investigated in removal of the dyes. Zhu et al. (2012) removed an acid dye in alkaline solution by chitosan-Fe (III) hydrogel. Monvisade and Siriphannon (2009) studied on adsorption of cationic dye on CTS/MMT and a good adsorption capacity (46-49 mg/g) was reported. Kittinaovarat et al. (2010) used CTS/MMT beads to remove acidic dye and obtained 5.61 mg/g maximum adsorption capacity. It proves that CTS has the potential to be use as dyes removal material. The modification of CTS onto OMMT results in the increasing of active functional groups on adsorbent surface which are amino and hydroxyl groups. The amino group can bind with anionic dye due to the charge difference which may promote the new chitosan modified organo-montmorillonite (CTS/OMMT) to an effective adsorbent for anionic dye removal from wastewater.

In the present study, MMT is modified by tetradecyltrimethylammonium bromide (TTAB) and cetyltrimethylammonium bromide (CTAB) then coated by CTS to improve the adsorption capability. Adsorption is tested with reactive red 120 in batch system for study in isotherm, kinetic, effect of pH and temperature and characterized the adsorbents by using FTIR, BET-method, SEM, and XRD. For fixed bed column experiments, due to the fine particle size of the MMT which lead to high pressure drop in the column, quartz sand is mixed making it possible for practical laboratory experiments. Dynamic adsorption is studied and analyzed the break through curves using Adam's-Bohart, Thomas and Yoon-Nelson models (Ahmad and Hameed, 2010).

1.2 Objectives

The objective of this study is to explore the feasibility of using modified CST/OMMT as a novel adsorbent for reactive dye removal.

1.3 Hypothesis

1.3.1 Addition of CTS into OMMT may improve the adsorption capacity of the adsorbent due to increasing the interlayer space and active site.

1.3.2 The factors such as time, pH and temperature may affect adsorption capacity of reactive dye to the adsorbent.

1.4 Scope of the research

1.4.1 Reactive dye was used in this work is Reactive red 120

1.4.2 MMT clay was obtained from a provider in Thailand.

1.4.3 CTS and cationic surfactants were used to modify the precursor.

1.4.4 Characterization of the adsorbent studied would be surface analysis, pore size, morphology and functional groups.

1.4.5 Adsorption was performed in batch system and studied on adsorption capacity, effect of pH, isotherms, kinetics and thermodynamics.

1.4.6 Dynamic adsorption was performed in fixed-bed column and studied on effect of initial dye concentration, bed height, flow rate was studied.

1.4.7 The feasibility of appropriate eluent for desorption process was investigated using distilled water and sodium hydroxide solution.

1.5 Expected benefits and application

1.5.1 This work could give the optimal conditions for maximum adsorption and desorption by using chitosan/cationic surfactants modified montmorillonite as an adsorbent.

1.5.2 The results should benefit in order to use in industrial applications.

CHAPTER 2
LITERATURE REVIEW

Reactive dyes differ from other classes of dyes in that they can become covalentlybound to nucleophiles in appropriate substrates (cotton, nylon, and wool). These properties are beneficialand have led to increased usage in many industries, such as textiles, leather, food processing, dyeing, and dye manufacturing. However, this increased usageresults in the possibility of contaminationof the water stream due to poor wastewater treatment systems. Contamination of the aquatic environment with dyes isa major concern because of the reactivityof the dyes. The intense coloration of the water reduces the transmission of light transmission in the water, hence affecting aquatic plants and the aquatic environment as a whole. Many of these effects are carcinogenic and pose serious health hazards to aquatic living organisms and humans in the areas of to the reproductive system, liver, brain and kidneys.

2.1 Reactive Red 120

Reactive Red 120 (RR120) is a diazo-base anionic dye which provides bright red color and high solubility. The dye molecule is synthesized by coupling two mono-functional dye molecules together through a diamines unit, providing good light and washing fastness due to high molecular weight (MW 1469.98 Da). RR120 give good yields irrespective of the Material to Liquor (M:L) ratio and have high substantivity The optimum fixation temperature of RR120 isbetween 80 and 85°C.

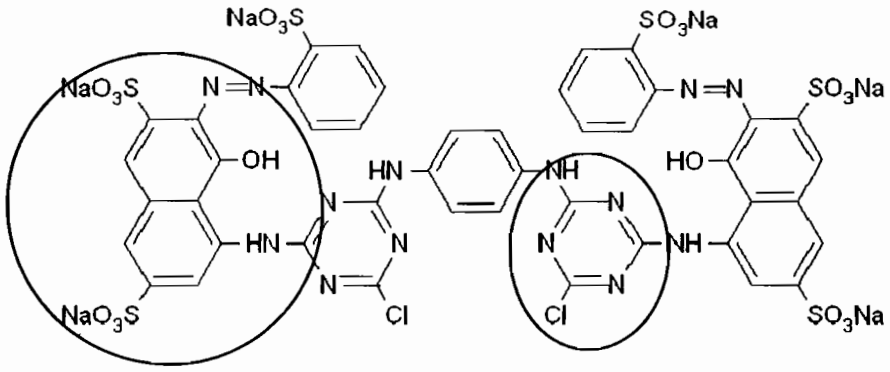

Chromophoric group

Figure 2.1 Reactive red 120 dye ($C_{44}H_{24}Cl_2N_{14}O_{20}S_6Na_6$) M_w 1469.98

In dyeing cotton fiber with reactive dyes, the addition of alkali is needed topromote the formation of the covalent bond between the dye and the cellulose. However, this alkali also causes hydrolysis of the reactive group of the dye, making it lose its fixability, and it must be removed by washing.

More details of the problems in the dyeing process and batch dyeing process were provided by Hehlen (1991) outline of three phases:

(1) The migration phase. In this first stage, the cotton is treated with dye solution in the presence of salt at about pH 6, but little reaction with the cellulose occurs. The dyeing is free to migrate from the more heavily to the lightly dyed areas of the material. The dye-bath exhaustion at the end of this phase is called the primary exhaustion

(2) The fixation phase. This begins when alkali is added to the dye-bath to raise the pH to the point where the dissociated hydroxyl groups of the cellulose begin to react with the dye. Migration of the fixed dye is impossible. During this stage, more dye is absorbed from the solution and reacts with the cellulose. The exhaustion of the dye-bath at the end of theprocess is called the secondary or final exhaustion.

(3) The washing phase. Once dyeing is completed, the material is washed several times to remove unfixed dye to achieve the final products.

As a result of the above dyeing process, dye molecules have to be treated before release intowater otherwise the ecosystem around that area isharmed.

2.2 Montmorillonite clay

Montmorillonite minerals are products of volcanism and hydrothermal activity. They are named after the Montmorillon commune in France, are composed of hydrous aluminum silicates in the form of microscopic crystals, and are a member of the smectite minerals group.

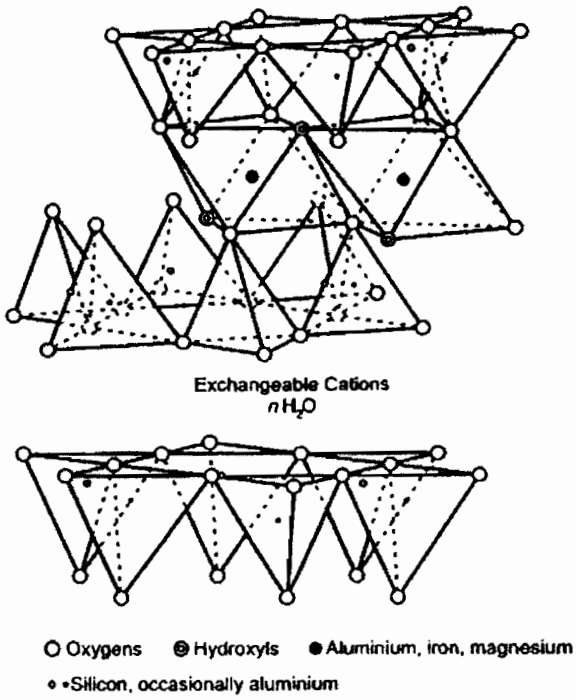

Figure 2.2 Smectite clay structure

Reference: Murray, 2006

Smectite is the mineral name given to a group of sodium (Na), calcium (Ca), Magnesium (Mg), iron (Fe), and Lithium-aluminum (Li-A1) silicates. The mineral names in the smectite group which are most commonly used are Na-montmorillonite (Na-MMT), Ca-montmorillonite (Ca-MMT), saponite (Mg), nontronite (Fe), and hectorite (Li). The rock in which these smectite minerals are dominant is bentonite. The term bentonite was defined by Ross and Shannon (Ross and Shannon, 1926) as a clay from a glassy igneous material, usually a tuff or volcanic ash. Ralph and Necip (1978) redefined the term bentonite to be any clay predominantly composed of a smectite mineral, regardless of its origin. Bentonites which are used industrially predominantly

comprise either Na-MMT or Ca-MMT and to a much lesser extent saponite and hectorite. The smectite minerals that comprise bentonites have significantly different physical and chemical properties which dictate their utility to a major degree.

Smectite is a 2:1 layer silicate in contrast to kaolinite which is a 1:1 layer silicate. Smectite has two silica tetrahedral sheets joined to a central octahedral sheet. There can be considerable substitution in the octahedral sheet, usually by Fe and Mg for Al, which creates a charge deficiency in the layer (Brindley and Brown, 1980). Also, there can be substitution in the tetrahedral sheets of Al for Si which again creates a charge imbalance.This net positive charge deficiency is balanced by exchangeable cations absorbed between the unit layers and around the edges. Thus, if the exchangeable cation is predominantly Na, the specific mineral is Na-MMT, and if it is predominantly Ca, it is Ca-MMT. Both the Na and Ca ions are hydrated in this interlayer position. Na-MMT generally have one water layer in the interlayer position and Ca-MMT generally have two water layers, which account for the basal spacing on the X-ray diffraction pattern of 15.4 Å for Ca-MMT and 12.6 Å. for Na-MMT.

The high charge on the smectite layer is satisfied by cations such as Na, Ca, Mg, Fe, and Li. Smectites have a high cation exchange capacity (CEC) which is generally of the order of 60 100 mEq/100 g of clay. These interlayer cations and water layers can be replaced by polar organic molecules such as ethylene glycol, quaternary amines, and poly-alcohols. This is an important property which can be translated into some very useful organo-clay products.

2.3 Cationic surfactants

Tetradecyltrimethyl ammonium bromide and Cetyltrimethyl ammonium bromide are cationic surfactants composed of a hydrocarbon chain (C_{14} and C_{16}) as a tail and quaternary amines which provide a permanent positive charge as a head (see Fig. 2.3).

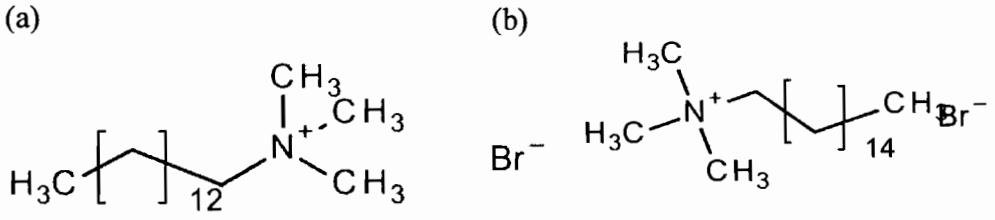

Figure 2.3 Cationic surfactants (a) Tetradecyltrimethyl ammonium bromide ($C_{17}H_{38}BrN$) Mw 336.40 (b) Cetyltrimethyl ammonium bromide ($C_{19}H_{42}BrN$) Mw 364.45

The modification of the surfactants could be possible to alter the nature of the interlayer region of clay by exchanging cations at the clay surface with cationic surfactant molecules which ultimately makes the clay surface more hydrophobic and hence causes an enhanced affinity towards the organics. The intercalation of the surfactants also increases the interlayers spaces of the clay (see Fig. 2.4), leading to an increased sorption capacity towards a variety of pollutants from aqueous solutions (Akçay and Akçay, 2004).

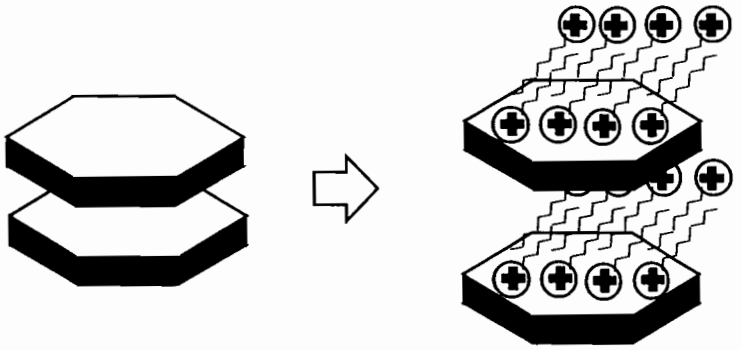

Figure 2.4 Surfactant modified montmorillonite.

2.4 Chitosan

Chitosan (CTS) is a linear polysaccharide composed of randomly distributed β-(1 - 4) - linked D-glucosamine (deacetylated unit) and N-acetyl-D-glucosamine (acetylated unit) (see Fig. 2.5). It is the second most abundant biodegradable material in the world after cellulose, made by treating shrimp and other crustacean shells with alkali sodium hydroxide(Kim, 2013).

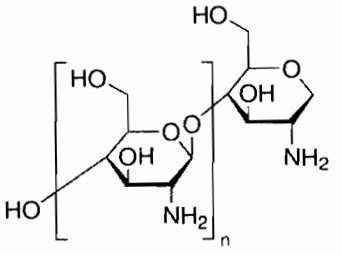

Figure 2.5 Chitosan

CTS has a number of commercial and possible biomedical uses. It can be used in agriculture as a seed treatment and bio-pesticide, helping plants to fight off fungal infections. In wine-making, it can be used as a fining agent and also helps to prevent spoilage. In industry, it can be used in a self-healing polyurethane paint coating. In medicine, it may be useful in bandages to reduce bleeding and as an antibacterial agent. It can also be used to help deliver drugs through the skin. In water processing engineering, it is used as a part of a filtration process. CTS causes the fine sediment particles to bind together, and is subsequently removed with the sediment during sand filtration. It also removes phosphorus, heavy minerals, and oils from the water. It is an important additive in the filtration process. Sand filtration apparently can remove up to 50% of the turbidity alone, while CTS with sand filtration removes up to 99% turbidity (Woodmansey, 2002).It has been used to precipitate caseins from bovine milk and cheese making(Ausar et al., 2002).

In acidic solutions, chitosan behaves as a cationic polyelectrolyte due to protonation of the amino groups. The pK_a value of chitosan is 6.3 but it is known that at pH 6.9 the amino-groups ($-NH^2$) are still partly (~20%) protonated ($-NH^{3+}$). Hence, at weak alkaline values (pH 7-8) chitosan is expected to have a very low positive charge(Jocic et al., 2010). To use it as the modification material for MMT, it is better to keep it in cationic to neutral form.

2.5 Absolubilization

The migration of organic solutes from aqueous solution into the interior of adsorbed surfactant aggregates is termed adsolubilization. This phenomenon is the surface form of solubilization, with adsorbed surfactant bilayers (admicelles) playing the role of micelles, as shown in Figure 2.6.

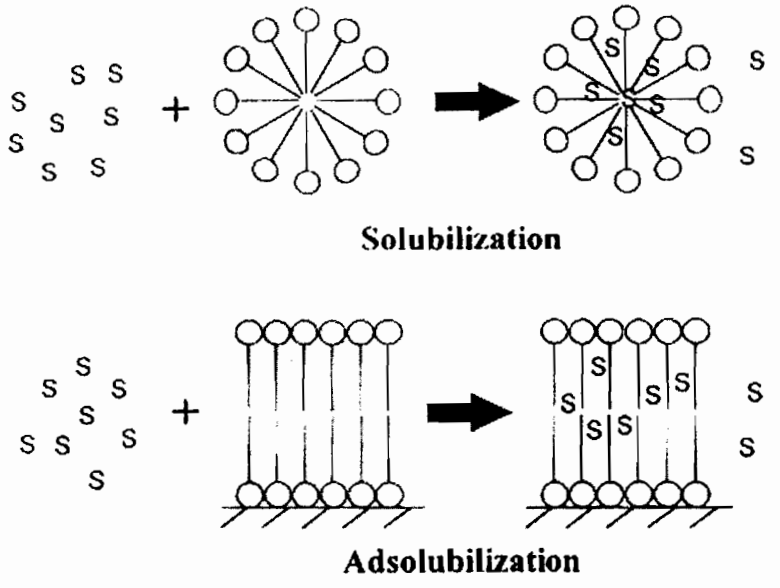

Figure 2.6 Phenomena of solubilization and adsolubilization

Reference: Kitiyanan et al., 1996

The suggested definition of adsolubilization is "the incorporation of compounds into surfactant surface aggregates, which compounds would not be in excess at the interface without surfactant"(Kitiyanan et al., 1996). This may lead to the formation of bilayers of surfactant or admicelles in the interlayer spaces of the modified clay which result in higher interlayer spaces and may have higher adsorption capacity.

2.6 Adsorption

Adsorption isthe result of interactive forces of physical attraction between the surface ofporous solids (adsorbent) and component molecules (adsorbate) being removed from the bulkphase. Thus adsorption is the accumulation of concentration at a surface (asopposed to absorption which is the accumulation of concentration within thebulk of a solid or liquid).

In general, the adsorption reaction is known to proceed through the following three steps:

(1) Transfer of adsorbate from bulk solution to adsorbent surface, which is usually mentioned as diffusion.

(2) Migration of adsorbate into pores.

(3) Interaction of adsorbate with available sites on the interior surface of pores.

Normally, the driving force for the adsorption process is the concentration difference between the adsorbate in the solution at any time and the adsorbate in the solution at equilibrium, but there are some important factors affecting adsorption, such as surface area of adsorbent, particle size of adsorbent, contact time or residence time, and affinity of the solute for the adsorbent.

2.6.1 Adsorption isotherms

Adsorption isotherms (or equilibrium data) are the fundamental requirements for the design of adsorption systems. The significance of adsorption isotherms is that they show how the adsorbate molecules are distributed between the solution and the adsorbent solids at equilibrium concentration, which can be described by adsorption isotherms using any of the mathematical models available.

The adsorption capacities at equilibrium are calculated by following equation (2.1) where $q_e$is the equilibrium dye capacity (mg/g), V is the suspension volume (L), m is the mass of adsorbent (g), C_0 is initial dye concentration (mg/l), and C_e is dye concentration at equilibrium (mg/l). The sorption uptake can be expressed in different units depending on the purpose of the exercise: for example, milligrams of solute sorbed per gram of the adsorbent material (the basic for engineering process-mass balance calculations), or mmol/g (when the stoichiometry and/or mechanism are to be considered).

$$q_e = \frac{V(C_0 - C_e)}{m} \qquad (2.1)$$

Models have an important role in technology from a laboratory to industrial scale. Table 2.1 summarizes some of the most frequently applied simple sorption isotherms(Volesky, 2003). Appropriate models can help in understanding process mechanisms, analyze experimental data, predict answers to operational conditions, and optimize processes. As an effective quantitative means to compare binding strengths and design adsorption processes, employing mathematical models for the prediction of binding capacities can be useful. Two adsorption isotherm models have been widely used in the literature. In this study, two equilibrium models were analyzed. These

included the linearized Langmuir and Freundlich isotherms equations for predicting the equilibrium behavior of dye adsorption onto modified montmorillonite clay.

Table 2.1 Frequently used single-component adsorption models

Isotherm	Advantage	Disadvantage
Langmuir	Interpretable parameters	Not structured, monolayer sorption
Freundlich	Simple expression	Not structured, no leveling off
Sips	Combination of above	Unnecessarily complicated
Reddlich–Peterson	Approaches Freundlich at high concentration	No special advantage

2.6.1.1 The Langmuir isotherm

The Langmuir isotherm assumes monolayer adsorption and is presented by following equation (2.2):

$$q_e = \frac{q_{max} b C_e}{(1+bC_e)} \qquad (2.2)$$

Where C_e (mg/l) and q_e (mg/g) are the equilibrium concentrations in the liquid and solid phase respectively, q_{max} is a Langmuir constant that expresses the maximum adsorption capacity (mg/g), and b is also a Langmuir constant related to the energy of adsorption and affinity of the sorbent.

This classical model incorporates two easily interpretable constants: q_{max}, which corresponds to the maximum achievable uptake by a system,nd b, which is related to the affinity between the sorbate and sorbent. The Langmuir constant "q_{max}" is often used to compare the performance of adsorbents while the other constant "b" characterizes the initial slope of the isotherm. Thus, for a good adsorbent, a high q_{max} and a steep initial isotherm slope (that is, high b) are generally desirable(Vijayaraghavan and Yun, 2008). However, the Langmuir isotherm is based on the following assumptions,the surface of the adsorbent is in contact with a solution containing an adsorbate which is strongly attracted to the surface, the surface has a specific number

of sites where the solute molecules can be adsorbed, and the adsorption involves the attachment of only one layer of molecules to the surface, that is monolayer adsorption(Pérez-Marín et al., 2007).

2.6.1.2 Freundlich isotherm

The Freundlich expression is as exponential equation and therefore assumes that the concentration of adsorbate on the adsorbent surface increases with the adsorbate concentration. Theoretically, using this expression, an infinite amount of adsorption can occur. This fairly satisfactory empirical isotherm can be used for non-ideal sorption that involves heterogeneous adsorption. It is presented by the following equation (2.3):

$$q_e = K_f C_e^{\frac{1}{n}} \tag{2.3}$$

Where K_F (mg/g) and n are Freundlich constants characteristic of the system, indicating the adsorption capacity and adsorption intensity, respectively.

For the intensity parameter, $\frac{1}{n}$ indicates the deviation of the adsorption isotherm from linearity. n = 1 indicates the adsorption is linear with homogeneous adsorption sites and there is no interaction between the adsorbed molecules. $\frac{1}{n} < 1$ shows that the adsorption is favorable, new adsorption sites are available, and the adsorption capacity increases. $\frac{1}{n} > 1$ indicates that the adsorption bonds are weak, and adsorption capacities decrease and are unfavorable(Fathy and El-Sherif, 2011).

2.6.2 Adsorption kinetics

An ideal adsorbent for wastewater pollution control must not only have a large adsorbate capacity but also a fast adsorption rate. Therefore, the adsorption rate is another important factor for the selection of the material and adsorption kinetics must be taken into account since they explain how fast the chemical reaction occurs and also provide information on the factors affecting the reaction rate (for example, chemical reaction, diffusion control, and mass transfer). Also, the kinetics describes the solute uptake, which in turn controls the residence time of adsorbate at the solid-solution

interface(Ho and McKay, 1998). Adsorption is a multi-step process comprised of four consecutive elementary steps in the case of immobilized beads(Guo et al., 2003): (1) transfer of solute from the bulk of solution to the liquid film surrounding the beads, (2) transport of the solute from the boundary liquid film to the surface of the bead (external diffusion), (3) transfer of solute from the surface to the internal active binding sites (intraparticle diffusion), and (4) interaction of the solute with the active binding sites. In general, the first two steps (external diffusion) are usually fast, as long as sufficient agitation is provided to avoid the formation of a concentration gradient within solution. If the fourth step is assumed to be rapid, the subsequent intraparticlediffusion becomes the rate-limiting step. Various models can be used to analyze the kinetics of sorption processes. Two kinetic models have been widely used in the literature for adsorption processes:

2.6.2.1 Pseudo-first order equation

The pseudo-first order equation (Lagergren model) is generally expressed as in equation (2.4):

$$\frac{dq_t}{dt}=k_1(q_e-q_t) \tag{2.4}$$

Where q_e and q_t (mg/g) are the amount of dyeadsorbed at equilibrium and at time t (minute) respectively, and k_1 (minute^{-1}) is the rate constant of the pseudo-first order equation. After integration and applying the boundary conditions, for $q_t = 0$ at $t = 0$ and $q_t = q_t$ at $t = t$, the equation becomes equation (2.5)(Ho and McKay, 1998):

$$\ln(q_e-q_t)=\ln q_e-k_1 t \tag{2.5}$$

2.6.2.2 Pseudo-second order equation

The pseudo-second order equation is expressed as in equation (2.6):

$$\frac{dq_t}{dt}=k_2(q_e-q_t)^2 \tag{2.6}$$

Integrating this equation for the boundary conditions for $q_t = 0$ at t = 0 and $q_t = q_t$ at t = tresults in equation (2.7):

$$\frac{t}{q_t} = \left(\frac{1}{k_2 q_e^2}\right) + \left(\frac{t}{q_e}\right) \quad (2.7)$$

where k_2 is the equilibrium rate constant of the pseudo-second order equation (g mg^{-1} min^{-1}) and $k_2 q_e^2$ is the initial adsorption rate (g mg^{-1} min^{-1})(Ho and McKay, 1998).

2.6.3 Adsorption Thermodynamics

Adsorption thermodynamics is determined using the thermodynamic equilibrium coefficients obtained at different temperatures and concentrations to verify possible adsorption mechanisms. The adsorption characteristics of a material can be expressed in terms of thermodynamic parameters such as ΔG_0 (Gibbs free energy change) which can be calculated by equation (2.8):

$$\Delta G_0 = -RT \ln K_0 \quad (2.8)$$

Where K_0 is the thermodynamic equilibrium constant, T is the solution temperature in Kelvin and R is a gas constant (8.314 J/mol/K). It can be obtained by plotting ln (q_e/C_e) vs. q_e and extrapolating q_e to zero. Its intercept with the vertical axis yields the values of K_0(Huang et al., 2007).

According to thermodynamics, the Gibbs free energy is the difference between the adsorption enthalpy (ΔH_0) and adsorption entropy (ΔS_0) multiplied by the temperature. In this manner, by applying this concept to the equation, the thermo-chemical parameters ΔH_0 and ΔS_0 can be determined using van't Hoff's plot (ln K_0 vs. 1/T) according to equation (2.9):

$$\ln K_0 = -\frac{\Delta H_0}{RT} + \frac{\Delta S_0}{R} \quad (2.9)$$

Where R is the universal gas constant (8.314 J mol^{-1} K^{-1}) and T is the temperature (K)(Piccin et al., 2011).

In general these parameters indicate that the adsorption process is spontaneous or not and exothermic or endothermic. The standard enthalpy change (ΔH_0) for the adsorption process is: (i) positive value indicates that the process is endothermic in nature; (ii) negative value indicates that the process is exothermic in nature and a given amount of heat is involved during the binding adsorbate molecule on the surface of adsorbent. This could be obtained from the plot of percent of adsorption (C_e/C_0) vs. Temperature (T). The percent of adsorption increase with increased temperature. This indicates the endothermic processes and the opposite is correct. The positive value of (ΔS_0) indicates an increase in the degree of freedom (or disorder) of the adsorbed species(Al-Anber, 2011).

2.7 Batchprocess

Batch processes are the simplest processes that involvemixing a batch of adsorbent with a batch of fluid, most commonly a liquid. After a pre-determined time the adsorbent can be separated from the fluid by sedimentation or filtration either for disposal or for re-use. If sufficient time is allowed for equilibrium to be reached then the loading of the adsorbate on the adsorbent is related to the final concentration of the adsorbate in the solution which can be determined by isotherms models. Powdered or granular adsorbents are usually added to the equipment in slurry form in such a way as to allow adequate dispersion and mixing. The adsorbent can be removed as a settled sludge(Thomas and Crittenden, 1998).

2.8 Fixed-bed column process

Separation in a fixed bed of adsorbent is, in virtually all practical cases, an unsteady state rate controlled process. This means that conditions at any particular point within the fixed bed vary with time. As fluid is passed through a fixed bed of adsorbent the transfer of adsorbate molecules from the feed to the solid initially occurs at the bed entrance. Once the adsorbent in this region becomes saturated with the adsorbate molecules, the zone in which the mass transfer occurs moves progressively through the bed towards the exit, as shown schematically in Figure 2.7 (Thomas and Crittenden, 1998).

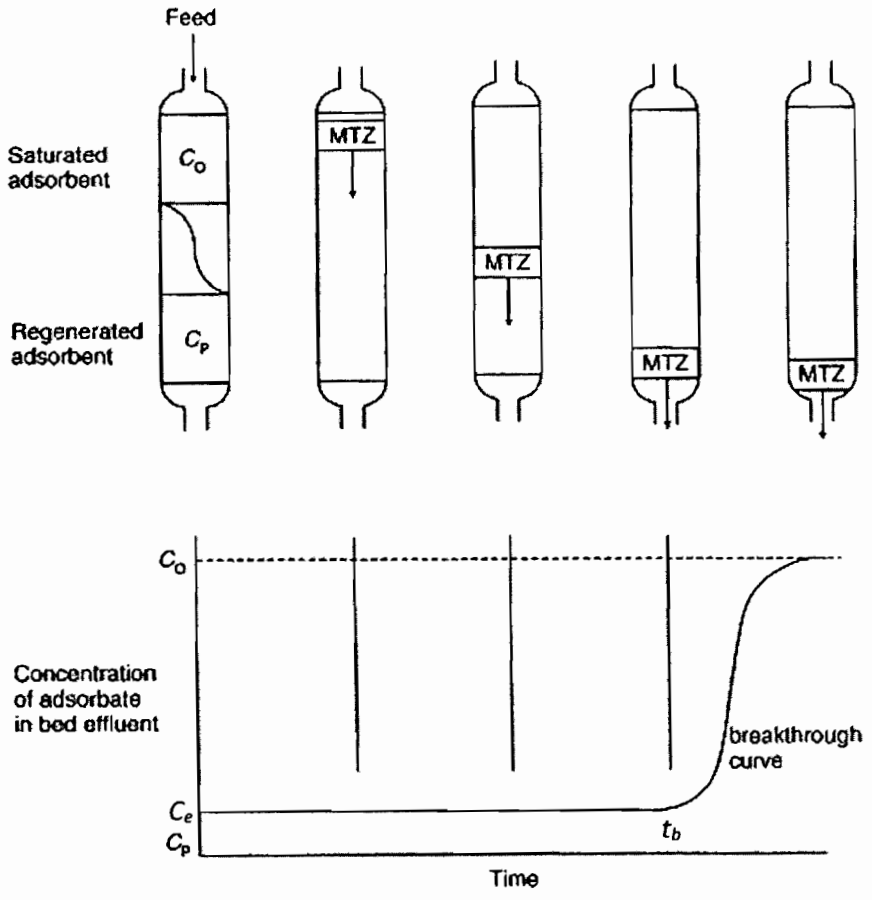

Figure 2.7 Sketch showing the concentration profile, mass transfer, and break-through curve in packed bed adsorption

Reference: Thomas and Crittenden, 1998

Much informationvaluable tothe design process canbe gleanedfromthe time tobreakthroughandfromthe shape of the break-through curve. Figure 2.7 shows the break-through curve for a single adsorbate from a fixed bed of adsorbent. Break-through is deemed to commence at a time t_b when the concentration of the adsorbate at the end of the bed increases beyond a certain level, c_e. This may be considered as the maximum allowable concentration for the effluent. As break-through continues, the concentration of the adsorbate in the effluent increases gradually up to the feed value c_0. When this has occurred no more adsorption can take place in the adsorption bed(Thomas and Crittenden, 1998). In practical operations the adsorption step must be terminated at some time earlier than t_b.

2.9 Dynamics adsorption models

In the practical application of adsorbents the situation is generally more complex since the adsorbent is usually contacted by fluid flowing through a packed bed, rather than in a well-mixed system of uniform composition. Therefore, its performance could be indicated by many parameters. One of the most important performance parameters is the outlet concentration from the fixed bed. Prediction of the outlet concentration is rather difficult, involvingthe solution of a set of non-linear partial differential equations governing the flow and mass transfer by a sophisticated numerical scheme with proper identification of many system parameters. Alternatively, the break-through curves of this work are analyzed by the following models.

2.9.1 The Adams and Bohart model

The fundamental equations describing the relationship between C_t/C_0 and t in a flowing system were estimated by Bohart and Adams. The Adams-Bohart model was used for the description of the initial part of the break-through curve. The expression is as follows:

$$\ln\left(\frac{C_t}{C_0}\right)=k_{AB}C_0t-KN\frac{Z}{F} \qquad (2.10)$$

Where C_0 and C_t are the inlet and outlet solute concentrations (mol L^{-1}) respectively. From the values of this equation describing the characteristic operational parameters of the column, (i) K is the kinetic constant (L mg^{-1} min^{-1}), (ii) Nis the saturation concentration (mg L^{-1}) that can be determined from a plot of $\ln C_t/C_0$ against time (t) at a given bed height (Z (cm)) and flow rate. F(cm min^{-1}) is the superficial velocity which can be calculated by dividing the flow rate by the cross-sectional area of the column(Aksu, 2005).

2.9.2 The Thomas model

The Thomas model assumes plug flow behavior in the bed and uses Langmuir isotherm for equilibrium and second-order reversible reaction kinetics. This model is suitable for adsorption processes where the external and internal diffusion limitations are absent. The linearized form of Thomas model can be expressed as follows:

$$\ln\left(\frac{C_0}{C_t}-1\right)=\frac{k_T q_0 w}{v}-k_T C_0 t \qquad (2.11)$$

Where k_{Th} is the Thomas rate constant (mL min^{-1} mg^{-1}), q_0 (mg g^{-1}) is the equilibrium solute uptake per g of the adsorbent, C_0 is the inlet solute concentration (mg L^{-1}), C_t is the outlet concentration at time t, W (g) the mass of adsorbent, v is the flow rate (mL min^{-1}), and t_{total} is flow time. The value of C_t/C_0 is the ratio of outlet and inlet RB5 concentrations. A linear plot of $\ln[(C_0/C_t) - 1]$ against time (t) was employed (figure not shown) to determine values of k_{Th} and q_0 from the intercept and slope of the plot(Ahmad and Hameed, 2010).

2.9.3 The Yoon-Nelsonmodel

Yoon and Nelson developed a model based on the assumption that the rate of decrease in the probability of adsorption of adsorbate molecule is proportional to the probability of the adsorbate adsorption and the adsorbate break-through on the adsorbent. The Yoon-Nelson a linearized model for a single component system and is expressed as:

$$\ln\left(\frac{C_t}{C_0-C_t}\right)=k_{YN}t-\tau k_{YN} \qquad (2.12)$$

Where k_{YN} is the rate velocity constant (min^{-1}) and τ is the time in required for 50% adsorbate break-through. A linear plot of $\ln[C_t/(C_0-C_t)]$ against sampling time (t) determined values of k_{YN} and τ from the intercept and slope of the plot (Dutta et al., 2012).

CHAPTER 3
MATERIALS AND METHODS

The experiment work for this study was carried out in the laboratory of the Department of Chemical Engineering, Faculty of Engineering, Ubon Ratchathani University. The studies of Fourier transform infrared analysis were conducted at Department of Chemistry, Faculty of Science, Ubon Ratchathani University. The studies of scanning electron microscopy analysis were conducted at Department of Biotechnology, Faculty of Science, Ubon Ratchathani University. The studies of X-ray diffraction analysis were conducted at Department of Physics, Faculty of Science, Ubon Ratchathani University. The studies of Brunauer–Emmett–Telleranalysis were conducted at Department of Chemistry, Faculty of Science Khon Kaen University. The materials and methods used in this study are reported below.

3.1 Chemicals and materials

MMT clay was purchase from Thai Nippon Chemical Industry Cp., Ltd. and used as received. All chemicals of analytical grade are listed in Table 3.1. Chemical solutions were prepared by distilled water.

Table 3.1 Chemicals used

Objectives	Chemicals
Adsorption	Reactive red 120 dye ($C_{44}H_{24}Cl_2N_{14}O_{20}S_6Na_6$) (RR120)
Adsorbent preparation	Tetradecyltrimethylammonium bromide ($C_{17}H_{38}NBr$) (TTAB)
	Cetyltrimethylammonium bromide ($C_{19}H_{42}NBr$) (CTAB)
	Chitosan $(C_6H_{11}NO_4)_n$(CTS)
	Montmorillonite clay CEC 80 meq/100 g (MMT)
	Acetic acid
Desorption	Sodium hydroxide (NaOH)
pH adjustment	Hydrochloric acid (HCl), Sodium hydroxide (NaOH)

3.2 Conceptual framework

MMT was modified by cationic surfactants and then further modified by CTS. The modified MMTs and MMT was characterized and tested for removal of RR120. The adsorbents were characterized by FTIR, BET-method, SEM, and XRD analyses. The adsorbent with highest percent dye removal was chosen and carried out for adsorption experiments in bath and fixed-bed column. Effect of contact time, initial dye concentration, pH, temperature, isotherm, and kinetic were studied for the batch adsorption. Effect of inlet dye concentration, flow rate, bed height, and dynamic adsorption models were studied for fixed bed column. The conceptual framework of this work has been shown in Fig. 3.1.

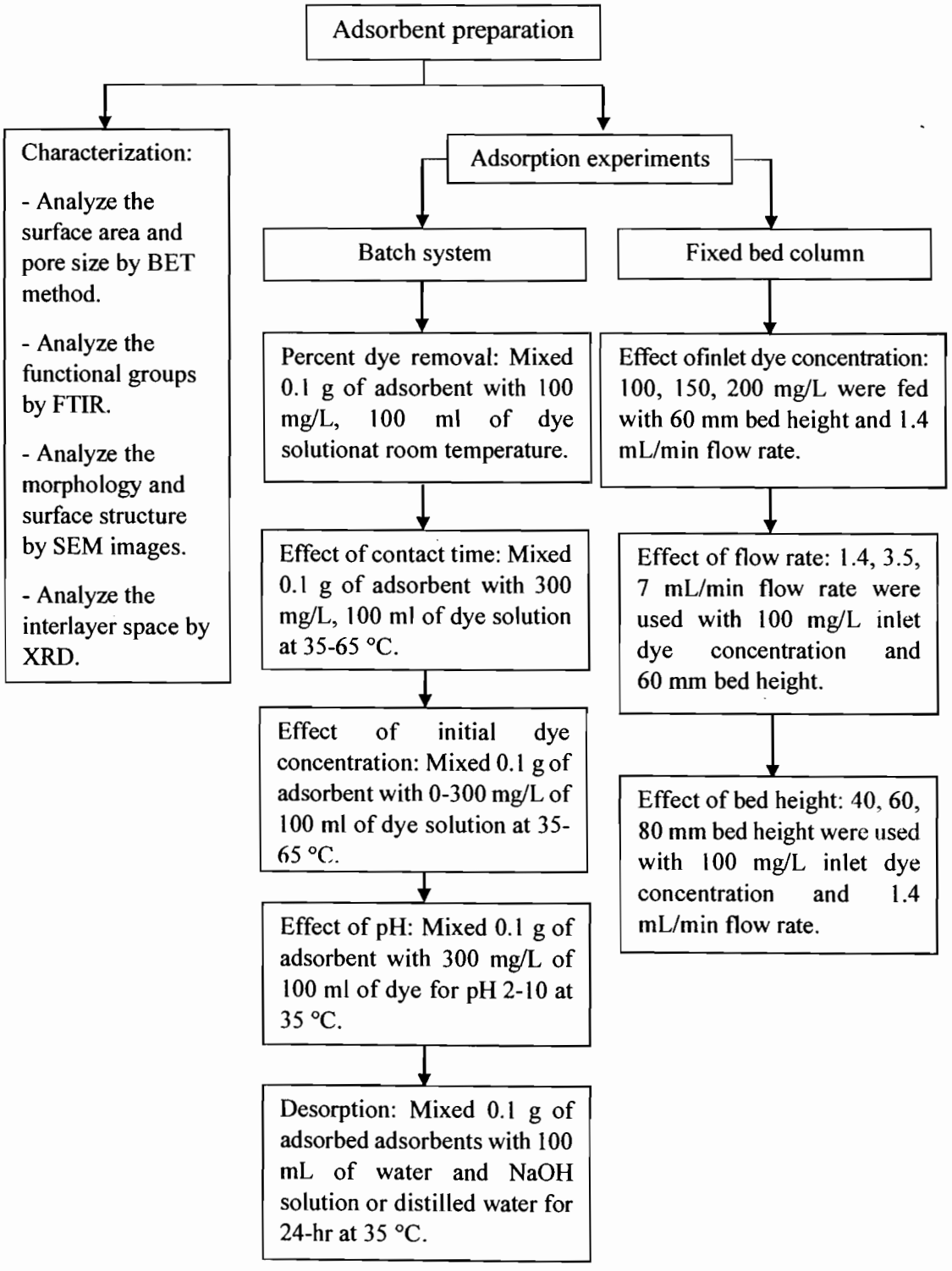

Figure 3.1 conceptual framework

3.3 Preparation of adsorbents

Before conducting the batch and fixed bed adsorption experiments, MMT was modified by several substances such as CTAB, TTAB, and CTS. The MMT modified by CTAB and TTAB were abbreviated as CTAB/MMT and TTAB/MMT and both also defined as OMMT. The MMT and OMMT modified by CTS were abbreviated as CTS/MMT and CTS/OMMT, respectively. The outline adsorbents preparation was shown in Fig. 3.2.

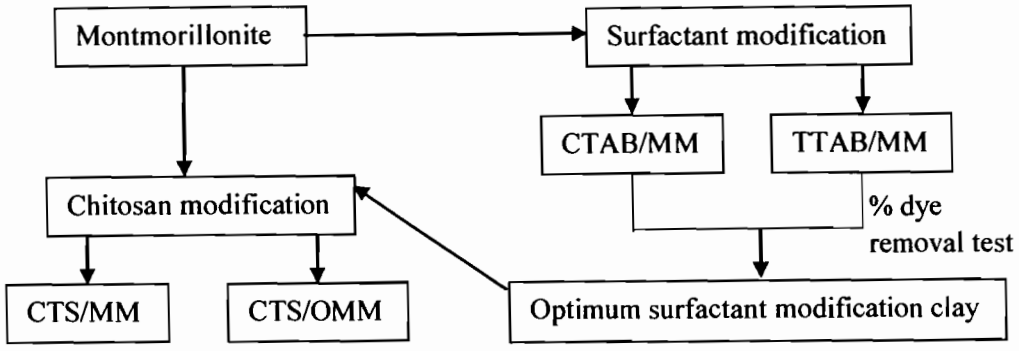

Figure 3.2 The outline adsorbents preparation.

3.3.1 Preparation of OMMT

The amounts of surfactants (CTAB or TTAB) equal to 0.25, 0.5, 0.75, 1.0, 1.5 and 2.0 CEC of MMT, the calculations were shown in appendix A, were dissolved in 100 mL distilled water. Then 1.0 g of MMT was added into each surfactant solution and continuously stirred for 12 h. The mixtures were separated using a centrifuge and washed several times by distilled water until the supernatant reach constant conductivity. Finally, the products were dried in a hot air oven at 105 °C until reached the weight constant then ground and screened througha 200 mesh screen. The adsorbents were tested for percent dye removal and the one with the highest percent dye removal was chosen and used in CTS/OMMT preparation.

3.3.2 Preparation of CTS/MMT

1.0 g of MMT was dispersed in 100 mL distilled water by continuously stirred on a stirrer.100 mL CTS solution, prepared by dissolving 2.0 g of CTS in 1% (v/v) aqueous glacial acetic acid (1000 mL) at 60 °C, pH 5.0 adjusted by 1.0 M NaOH solution, was slowly added. The solution was stirred further for 2-hrthen separated and

washed with distilled water until the supernatant reach pH7. Finally, the product was dried at 80 °C until constant weight then ground and screened through a200 mesh screen.

3.3.3 Preparation of the CTS/OMMT

1.0 g of OMMT (from 3.3.1) was dispersed in 100 mL distilled water by continuously stirred on a stirrer. 100 mL CTS solution, prepared by dissolving 2.0 g of CTS in 1% (v/v) aqueous glacial acetic acid (1000 mL) at 60 °C, pH 5.0 adjusted by 1.0 M NaOH solution, was slowly added. The solution was stirred further for 2-hrthen separated and washed with distilled water until the supernatant reach pH 7. Finally, the product was dried at 80 °C until constant weight then ground and screened through a 200 mesh screen.

3.4 Characterization of the adsorbent

3.4.1 Fourier transforms infrared analysis (FTIR analysis)

The functional groups of the adsorbent were analyzed with Perkin Elmer Spectrum Two ATR-FTIR spectrometer for as MMT and the modified-MMTs.

3.4.2 Morphology observation

The morphologies of the adsorbent were analyzed with JSM-5410LV scanning electron microscopy, SEM,at 20 kv and 10,000× magnification for as MMT and the modified-MMTs.

3.4.3 Brunauer–Emmett–Teller analysis (BET analysis)

The surface areas and pore sizes were analyzed by Nitrogen adsorption-desorption technique with Automatic Surface Analyzer, for as MMT and the modified-MMTs.

3.4.4 X-ray diffraction analysis (XRD analysis)

The interlayer spaces of the adsorbent were analyzed with X-ray fluorescence spectrometer with CuK alpha-radiation λ = 1.542 Å at 40 kv 20 mA and step size = 0.02 °2Θfor MMT and the modified-MMTs.

3.5 Analytical methods

3.5.1 Dye concentration analysis

Construct the calibrate graph of dye for dye concentration determination by measuring the absorbance according to the Beer's law which states that "attenuation is proportional to the concentration of attenuating species in the material". UV-VIS spectrophotometer was used to measure the absorbance by the following procedure.

First, 1 g of dye was dissolvedin distilled water then added into 1.0 L volumetric flask and made up with distilled water. The dye solution was kept in 1 L bottle as 1000 mg/L stock solution. The stock solution was diluted into several lower concentrations (50, 100, 150, 200, 250, and 300) with distilled water using mass balance equation (3.1).The spectrophotometer was used to scan for the maximum weave length that give the highest absorbance value and used as the lambda max, λ_{max}. The absorbance of the dye solutions were determined by UV-VIS spectrophotometer at λ_{max} = 534 nm.

$$C_1V_1=C_2V_2 \tag{3.1}$$

Where C_1 is the concentration of stock solution, 1000 mg/L.
C_2 is the concentration of wanted diluted solution (mg/L).
V_1 is the volume of stock solution that has to be used (mg/L).
V_2 is the volume of desired diluted solution (mL).

Finally, calibrate graph was conducted by plotting the absorbances of known concentration value of dye solution using the weave length at lambda max value against their concentrations, as shown in figure 3.3.

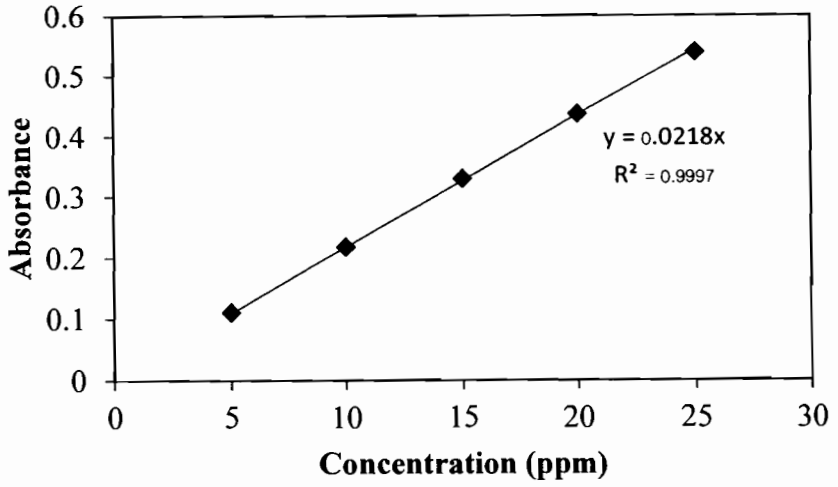

Figure 3.3 calibrate graph of dye solution, Reactive red 120, λ_{max} at = 534 nm

Table 3.2 Standard equation and λ_{max} of dye solution.

Dye	λ_{max} (nm)	Standard equation	R^2
Reactive red 120	534	Absorbance = 0.0218×Concentration	0.9997

3.5.2 pH measurement and adjustment

A combination pH electrode (EUTECH pH 700) was used to measure pH. The pH meter was calibrated before measurement using three standard pH solution of pH 4, 7 and 10. Between samples, the electrode was rinsed with distilled water to minimize the deviation of the pH meter reading. The pH was adjusted by adding HCl (0.1M) or NaOH (0.1M) drop wisely with vigorously stirred for 2 min before measured.

3.6 Adsorption studies in batch system

3.6.1 Percent Dye Removal

100 mL of 100 mg/L dye solutions were prepared in 250 mL Erlenmeyer flasks. Added 0.2 g of the adsorbents (MMT, OMMTs CTS/MMT and CTS/OMMT) intoeach flask and stirred for 12 h, 200 rpm, at room temperature. Thereafter, separated theadsorbents from the solutions by centrifugation at 8000 rpm for 5 min with a Fisher Scientific 225 centrifuge and the liquid phase was subjected to residual dye concentration determination. The residual concentrations of dye were analyzed by UV-

VIS spectrophotometer. Finally, calculated the percent dye removal by using the following equation:

$$\% \text{ Dye Removal} = \frac{C_0 - C_e}{C_0} \times 100 \quad (3.1)$$

Where C_0 is initial dye concentration (mg/L)

C_e is equilibrium dye concentration (mg/L)

The adsorbent with the highest percent dye removal was chosen to use in further experiments.

3.6.2 Effect of initial concentration

First, prepared 100 mL of 50, 100, 150, 200, 250, 300 mg/L dye solutions in 250 mL Erlenmeyer flasks. Added 0.1 g of adsorbent were added into each flask and stirred for 12 h, 200 rpm at 35°C in an incubator. Thereafter, separated the adsorbents from the solutions by centrifugation at 8000 rpm for 5 min in a Fisher Scientific 225 centrifuge and the liquid phase was subjected to residual dye concentration determination. The residual concentrations of dye were analyzed by UV-VIS spectrophotometer. Finally, calculated the adsorption capacity using equation 2.1 and fitted the experimental data with the models, Langmuir and Freundlich, according to the adsorption isotherms equation in topic 2.6 in chapter 2.

3.6.3 Effect of contact time

Before conducting this experiment, the preliminary study was tested to determine the equilibrium time with 300 mg/L dye solution and 0.1 g adsorbent, 200 rpm, 35°C. The equilibrium time was found to be 360 min. To test effect of contact time, thirteen 100 mL of 300 mg/L dye solution were preparedin250 mL Erlenmeyer flasks. Added 0.1 g of adsorbent was added into each flask and stirred at 200 rpm, 35°C in an incubator. The samples were measured at 0, 5, 15, 30, 60, 90, 120, 150, 180, 240, 360, 480, and 600 min. The collected samples were separated as soon as possible after collecting by centrifugation. The residual concentrations of dye were analyzed by UV-VIS spectrophotometer. Finally, the adsorption capacities were calculated using equation 2.1 and experimental data were fitted with the models, Pseudo-first order and

Pseudo-second order, according to the adsorption kinetics equation in topic 2.6 in chapter 2.

3.6.4 Effect of temperature

To test the effect of operating temperature, the similar procedures with the topics 3.6.2 and 3.6.3 were applied with different temperatures of 45, 55 and 65°C. The results were analyzed and studied in term of adsorption thermodynamics and the effect of temperature to adsorption capacity.

3.6.5 Effect of initial solution pH

To test the effect of initial dye solution pH, five100 mL of 300 mg/Ldye solution were prepared in250 mL Erlenmeyer flasks. The pH of each flasks were adjusted to 2, 4, 6, 8 and 10, respectively, by adding 0.1 M HCl or 0.1 M NaOH. After that, 0.1 g of adsorbent was added into each flask and stirred for 12-hr at 200 rpm,35°C in an incubator. Thereafter, the adsorbent was separated from solution by centrifugation at 8000 rpm for 5 min in a Fisher Scientific 225centrifuge and the liquid phase was subjected to residual dye concentration determination. The residual concentrations of dye were analyzed by UV-VIS spectrophotometer. Finally, analyzed the experimental data for the effect of initial pH to adsorption capacity.

3.6.6 Desorption

Before desorption test, 0.2 g of adsorbent was added into 200 mL of 300 mg/L dye solution and stirred for 24-hr at 35°C and separated from solution by centrifugation at 8000 rpm for 5 min in a Fisher Scientific 225 centrifuge to obtain dye adsorbed-adsorbent. The liquid phase was subjected to residual dye concentration determination by UV-VIS spectrophotometer. Dye adsorbed-adsorbent was dried in a hot air oven at 80 °C for until weight constant. 0.1 g of dye adsorbed-adsorbent was added into 200 mL of 0.1 M NaOH or distilled water and stirred for 24-hr at room temperature. The adsorbents were separated from solution by centrifugation at 8000 rpm for 5 min in a Fisher Scientific 225centrifuge and the liquid phase was subjected to residual dye concentration determination. The residual concentrations of dye were analyzed by UV-VIS spectrophotometer.

3.6.7 Regeneration

0.2 g of adsorbent was added into 100 mL of 300 mg/L dye solution and stirred for 24-hr at 35°C. The adsorbent was separated from solution by centrifugation

at 8000 rpm for 5 min in a Fisher Scientific 225 centrifuge and the liquid phase was subjected to residual dye concentration determination. The residual concentrations of dye were analyzed by UV-VIS spectrophotometer. Dye adsorbed-adsorbent was regenerated by shaking for 24-hrat 35°C, 200 rpm with effective eluent from the desorption experiment. Regenerated-adsorbent was dried in a hot air oven at 80 °C until weight constant. Regenerated-adsorbent was used as a new adsorbent and used for 3 cycles.

3.7 Adsorption study in fixed bed column

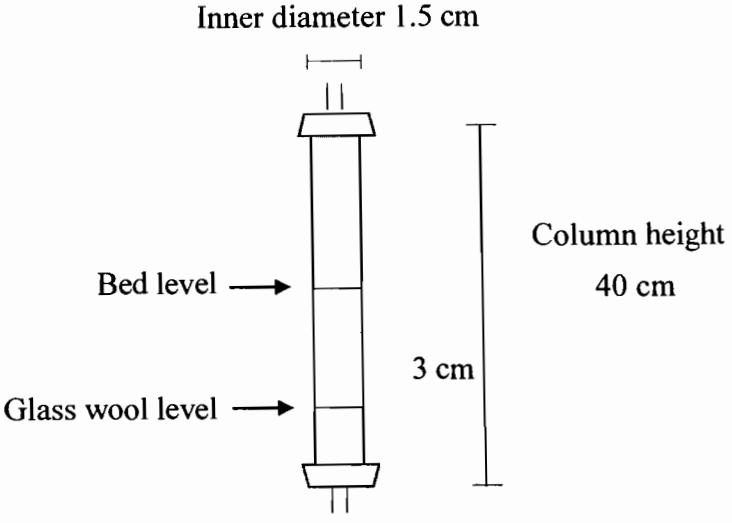

Figure 3.4 Fixed bed column diagram.

For more viewpoint of practical use, the glass tube with inner diameter of 1.5 cm and 40 cm height was used for fixed-bed column. Due to the fine particle of the clay, quartz sand was mixed at 1.75 % by mass of adsorbent clay to eliminate the fouling in the column. The column was filled with adsorbent clay-sand mixture for the desired bed height on a glass wool support and the dye solution was fed to the top of the column by a perimatic pump with the desired flow rate. Theadsorbent clay prepared from optimal condition obtained from batch experiment and all experiment was performed in room temperature.

3.7.1 Effect of inlet dye concentration

1 L of100, 150, 200 mg/L of dye solutions were prepared. The column was filled with the clay-sand mixture to obtain 60 mm bed height. The dye solution was fed with 1.4 mL/min flow rate to the top of the column and the effluent was collected. The sample was collected every 5 min andmeasured the concentration by UV-VIS spectrophotometer. The total adsorption, maximum capacity were calculated and experimental data were fitted with the model (Adam's-Bohart model, Thomas and Yoon-Nelson models) according to the equations in topic 2.9 in chapter 2. The optimal dye concentration was chosen for further experiment.

3.7.2 Effect of influent flow rate

1 L of dye solution with concentration equal to optimal values from previous experiment was prepared. The column was filled with the adsorbent clay-sand mixture to obtain 60 mm bed height. The dye solution was fed with 3.5 ml/min flow rate to the top of the column and the effluent was collected. The sample was collected every 5 min and measured the concentration by UV-VIS spectrophotometer. Similar procedure was performed except changed the flow rate to 7 mL/min. The total adsorption, maximum capacity were calculated and experimental data were fitted with the model (Adam' s-Bohart model, Thomas and Yoon-Nelson models) according to the equations in topic 2.9 in chapter 2.The optimal flow rate was chosen for further experiment.

3.7.3 Effect of bed height

1 L of dye solution with concentration equal to optimal values obtain from previous experiment was prepared. The column was filled with the adsorbent clay-sand mixture to obtain 40 mm bed height. The dye solution was fed with the optimal flow rate value from previous experiment to the top of the column and the effluent was collected. The sample was collected every 5 min and measured the concentration by UV-VIS spectrophotometer. The similar procedure was performed except changed the bed height to 80 mm. The total adsorption, maximum capacity were calculated and experimental data were fitted with the model (Adam's-Bohart model, Thomas and Yoon-Nelson models) according to the equations in topic 2.9 in chapter 2.

CHAPTER 4
RESULTS AND DISCUSSION

In this study, MMT clay modified by several substances namely CTS, Cetyltrimethylammonium bromide (CTAB), and Tetradecyltrimethylammonium bromide (TTAB) were characterized by FTIR, BET-method, SEM, and XRD analyses. Furthermore, batch adsorptions for RR120 uptake were tested in the effect of initial dye concentration, contact time, pH, and temperature. Two adsorption isotherm models, Langmuir and Freundlich, and two adsorption kinetic models, pseudo-first order and pseudo-second order, were used to analyses the experimental data. The sorbed-adsorbent was desorbed in NaOH solution and tested for reusability for three cycles. The fixed bed column was used to tested dynamic adsorption of RR120 in the effect of inlet dye concentration, flow rate, and bed height and fitted the data with Thomas, Adams–Bohart, Yoon–Nelson model and models.

4.1 Characterization

4.1.1 FTIR analysis of adsorbents

The FTIR spectrum of MMT (Fig.4.1a) is obviously different from CTS/MMT spectrum (Fig. 4.1b). The band at 2,945 and 2,879 cm^{-1}areattributed to aliphatic C-H stretching (Lertsutthiwong et al., 2012)which contributed to pyranose ring in chitosan structure (Pawlak and Mucha, 2003). The peaks at 2,945 and 2879 cm^{-1} in the spectrum of CTS/MMT are observed the difference between CTS/MMT and MMT(Pereira et al., 2013). This phenomenon is often used to confirm an ionic exchange reaction occurred between CTS and MMT and consequently CTS is intercalated into the MMT structure.

The differences FTIR spectrum of CTS (Fig.4.1b) and surfactants (Fig.4.1c, d, e) modifications are observed at peak 1,488 $cm^{-1}$and peaks around 2,900 cm^{-1}. At peak around 2,900 cm^{-1}, the surfactants modifications adsorbents show solely peaks at 2,920, 2933, and 2922cm^{-1} indicate the C-H stretching of the alkyl chain of surfactants. The occurrences of peaks at 1,488 $cm^{-1}$are characterized to C-H bending of the alkyl

chain in surfactants structure (Hu et al., 2013). The FTIR spectra of CTAB/MMT (Fig.4.1c), TTAB/MMT (Fig.4.1d) and CTS/OMMT (Fig. 4.1e) are much similar, except the C-H stretching peaks at 2,933 cm^{-1} for CTAB/MMT, 2,920 cm^{-1} for TTAB/MMT and 2,922 $cm^{-1}$for CTS/MMT are observed. The differences come from the fact that the difference in the hydrocarbon chain length group between CTAB (C-16) and TTAB (C-14) causes the C-H stretching peaks appeared at different position. The alkyl groups which observed from the spectra of CTAB/MMT, TTAB/MMT and CTS/OMMT while it is not shown in the spectra of CTS/MMT and MMT should be the evidence of the intercalation of cationic surfactant into the MMT.

For CTS/MMT and CTS/OMMT comparison, the aliphatic C-H stretching of CTS/OMMT could not be clearly detected, compared to CTS/MMT, might due to the domination of alkyl group of surfactant or low intercalation of CTS into OMMT structure.

Table 4.1 FTIR peaks differentiation of adsorbents.

Adsorbent	Peak (cm^{-1})	Functional group
MMT	-	-
CTS/MMT	2945, 2879	Aliphatic C-H
CTAB/MMT	2920, 1488	Alky C-H stretch, Alky C-H bend
TTAB/MMT	2933, 1488	Alky C-H stretch, Alky C-H bend
CTS/OMMT	2922, 1488	Alky C-H stretch, Alky C-H bend

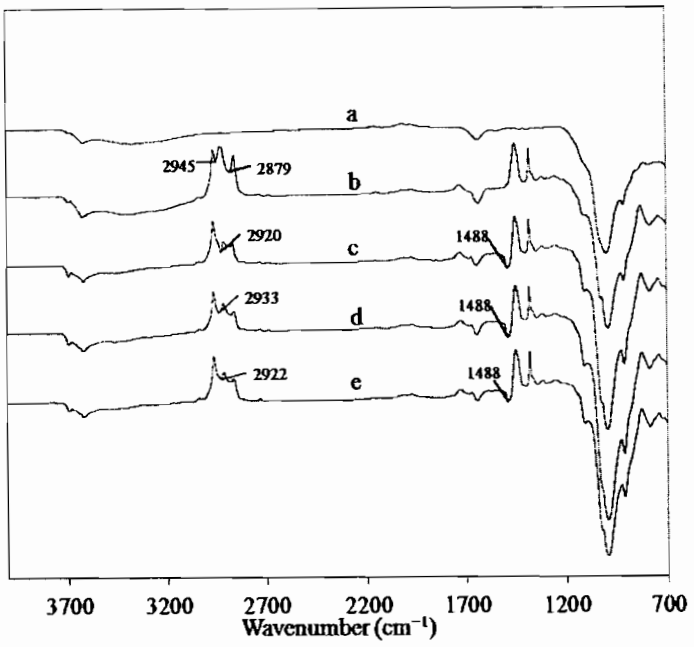

Figure 4.1 IR spectra of as received MMT (a), CTS/MMT (b), CTAB/MMT (c), TTAB/MMT (d) and CTS/OMMT (e).

4.1.2 BET analysis of adsorbents

The nitrogen adsorption-desorption isotherms of as received MMT, CTS/MMT, CTAB/MMT, TTAB/MMT, and CTS/OMMT are shown in Fig. 4.2. All adsorbents show type II isotherm with a type H3 hysteresis loop, characteristics of non-rigid aggregates of plate-like particles. Moreover, the average pore size of all adsorbents is in range of mesopores (2-50 nm) classified by the International Union of Pure and Applied Chemistry (IUPAC).

From Table 4.2, the increases in pore size of all modified MMT indicate the intercalation of modified substances which agree with the fact that MMT has the capability of interlamellar expansion and larger organic cations often act as "pillars" which keep the aluminosilicate sheets permanently apart (Huang et al., 2002). The decreases in BET surface area of all modified MMT may be induced by two mechanisms; one is that the larger organic ion may screen some MMT surface roughness, which becomes inaccessible for the nitrogen molecules, and the other is the pore blocking effect that a larger organic cations may clog some smaller pores and inhibit the passage of nitrogen molecules into these pores (C.-C. Wang et al., 2004).

After intercalation, the specific surface area of the modified MMTs was lower than that of MMT. The decrease in specific surface area comes from that fact that the cationic surfactants and/or CTS screens on the external surface of MMT which causes blocking of internal surface area of the modified MMTs. On the other hand, the adsorption capacity of RR120 on the modified MMTs was still higher than that of the precursor (see Fig.4.6). The disagreement between the specific surface area and the dye adsorption capacity might occur because the adsorption was dominated by chemical adsorption. The average pore size of surfactants modified MMT (CTAB/MMT and TTAB/MMT) was much larger than as received MMT and CTS/MMT. The larger average pore size might be due to the hindrance of large molecules of the modifying agents on the small pores of MMT. Again, the higher dye uptakes were found by using the modified MMTs as adsorbents indicating chemosorption dominated. The addition of CTS molecules into admicelle of OMMT caused lower specific surface area and larger pore size. However, the dye uptakes of CTS/OMMT and CTS/MMT are very similar (Fig. 4.6). The difference of physical characteristics between CTS/OMMT and CTS/MMT was quite independent with the adsorption capacities because the chemical sorption is the process.

Table 4.2 Specific surface areas, specific pore volumes, and average pore diameters of the adsorbents.

Adsorbent	Specific surface area (m^2/g)	Total pore volume (mL/g)	Average pore size (nm)	d-spacing (nm)
MMT	54.17	0.1701	12.56	13.5
CTS/MMT	36.45	0.144	15.8	15.3
CTAB/MMT	6.944	0.07334	42.24	-
TTAB/MMT	15.98	0.1341	33.56	-
CTS/OMMT	5.583	0.04866	34.86	-

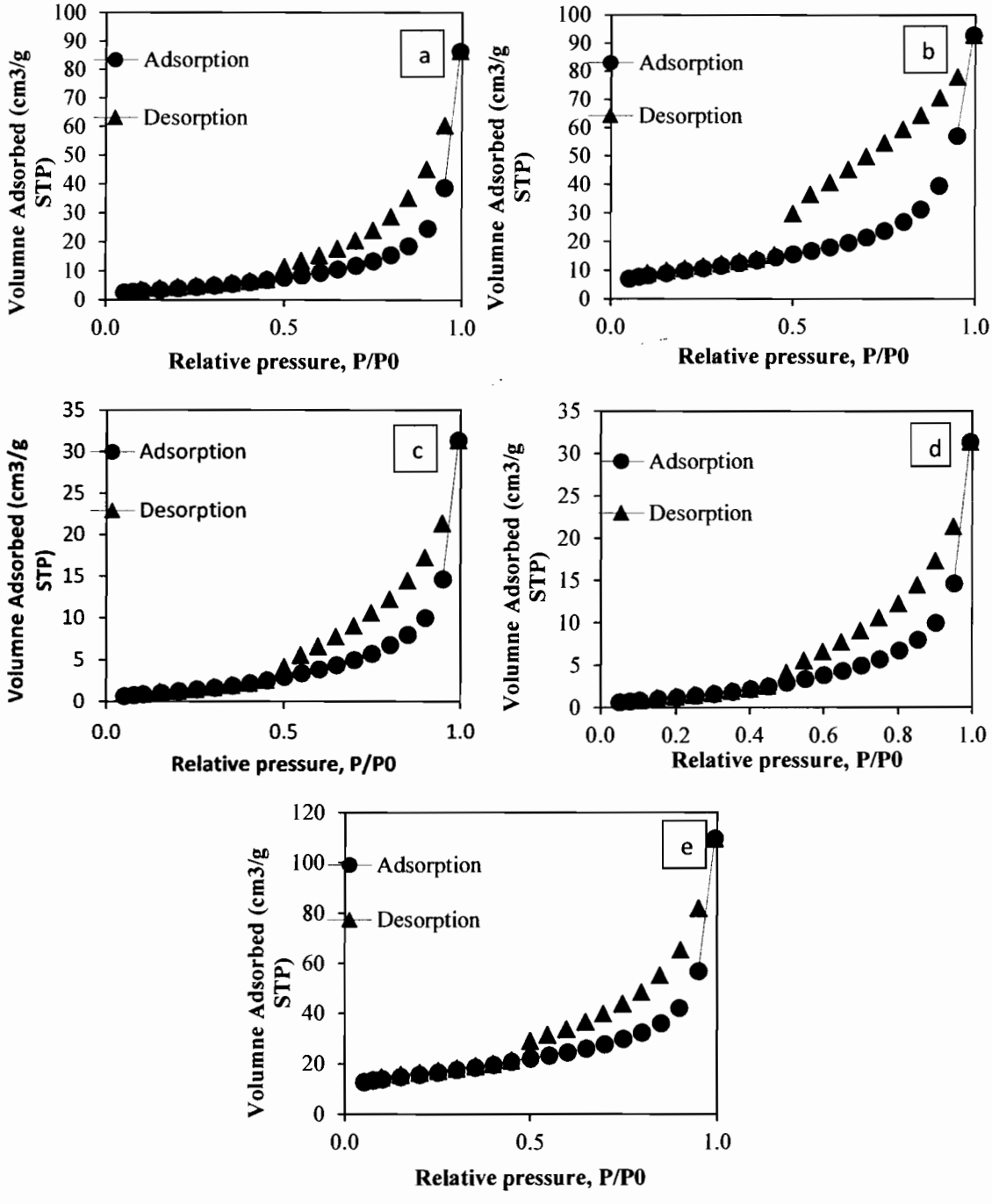

Figure 4.2 Nitrogen adsorption-desorption isotherms of as received MMT (a), CTS/MMT (b), CTAB/MMT (c), TTAB/MMT (d), and CTS/OMMT (e)

4.1.3 XRD analysis of adsorbents

XRD patterns of as received MMT, CTS/MMT, CTAB/MMT, TTAB/MMT and CTS/OMMT are shown in Fig. 4.3. Peak for MMT were observed at 2Θ = 6.55°. After intercalation MMT with CTS, the diffraction peak of MMT is boarded and a new peak is observed at 2Θ = 5.79°. The movement of the diffraction peak of MMT to a lower angle indicated formation of an intercalated nanostructure(Yu et al., 2014).

The d-spacing of MMT is 13.5 Å, corresponding to MMT intercalated with a monolayer of water, whereas the d-spacing of CTS/MMT at 2Θ =5.79° is about 15.3 Å. It is possible that a CTS monolayer was formed between the interlayer of MMT, resulting in expansion of the MMT layers. A similar result was also observed by Monvisade and Siriphannon (Monvisade and Siriphannon, 2009), based on which it was proposed that the d-spacing of about 13.6 Å was due to monolayers of CTS in MMT, whereas the d-spacing around 22.5 Å was related to the intercalation of CTS bilayers. Dader et al. (Darder et al., 2005) also suggested that the first CTS layer is adsorbed in MMT layers through a cationic exchange process.

The low intensity peaks which illustrated in XRD patterns of CTS/MMT, CTAB/MMT, TTAB/MMT, and CTS/OMMT could be due to a non-intercalated phase which was suggested by Zhou (Zhou et al., 2007). According to the limitation of the equipment which could not operate below 5 degree 2Θ, the actual peaks of CTAB/MMT, TTAB/MMT and CTS/OMMT could not be determined in this work. However, by extrapolating their XRD patterns into the lower than 5 degree 2Θ region, CTAB/MMT and CTS/OMMT seem to have the peaks at lower angle indicating the higher d-spacing. However, there has had a result of CTAB/MMT d-spacing from similar work (Zhang et al., 2013). The result shows d-spacing of CTAB/MMT at 2Θ =2.20° is 40.5 Å similar to the result of pore size in BET analysis. Another possibility is the exfoliation of the MMT structure when the peak is disappeared (Yu et al., 2014).

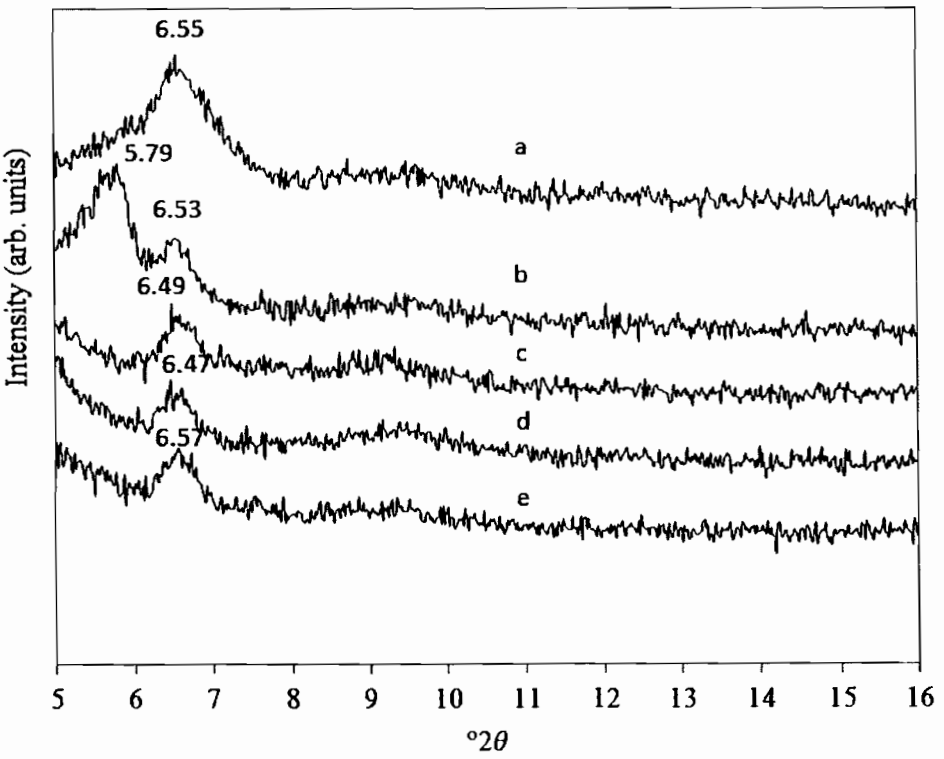

Figure 4.3 XRD powder patterns of as received MMT (a), CTS/MMT (b), CTAB/MMT (c), TTAB/MMT (d), and CTS/OMMT (e).

4.1.4 SEM images analysis of adsorbents

As can be seen in Fig.4.4a, the small particles of the MMT were close together and form an aggregate clump. After modifications with CTS (Fig. 4.4b), CTAB (Fig. 4.4c) and TTAB (Fig. 4.4d), the clay particles become larger and separated from each other leading to cavity-like structure which should be convenient for the dye molecules to diffuse into the interior structure resulting in adsorption capacity increased. According to percent dye removal experiments (section 4.2.1), the larger particle size of CTAB/MMT also corresponded to increase in dye removal efficiency. The larger portion of the modified clays is expected as admiclle adhering on the external surface of MMT. However, with further modified OMMT to CTS/OMMT (Fig. 4.4e) the cavity-like structure was covered decreasing in external surface area and reducing in adsorption capacity.

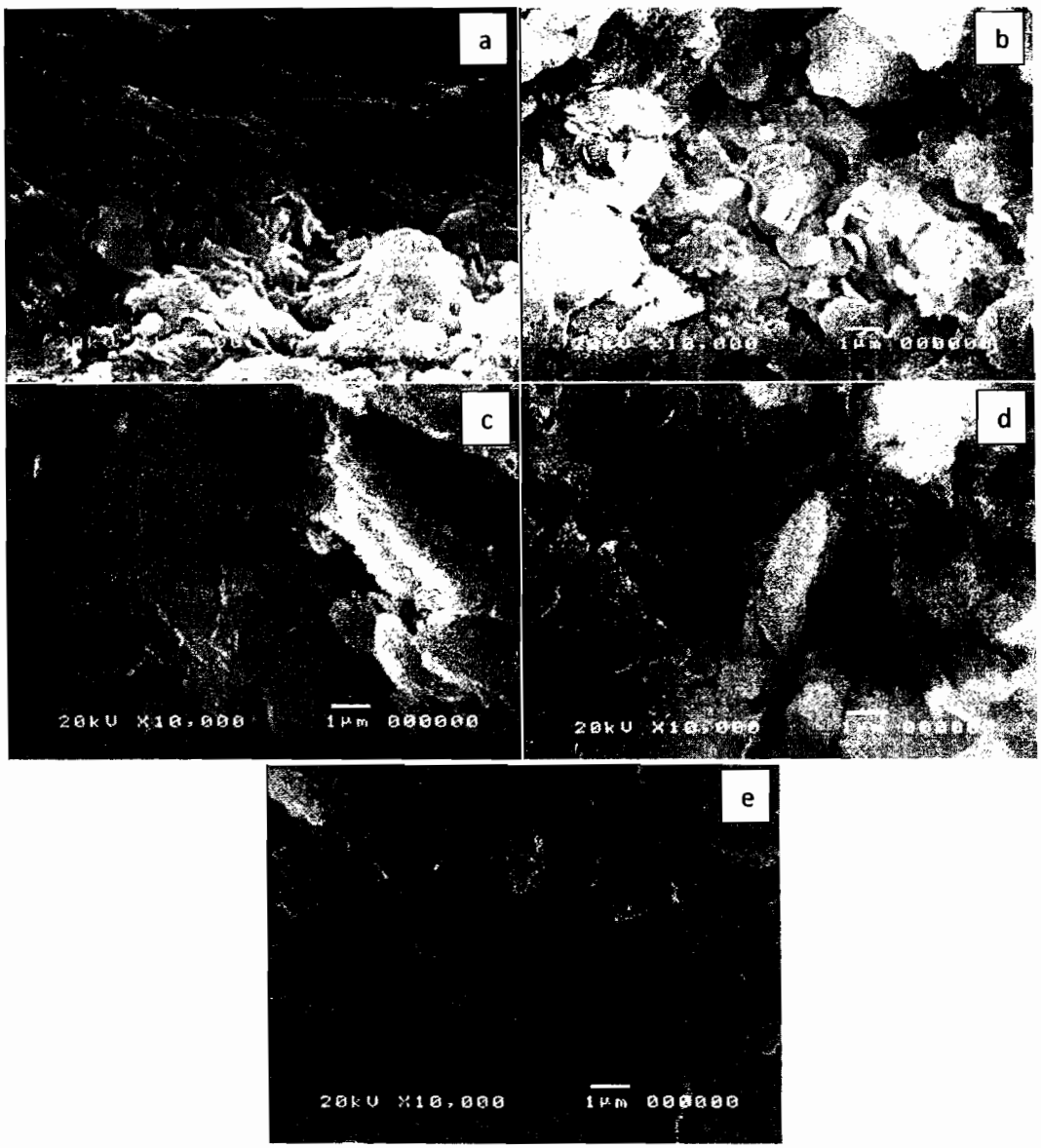

Figure 4.4 SEM images of as received MMT (a), CTS/MMT (b), 1.5 CEC CTAB/MMT c), 1.5 CEC TTAB/MMT (d), and CTS/OMMT (e).

4.2 Batch adsorption studies

4.2.1 Effect of modifications on percent dye removal

Before further modification of OMMT to CTS/OMMT, the preliminary study of the effect of surfactant types on percent dye removal was investigated. The result is shown in Fig. 4.5 demonstrating that percent dye removal increases with the percent of CEC value on the MMT to a maximum point (1.5 for CTAB and 1.0 for

TTAB) and then decrease. The increase may be due to the fixed negative charged of MMT being adsorbed the counter ions of the surfactant altering its surface property to organophilic. The further increase in percent CEC value causes the decrease of the percent dye removal. It comes from the fact that the overloading of surfactant causes too compact admiclle and blocking RR120 to penetrate into the interior portion of admiclle. The number of carbon atom of surfactant which is 14 for TTAB and 16 for CTAB may also effect the percent dye removal. The result may be due to the longer alkyl chain of CTAB increases more interior space of the adsorbent. Hence, the OMMT modified by 1.5 CEC CTAB will be used in modification of CTS/OMMT.

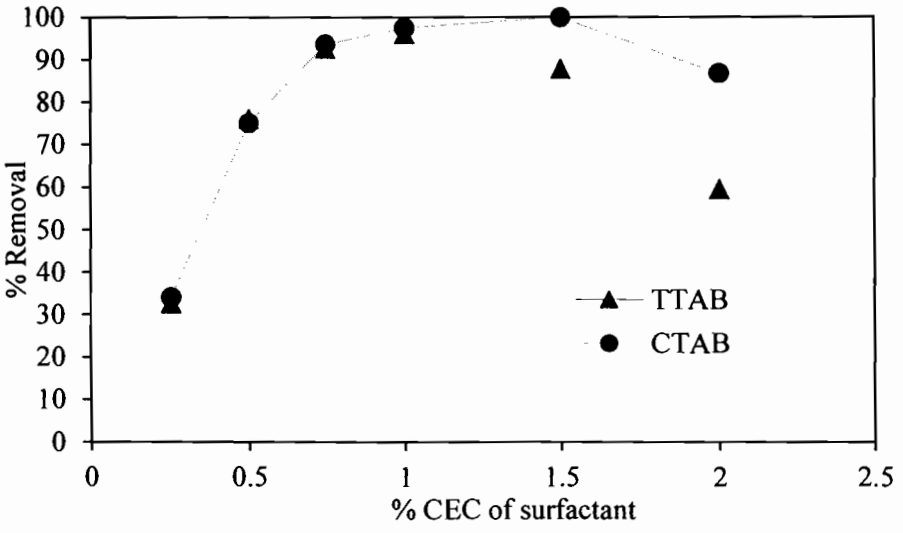

Figure 4.5 Effect of the surfactants (0.25-2.0 CEC used for each of the different surfactant types) on percent dye removal. Initial RR120 concentration: 200 ppm, adsorbent concentration: 0.1 g/100mL, room temperature and pH 5.76.

After finishing all modifications, four adsorbents (CTS/OMMT, CTS/MMT, OMMT and MMT) were obtained and tested on percent dye removal. As can be seen from Fig. 4.6, the percent dye removal could be significantly increased when MMT is modified compared to original MMT. Among the tested adsorbents, OMMT provides the highest percent dye removal (100 %) and CTS/OMMT and CTS/MMT give the similar results (47.47 and 45.62 %).In case of OMMT, the fixed positive charged on the

external surface of the admicelle induced the dye molecule to get closer to the admicelle by electrostatic force and could be easily adsorbed into the admicelle. In case of CTS/OMMT, the external surface of the admicllеis covered by the large molecule of the biopolymer allowing the adsorption occurred only on the external surfaces. This results in significant decrease of percent dye removal of CTS/OMMT compared to OMMT. According to SEM images (Fig. 4.6b), CTS/MMT shows no biopolymer coverage at the surface like CTS/OMMT. Therefore the decrease in percent dye removal of CTS/MMT might be due to the fixed positive charged of CTS (amine groups) was attached to the fixed negative charged of MMT leading to remaining of net negative charged of the adsorbent repulsing dye molecules from getting close to the adsorbent surface. Hence, OMMT modified by 1.5 CEC CTAB is chosen as a suitable adsorbent for RR120 removal from aqueous solution and used in further experiments in this research work.

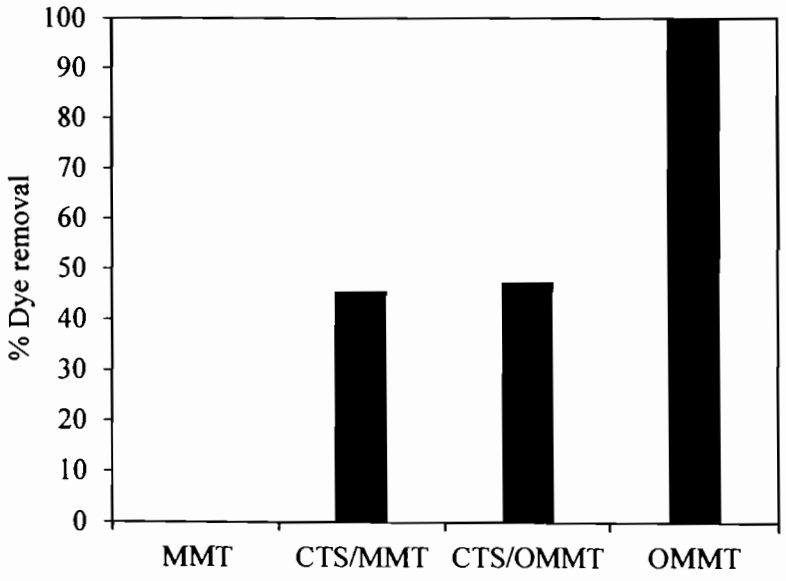

Figure 4.6 Effect of the adsorbents (2g/L CTS used for CTS/OMMT and CTS/MMT and 1.5 CEC for OMMT) on percent dye removal. Initial RR120 concentration: 200 ppm, adsorbent concentration: 0.1 g/100mL, room temperature and pH 5.5±0.4.

4.2.2 Effect of contact time

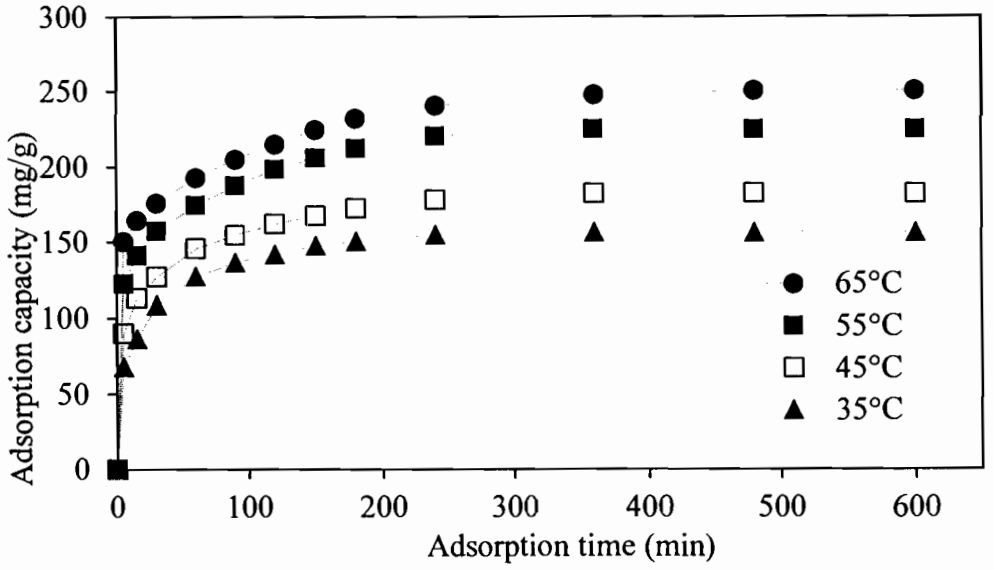

Figure 4.7 Effect of contact time and temperature on the adsorption capacities of OMMT. Initial RR120 concentration: 300 mg/L, adsorbent concentration: 0.1g/100 mL, temperature: 35 to 65 °C and pH 5.5±0.4.

The effect of contact time on the adsorption capacities of RR120 is shown in Fig. 4.7. The adsorption capacity increases rapidly at first 30 minutes and then kept slower increase until reached constant, which is assigned as equilibrium stage. Under the experimental conditions, the equilibrium time for the adsorption of RR120 on OMMT is 360 minutes. The results show that at the initial stage, the large amount of dye molecules are adsorbed onto the available active site at the external surface of admicelle which is rapidly and then slowly diffuse into the interior spaces of the adsorbent. Eventually, the available sites are fully occupied causing constant adsorption capacity at the equilibrium time.

4.2.3 Effect of initial dye concentration

In general, the removal of dye was dependent on the initial concentration of the dye (Namasivayam and Kavitha, 2002; Namasivayam et al., 1996). The relationship between the initial dye concentration and adsorption capacity of RR120 on OMMT is

presented in Fig. 4.8. It can be seen that at 35 °C the RR120 uptake increases from 42.06 to 115.99 mg/g with increasing in initial dye concentrations from 50 to 150 mg/l and then increases slightly from 115.99 to 148.75 mg/g with increasing in initial concentrations from 150 to 300 mg/l. The initial dye concentration provided an important driving force to overcome the mass transfer resistances of the pollutant between the aqueous and solid phases. At low initial dye concentration, the adsorption capacity was low because the dye molecules could not overcome the mass transfer resistances leading to unsaturated of the active sites of the adsorbent. At higher initial dye concentrations, the dye molecules have more driving force allowing dye molecule to overcome the mass transfer resistances and more internal active sites could be more occupied (Mobasherpour et al., 2014). The saturation of the dye in the adsorbent may occur when the curve reach plateau. This result shows that initial dye concentrations provide an important driving force for RR120 uptake onto OMMT which in agreement with the study of adsorption of RR120 onto *S. majuscula alga* (Çelekli et al., 2009).

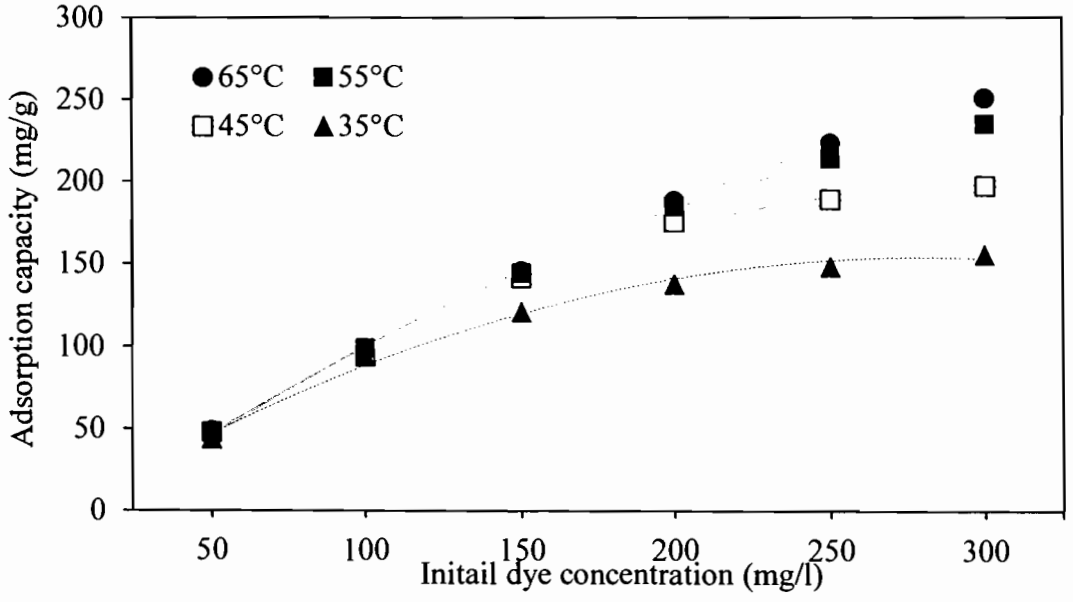

Figure 4.8 Effect of initial dye concentration and temperature on the adsorption capacities of OMMT. Initial RR120 concentration: 50 to 300 mg/L, adsorbent dose: 0.1 g/100 mL, temperature: 35 to 65 °C, pH 5.5±0.4, adsorption time: 12 h.

4.2.4 Effect of temperature

The effect of temperature on adsorption is studied by varying temperatures in a range of 35 - 65°C, initial dye concentration 300 mg/L, adsorbent dose 0.1 g/100 mL and 12 h, the results are shown in Table 4.3. The amount of RR120 adsorbed on OMMT increases from 148.75 to 245.91 mg/g when increasing in operating temperatures from 35 to 55°C. It is found that the increase of temperature facilitates to the adsorption capacity. It has been well documented that increase of temperature may cause swelling effect which denotes as an expansion of basal spacing inside the internal structure of adsorbent (Bhattacharyya and Sarma, 2003). This swelling effect allows higher amount of dye molecules penetrating into the wider intercalated space. The results from contact time and initial dye concentration (Fig. 4.7 and Fig. 4.8) also show that increasing of temperature can increase the adsorption capacity. The similar trend has been observed for the adsorption of reactive dyes on activated carbon (Al-Degs et al., 2008) and RR120 on Fe_3O_4 magnetic nanoparticles (Absalan et al., 2011).

Table 4.3 Effect of the temperature on adsorption capacity of OMMT for RR120

Temperature (°C)	Adsorption capacity (mg/g)
35	148.75
45	185.36
55	230.45
65	245.91

4.2.5 Effect of initial pH

The effect of the pH value of the original solution on the adsorption capacity of RR120 dye is shown in Fig. 4.9. It can be seen that the effect of the pH on the adsorption capacity is weak. When the pH value of the dye solution raises from 2 to 10, the adsorption capacity reduces slightly from 163.60 to 144.46 mg/g at 35°C. At low pH values, the net positive charge increases as a result of the penetration of cationic ions into the interlayer which allows dye molecules reach the external surface of OMMT more easily due to electrostatic attraction (Tabak et al., 2010). The slight decrease in adsorption may be attributed to the competition between anionic dye molecules and the

excessive hydroxyl ions to the positive active site in alkaline pH values. The dyes also could be adsorbed into interior bilayer space by hydrophobic-hydrophobic interaction. The hydrophobicity of the dye and its conjugated base are different and have lower value at higher solution pH (Yan et al., 2007). However, comparatively high adsorption capacity of the anionic dye on the adsorbent still occurred at pH 10 due to the fact that hydrophobic interactions between RR120 dye and OMMT taken place (L. Wang and Wang, 2008).

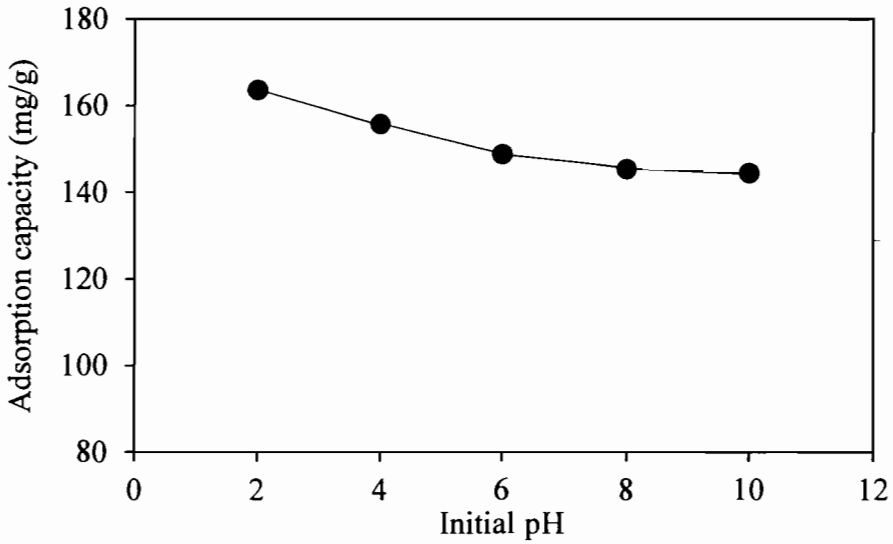

Figure 4.9 Effect of initial pH on the adsorption capacities of OMMT. Initial RR120 concentration: 300 mg/L, adsorbent concentration: 0.1 g/100 mL, temperature: 35°C, adsorption time: 12 h.

4.2.6 Adsorption isotherms

Fig. 4.10 shows adsorption isotherm which is a plot of adsorption capacity versus equilibrium dye concentration for the adsorption. It can be seen that adsorption capacity significantly increases at low equilibrium dye concentration and then increases gradually with increasing in equilibrium dye concentration.

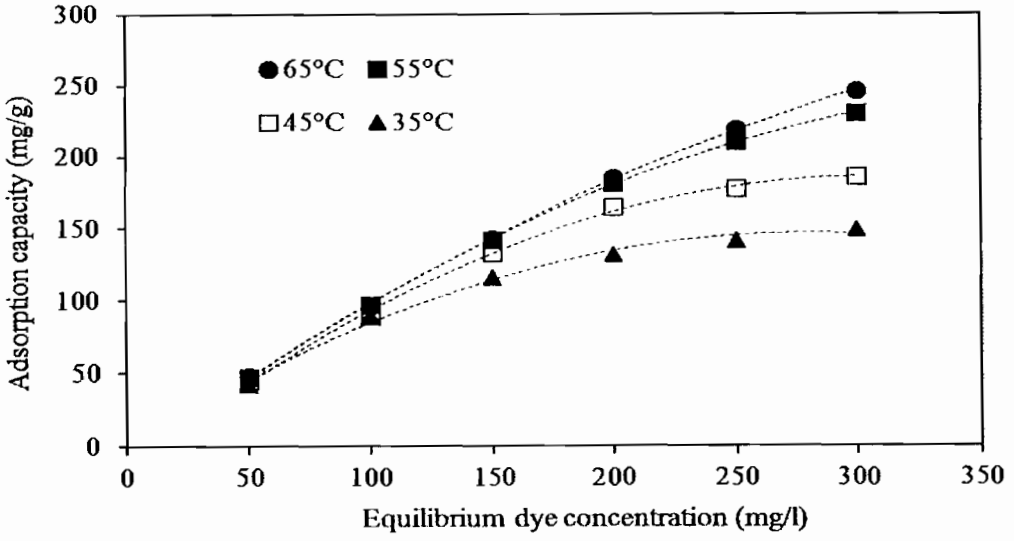

Figure 4.10 Adsorption isotherm for the adsorption of RR120 on OMMT. Adsorbent concentration: 0.1 g/100ml, pH 5.5±0.4, adsorption time: 12 h.

The equilibrium data at different temperature are interpreted using Langmuir and Freundlich adsorption isotherm models.

4.2.6.1 Langmuir model

The Langmuir model was developed based on the assumption of the formation of monolayer adsorption and also the surface is energetically homogeneous (Langmuir, 1918). Linear form of the rearranged Langmuir model is

$$\frac{C_e}{q_e} = \frac{1}{bq_m} + \frac{C_e}{q_m} \qquad (4.1)$$

where q_e is the amount of dye adsorbed at equilibrium (mg/g), C_e is the dye concentration in solution at equilibrium (mg/L), q_m is a constant related to maximum adsorption capacity (mg/g) at equilibrium and b is Langmuir constant related to energy of adsorption (L/mg).

The constants q_m and b can be calculated from the slope and intercept of the plot of C_e/q_e vs C_e as shown in Fig. 4.11 and results are presented in Table 4.4.

The Langmuir monolayer maximum adsorption capacity (q_m) increases from 162.60 to 265.00 mg/g while increasing the temperature from 35 to 65°C.

The essential characteristics of Langmuir isotherm can be expressed by dimensionless constant called equilibrium parameter, R_L.

$$R_L = \frac{1}{1+b \cdot C_0} \quad (4.2)$$

where b is the Langmuir constant and C_0 is the initial concentration (mg/L). The value of R_L indicates the nature of the adsorption process as unfavorable ($R_L > 1$), linear ($R_L = 1$), favorable ($0 < R_L < 1$), and irreversible ($R_L = 0$).

As the results from Table 4.4, the R_L value ranges between zero and one for the range of temperatures studied indicate that the adsorption is favorable.

4.2.6.2 Freundlich model

The Freundlich model is usually adopted for heterogeneous adsorption. One of its limitations is that the amount of adsorbed solute increases indefinitely with the concentration of solute in the solution (Umpuch and Sakaew, 2013). The linear form of this isotherm can be described as:

$$\ln q_e = \ln K_f + \frac{1}{n} \ln C_e \quad (4.3)$$

where K_f (mg/g) is the measure of adsorption capacity and n is the adsorption intensity. For the intensity parameter, 1/n indicates the deviation of the adsorption isotherm from linearity. n = 1 indicates the adsorption is linear with homogeneous adsorption sites and there is no interaction between the adsorbed molecules. 1/n < 1 shows that the adsorption is favorable, new adsorption sites are available, and the adsorption capacity increases. 1/n > 1 indicates that the adsorption bonds are weak, and adsorption capacities decrease and are unfavorable (Fathy and El-Sherif, 2011).

A plot of ln q_e vs log C_e gives a linear trace with a slope of 1/n and intercept of ln K_f, as shown in Fig. 4.12 and results are presented in Table 4.4.

The Freundlich constants are reported in Table 4.4, K_f increases from 9.10 to 10.51 with increasing in temperature. The value of n varies from 2.76 to 2.54 indicating that the adsorption of RR120 onto OMMT is favorable. Both Freundlich

and Langmuir model describes the nature of adsorption with good correlation coefficients.

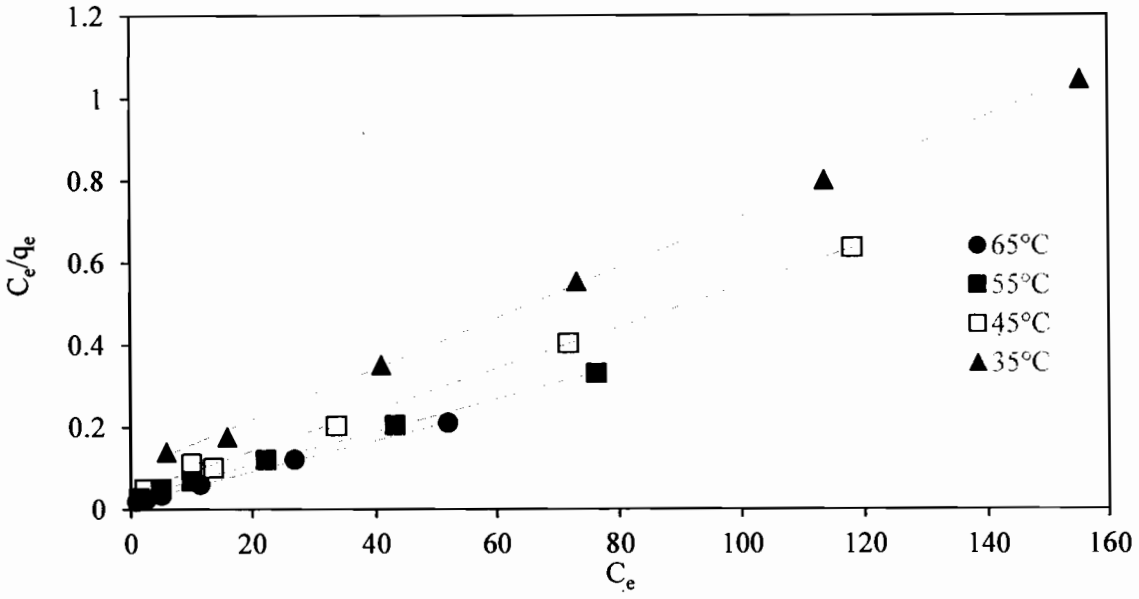

Figure 4.11 Linear plot of Langmuir isotherm model. Conditions: Adsorbent concentration: 0.1 g/100ml, and pH 5.5±0.4.

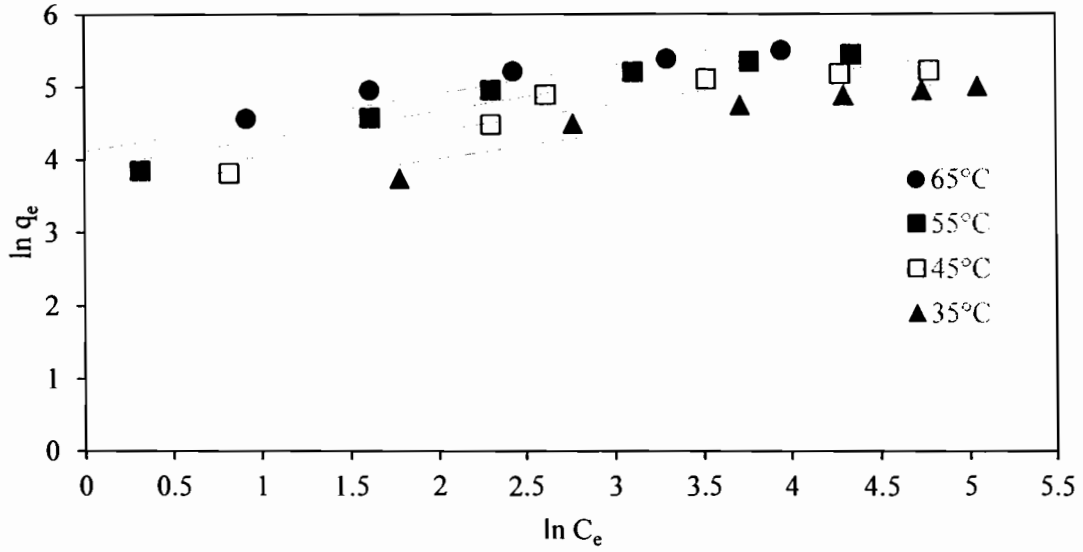

Figure 4.12 Linear plot of Freundlich isotherm model. Conditions: Adsorbent concentration: 0.1 g/100ml, and pH 5.5±0.4.

Table 4.4 Results of isotherm plot for the adsorption of RR120 onto OMMT.

Parametures	Temperature (°C)			
	35	45	55	65
q_{exp} (mg/g)	148.75	185.36	230.46	248.95
Langmuir isotherm				
q_m (mg/g)	162.60	199.21	250.67	265.00
b (l/mg)	0.2179	0.0635	0.1164	0.1333
R^2	0.9992	0.9979	0.9987	0.9991
R_L	0.2396	0.1466	0.1304	0.0841
Freundlich isotherm				
n	2.7639	2.7881	2.5405	2.5484
K_f (mg/g)	9.0980	10.2852	9.8673	10.5128
R^2	0.9013	0.8942	0.9521	0.9187

4.2.7 Adsorption kinetics

In order to understand the adsorption mechanisms of RR120 on the adsorbents, pseudo-first-order and pseudo-second-order models are used.

4.2.7.1 Pseudo-first-order kinetic model

The pseudo-first-order equation proposed by Lagergren (Yuh-Shan, 2004) can be expressed in the integrated form as equation 2.5.

The pseudo-first order kinetic plot at various temperatures are shown in Fig. 4.13 and the results are given in Table 4.5. The calculated equilibrium sorption capacity $q_{e(cal)}$ and the $q_{e(exp)}$ values have shown large deviation. The pseudo-first-order rate law fails to explain the adsorption of RR120 by OMMT with poor fit as the correlation coefficient ranged between 0.9402 and 0.9608.

4.2.7.2 Pseudo-second-order kinetic model

The pseudo-second-order model is based on the assumption of chemisorption of the adsorbate on the adsorbents (Ho and McKay, 1999). Its linearized form is given as equation 2.7.

A plot of t/q_t and t should give a linear relationship if the adsorption follows second order. q_e and k_2 can be calculated from the slope and intercept of the plot. The pseudo-second-order plots at various temperatures are given in Fig. 4.14 and results are given in Table 4.5. The equilibrium sorption capacity $q_{e(cal)}$ and $q_{e(exp)}$ are very much similar to the experiment data. From the results it is clear that equilibrium sorption capacity q_e increases with increasing the temperature. However, the pseudo-second-order rate constant k_2 decreases on increasing the temperature. These results indicate that at higher temperature the equilibrium trends to reach slower but greater in capacity. The adsorption of RR120 by OMMT is explained well by pseudo-second-order kinetics with a very high correlation coefficient of $0.9939<R^2<0.9982$, indicated that the formation rate of adsorbate and adsorbent interaction on the external surface of adsorbent is the rate of limiting step.

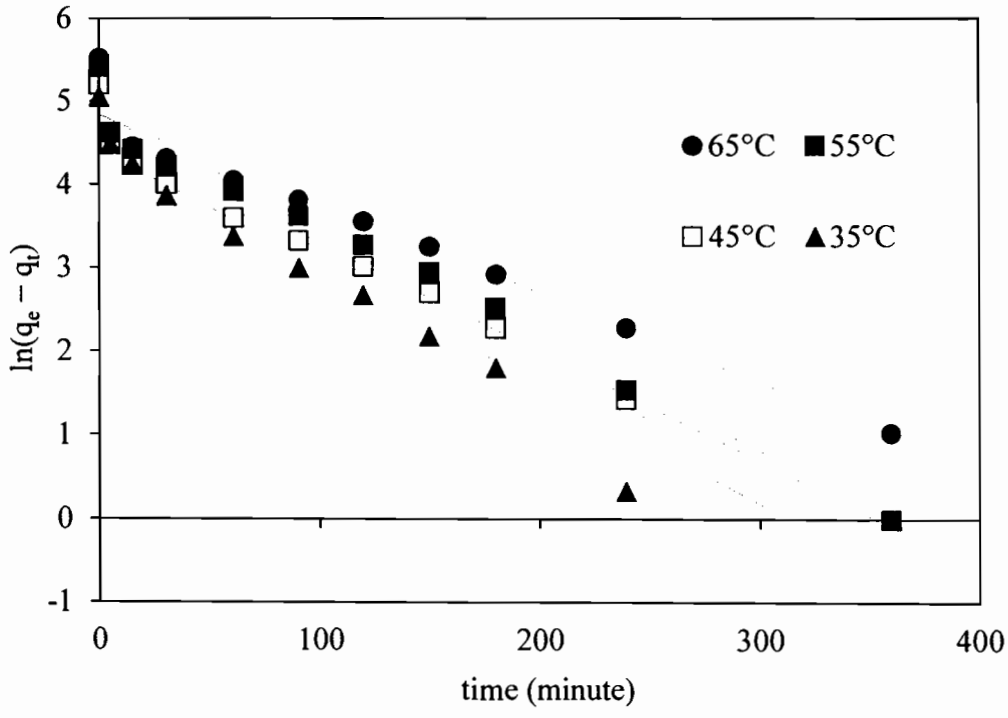

Figure 4.13 Linear plot of pseudo-first-order kinetic model. Conditions: Adsorbent concentration: 0.1 g/100ml, and pH 5.5±0.4.

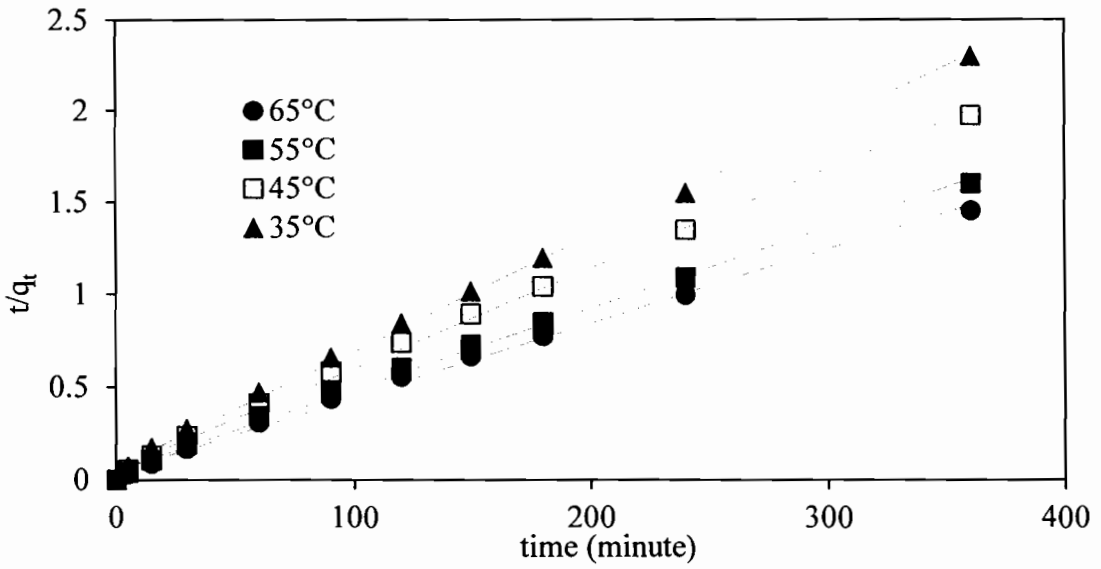

Figure 4.14 Linear plot of pseudo-second-order kinetic model. Conditions: Adsorbent concentration: 0.1 g/100ml, and pH 5.5±0.4.

Table 4.5 Results of kinetic modeling for the adsorption of RR120 onto OMMT.

Parameters	Temperature (°C)			
	35	45	55	65
$q_{e(exp)}$ (mg/g)	156.48	182.41	225.00	250.46
Pseudo-first-order model				
k_1 (min^{-1})	0.00613	0.00539	0.00532	0.00466
$q_{e(cal)}$ (mg/g)	83.17	99.46	127.61	125.56
R^2	0.9456	0.9608	0.9402	0.9601
Pseudo-second-order model				
$k_2 \times 10^3$(g/mg/min)	0.5724	0.4898	0.3812	0.3563
$q_{e(cal)}$ (mg/g)	160.00	184.84	228.31	250.00
R^2	0.9982	0.9970	0.9939	0.9960

4.2.8 Thermodynamic parameters

The activation energy for the adsorption of RR120 onto OMMT is evaluated using the following form of Arrhenius equation.

$$\ln k_2 = \ln A - \frac{E_a}{RT} \quad (4.6)$$

where k_2 (g/mg/min) is the rate constant derived from pseudo-second-order kinetic model, E_a (kJ/mol) is the Arrhenius activation energy of adsorption and A is the Arrhenius factor, R is the gas constant which is equal to 8.314 J/mol/K, and T (K) is the system temperature. The activation energy for the adsorption and the Arrhenius factor can be calculated from the plot of ln k_2 vs 1/T given in Fig. 4.15. The activation energy obtained for the adsorption of RR120 by OMMT is -14.52 kJ/mol. The negative value of activation energy suggests that the rates of adsorption decrease with an increase in the solution temperature. Reactions exhibiting these negative activation energies are typically barrierless reactions, in which the reaction proceeding relies on the capture of the molecules in a potential well. Increasing the temperature leads to a reduced probability a reduction in the probability of the colliding molecules capturing one another and this results in a negative activation energy (Umpuch and Sakaew, 2013).

The thermodynamic parameters such as Gibbs free energy change (ΔG°), standard enthalpy (ΔH°), and standard entropy (ΔS°) are also calculated to identify the influence of temperature on the adsorption process. These parameters are calculated based onthe isotherm data collected for 50-300 mg/L of RR120 solution at various temperatures range from 35 to 65°C. The thermodynamic parameters are evaluated using equations 2.8 and 2.9.

The values ofΔH° and ΔS°are evaluated from the slope and intercept of van't Hoff plot of ln K_0 vs 1/T as shown in Fig. 4.16 and the results are presented in Table 4.6.

The negative standard Gibbs free energy change depicts the spontaneous nature of adsorption. However, the adsorption of RR120 by OMMT is less favored by high temperature as indicated by the less negative Gibbs free energy (from -7.06 to -4.28 kJ/mol) during the temperature increase. Standard enthalpy change ΔH°is 33.25

kJ/mol (less than 80 kJ/mol) substantiates the physisorption and the positive sign indicates the endothermic nature of RR120 adsorption by OMMT. The randomness increases at the interface during the adsorption of RR120 by OMMT as indicated by the positive ΔS°(85.50 J/K/mol).

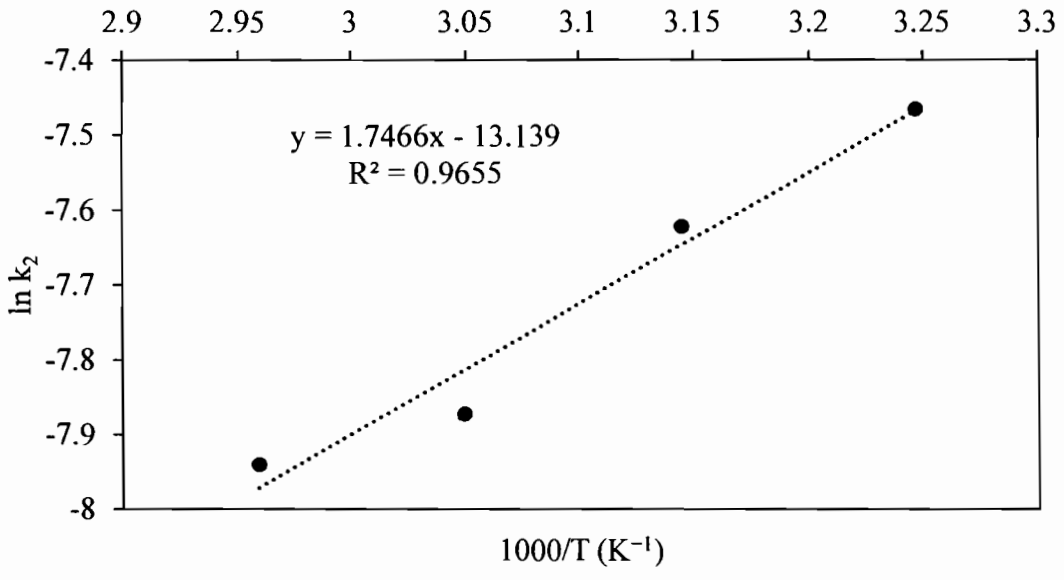

Figure 4.15 Plot of ln k_2 versus 1/T: estimation of the activation energy, E_a, for the adsorption of RR120 onto OMMT.

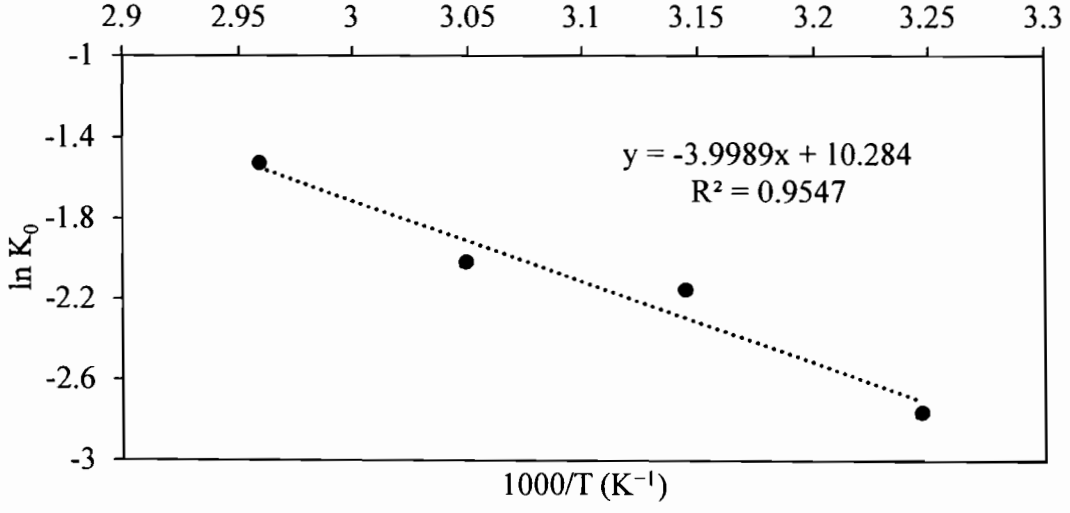

Figure 4.16 Plot of ln K_0 versus 1/T: estimation of the enthalpy (ΔH°), entropy (ΔS°), and Gibb free energy (ΔG°) for the adsorption of RR120 onto OMMT.

Table 4.6 Thermodynamic parameters for the adsorption of RR120 onto OMMT.

Temperature (°C)	$\Delta G°$ (kJ/mol)	$\Delta H°$ (kJ/mol)	$\Delta S°$ (J/K/mol)	Activation energy, E_a (kJ/mol)	Frequency factor, A
35	-7.06	33.25	85.50	-14.52	1.97×10^{-6}
45	-5.69				
55	-5.49				
65	-4.28				

4.2.9 Desorption of RR120

Desorption experiments were carried out in0.1 M NaOH solution, 100 mL, 0.1 g OMMT, 200 rpm, 35°C, and 24-hr desorption time. From Fig. 4.17, the percent desorptiondecreases drastically since the first cycle to 38.86 %.A low desorption capacity of RR120 might be due to RR120 becomes trapped into the intra-pores of the adsorbent and be difficult to release (Vijayaraghavan and Yun, 2008). The large molecule size of RR120 might provide the sufficient van der waals force leading to the desorption difficulty of trapped molecules and allowing only external-sorbed molecules to desorb. For the next two cycle, the adsorption and desorption might occur only on the external surface of OMMT which got less effect of interior-trapped leading to increase of percent desorption to89.20 and 87.84 for second and third cycle, respectively. In addition, the preliminary study of desorption using distilled water was conducted and obtained only 1.72 % of desorption. It indicates that the adsorption process is chemisorption and adsorbate-adsorbent interaction is the ion exchange which could be contested by OH molecule in alkali solution.

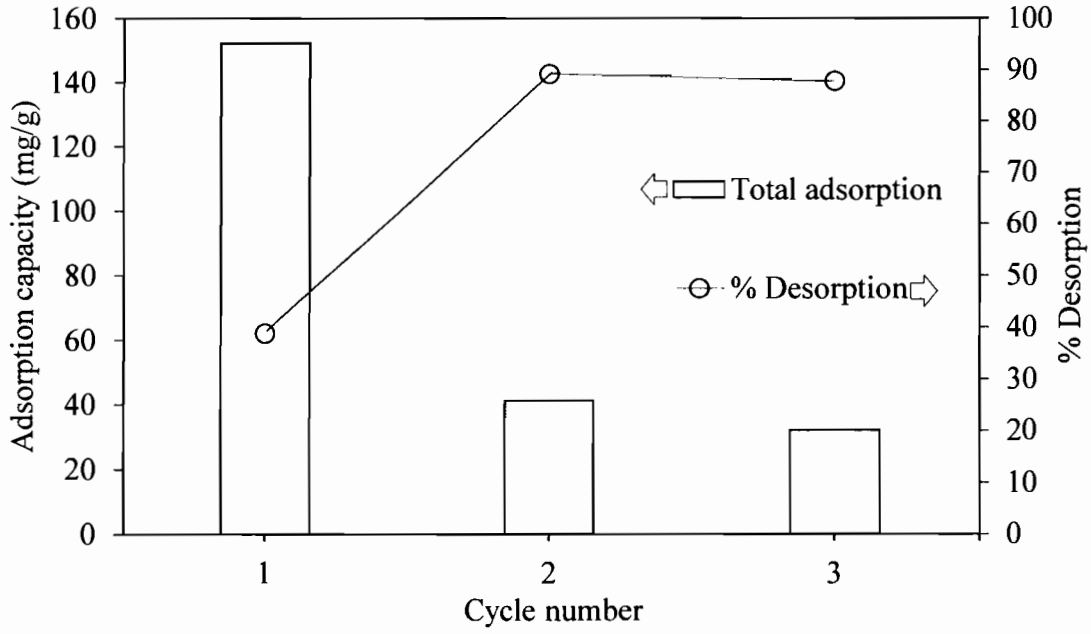

Figure 4.17 Desorption and regeneration study of RR120 on OMMT. Initial dye concentration: 300 mg/L, adsorbent concentration: 0.1 g/100ml, temperature: 35°C and pH 5.5±0.4.

4.3 Fixed bed adsorption study

4.3.1 Effect of adsorbate inlet concentration

The effect of adsorbate RR120 concentration on the column performance was studied by varying the inlet concentration of 100, 150, and 200 mg/L for the same adsorbent bed height of 60 mm and feed flow rate of 1.4 mL/min were used. The breakthrough curve is illustrated by Fig.4.18.

As can be observed from the plots, OMMT beds are exhausted faster at higher adsorbate inlet concentration. The earlier breakthrough point was reached faster at higher concentration. The breakthrough times are 111.28, 76.68, and 65.23 minutes decreasing with increasing inlet concentrations from 100 to 150, and 200 mg/L, respectively. The results indicate that the binding sites became more quickly saturated in the column with higher inlet dye concentration due to higher driving force. Furthermore, the high inlet dye concentration may cause reduce opportunity of dye contacting to the active site and the some portion of dye left the fixed-bed column without adsorption. A decrease in inlet concentration gives an extended breakthrough curve indicating that a higher volume of solution could be treated. This is due to the fact

that lower concentration gradient causes a slower transport by decreasing in diffusion coefficient or mass transfer coefficient. On the other hand, the lower concentration may cause directly in increasing the opportunity of dye contacting to the active site resulting in higher adsorption capacity.

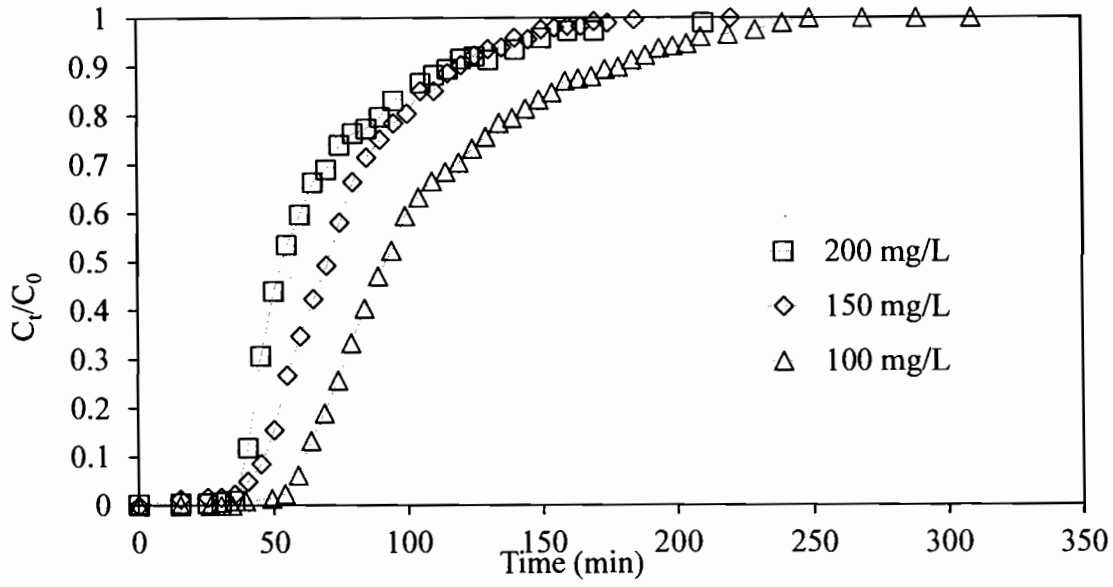

Figure 4.18 Breakthrough curves for adsorption of RR120 on OMMT at different inlet concentration (pH 5.5±0.4, flow rate 1.4 mL/min, bed height 60 mm).

4.3.2 Effect of flow rate on the breakthrough curve

To investigate the effect of flow rate on RR120 adsorption, the influent RR120 concentration and the bed height were held constant at 100 mg/L, and 60 mm. The flow rate was varied to 1.4, 3.5 and 7.0 mL/min, respectively. The breakthrough curves for OMMT are shown in Fig. 4.19. It is shows that breakthrough generally occurred faster with a higher flow rate. The breakpoint times are 111.28, 31.58, and 22.65 minutes for the flow rate of 1.4, 3.5, and 7.0 mL/min, respectively. The break point of the curve reaching saturation significantly increases with a decrease in flow rate. At a low flow rate of influent, RR120 has more time to contact with OMMT resulting in a higher removal of RR120 in column.

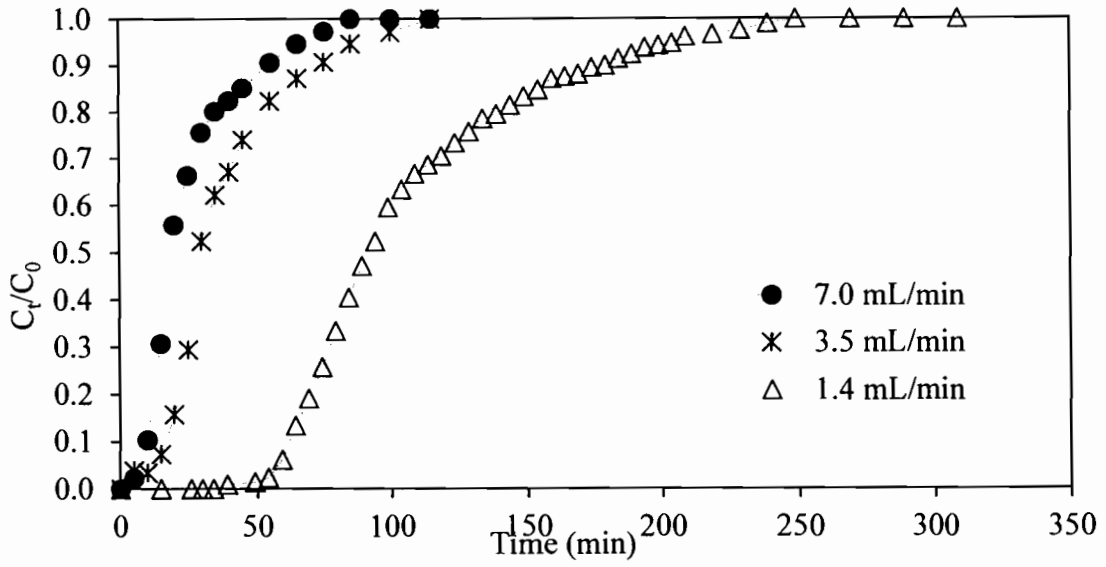

Figure 4.19 Breakthrough curves for adsorption of RR120 on OMMT at different flow rate (pH 5.5±0.4, inlet concentration 100 mg/L, bed height 60 mm).

4.3.3 Effect of bed height on the breakthrough curve

In order to perform this investigation, the breakthrough curves at different bed height (40 to 80 mm) and the same influent concentration (C_0 =100 mg/L) and flow rate (v =1.4 mL/min) for OMMT, are plotted. The results obtained are shown in Fig. 4.20.The breakpoint timesare 64.65, 111.28, and 130.72 minutes for the bed height of 40, 60, and 80 mm, respectively. It is seen that with increasing of the column bed height, a much higher removal efficiency of RR120 was observed for the employed adsorbent. When the bed height increases, RR120 has more time to contact with the OMMT, and this resulted in higher removal efficiency of RR120. The increase of bed height cause higher dye uptake which is due to an increase in the surface area of the adsorbent providing more binding sites for the adsorption.

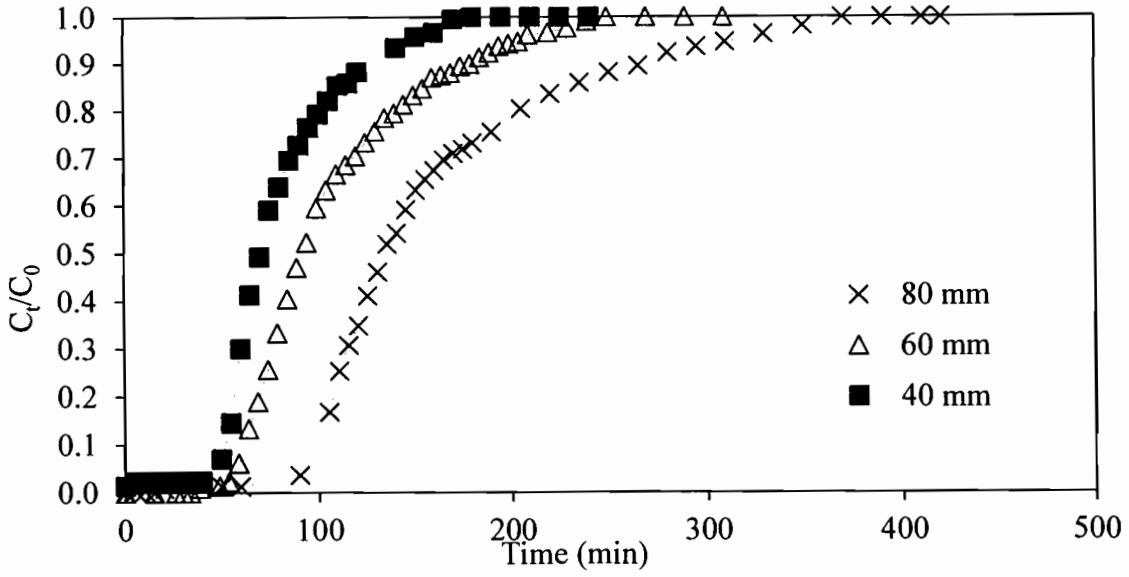

Figure 4.20 Breakthrough curves for adsorption of RR120 on OMMT at different bed height (pH 5.5±0.4, inlet concentration 100 mg/L, flow rate 1.4 mL/min).

4.3.4 Modeling of breakthrough curves

4.3.4.1 Thomas model

The basic assumptions of Thomas or reaction model are: (1) negligible axial and radial dispersion in the fixed bed column; (2) the adsorption is described by a pseudo second-order reaction rate principle which reduces a Langmuir isotherm at equilibrium; (3) constant column void fraction; (4) constant physical properties of the biomass (solid-phase) and the fluid phase; (5) isothermal and isobaric process conditions; (6) the intra particle diffusion and external resistance during the mass transfer processes are considered to be negligible (Dolphen et al., 2007). The experimental data are calculated using equation 2.11.

A linear plot of $\ln((C_0/C_t)-1)$ against time (t) is givenin Fig. 4.21 to determine values of q_0 and k_T from the intercept and slope of the plot. The column data are fitted to the Thomas model to determine the Thomas rate constant (k_T) and maximum solid-phase concentration (q_0). The determined coefficients and relative constants are obtained using linear regression analysis and the results are listed in Table 4.7.

The Thomas adsorption capacity q_0 increase from 56.68 to 64.98 mg/g on increasing the inlet dye concentration from 100 to 200 mg/L. Increase of flow rate and bed height lead to decrease of adsorption capacity. Though higher bed height enhances the quantity of treated effluent, but the amount of solute per unit quantity of adsorbent decreases. The Thomas model adsorption capacity q_0 show substantial difference with the experimental adsorption capacity (q_{exp}) meaning that the adsorption of RR120 onto OMMT is not agreed well with Thomas model assumption.

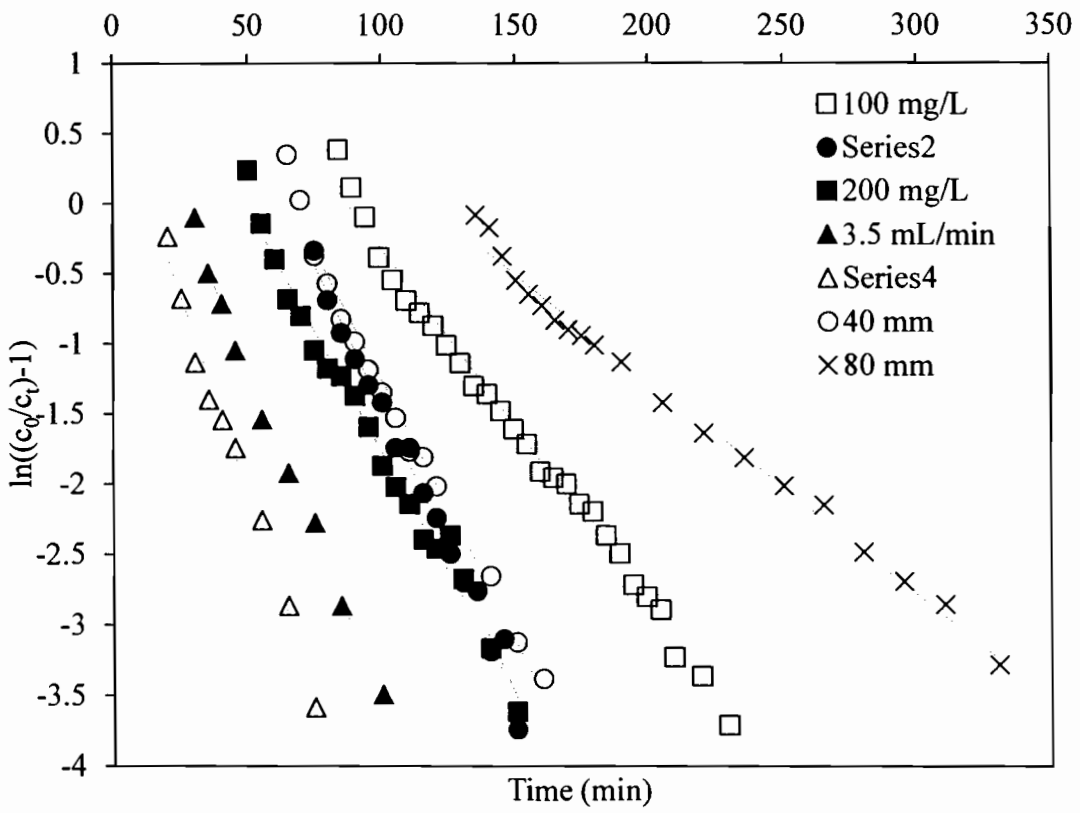

Figure 4.21 Linear plot of Thomas model with experimental data at different conditions. Flow rate 1.4 mL/min and bed height 60 mm for 100, 150 and 200 mg/L. C_0 100 mg/L and bed height 60 mm for 3.5 and 7.0 mL/min. C_0 100 mg/L and flow rate 1.4 mg/L for 40 and 80 mm.

4.3.4.2 The Adams–Bohart model

Adams–Bohart model (Bohart and Adams, 1920) based on the surface reaction theory assumes that equilibrium is not instantaneous; therefore, the rate

of the adsorption is proportional to the adsorption capacity which still remains on the sorbent. This model established the fundamental equations describing the relationship between C_t/C_0 and t in a continuous system. The Adam's–Bohart model is used for the description of the initial part of the breakthrough curve. This approach focused on the estimation of characteristic parameters such as maximum adsorption capacity (N) and kinetic constant (K) using a quasi-chemical kinetic rate expression. The experimental data are calculated using equation 2.10.

The validity of this model is limited to the range of conditions used(Ahmad and Hameed, 2010). The values of N and K can be obtained from the intercept and slope the linear plot of $\ln(C_t/C_0)$ against time (t), as show in Fig. 4.22. For all breakthrough curves, respective values of N, and Kare calculated and summarized in Table 4.7 together with the corresponding correlation coefficients. K values increase with flow rate increase this showed that the overall system kinetics is dominated by external mass transfer in the initial part of adsorption in the column.

Adsorption rate coefficient (K) is an indication of volume of influent treated by unit amount of adsorbent at unit time. On increasing the concentration from 100 to 150 mg/L more solute molecules form greater concentration gradient which reduces the adsorption rate coefficient from 1.0×10^{-3} to 0.6×10^{-3}L/mg/min. When the flow rate increased from 1.4 to 7.0 mL/min the adsorption rate coefficient increases from 1.0×10^{-3} to 2.1×10^{-3}L/mg/min and it does not show any variation while increasing the bed height from 40 to 80 cm. The adsorption capacity coefficient (N) increases while increasing the inlet dye concentration from 100 to 200 mg/L due to more availability of solute molecules in the vicinity of adsorbent. Due to high deviation of correlation, the Adams-Bohart model is not well described the adsorption data of RR120 onto OMMT in fixed bed column.

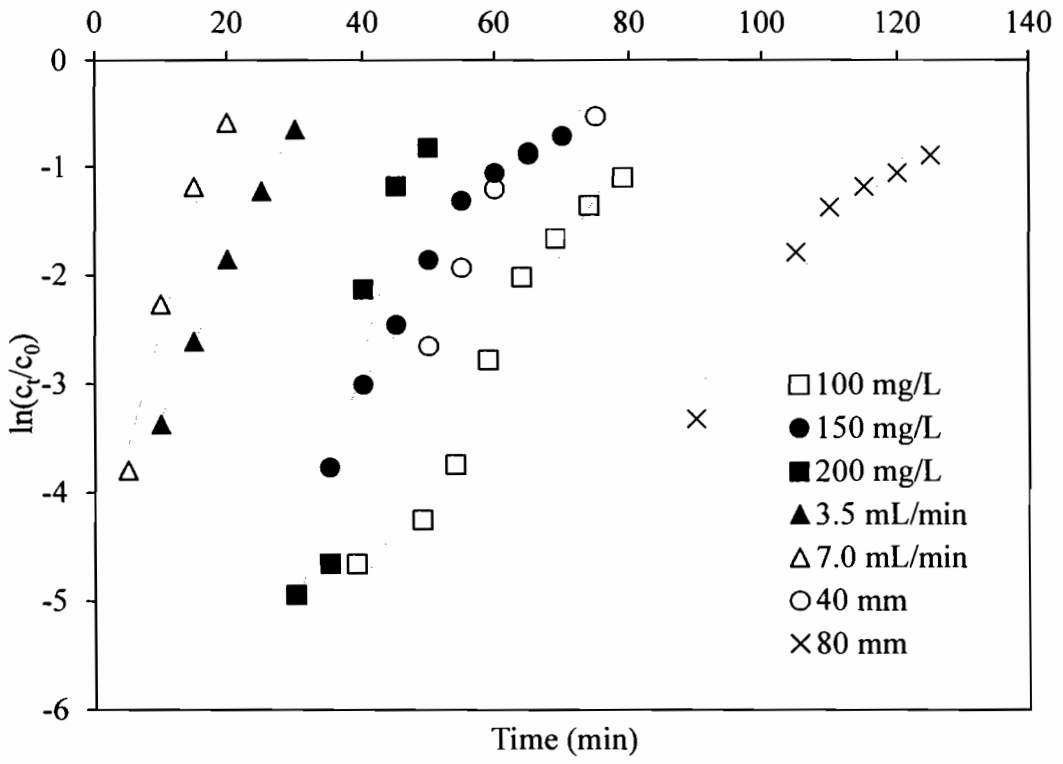

Figure 4.22 Linear plot of Adams-Bohart model with experimental data at different conditions. Flow rate 1.4 mL/min and bed height 60 mm for 100, 150 and 200 mg/L.C_0 100 mg/L and bed height 60 mm for 3.5 and 7.0 mL/min. C_0 100 mg/L and flow rate 1.4 mg/L for 40 and 80 mm.

4.3.4.3 The Yoon–Nelson model

Yoon and Nelson (Yoon and NELSON, 1984)developed a model based on the assumption that the rate of decrease in the probability of adsorption of adsorbate molecule is proportional to the probability of the adsorbate adsorption and the adsorbate breakthrough on the adsorbent. The experimental data are calculated using equation 2.12. A linear plot of $\ln(C_t/(C_0 - C_t))$ against sampling time (t) given in Fig. 4.23 determined values of τ and k_{YN} from the intercept and slope of the plot. The values of k_{YN} and τ are listed in Table 4.7.

From Table 4.7, the rate constant k_{YN} increases and the 50% breakthrough time (τ) decreases with increasing both flow rate and RR120 influent concentration. With the bed heights increases, the values of τ increases while the values of k_{YN} decreases.

The adsorption capacity based on Yoon-Nelson model increases with concentration and decreases while increasing the flow rate and bed height. The Yoon-Nelson adsorption capacity and the experimental adsorption capacity were very close, which substantiates the fitness of Yoon-Nelson model. As the adsorbent gets saturated quickly at higher concentration as well as at higher flow rate which leads to decrease of τ. Bed depth increase gives more and more adsorption sites there by increasing the value of τ which in-terms increases quantity of treated dye effluent. In case of breakthrough time prediction, the Yoon-Nelson model fits quite well with experimental data for the adsorption of RR120 onto OMMT with respect to other models.

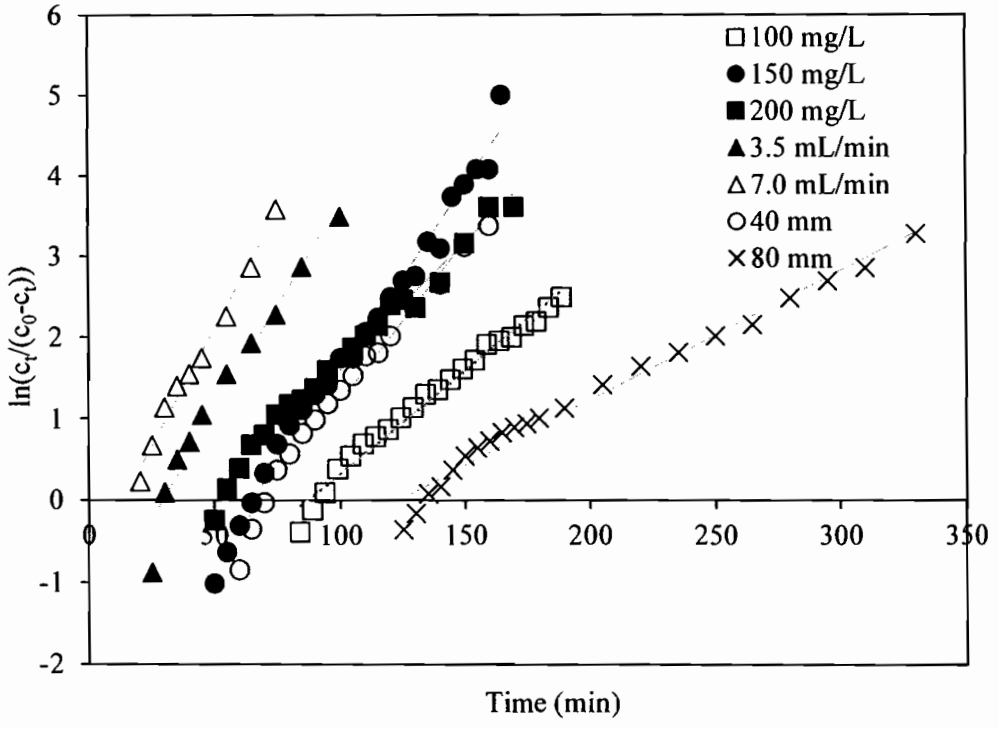

Figure 4.23 Linear plot of Yoon-Nelson model with experimental data at different conditions. Flow rate 1.4 mL/min and bed height 60 mm for 100, 150 and 200 mg/L. C_0 100 mg/L and bed height 60 mm for 3.5 and 7.0 mL/min. C_0 100 mg/L and flow rate 1.4 mg/L for 40 and 80 mm.

Table 4.7 Results of column models for the adsorption of RR120 onto OMMT.

Parameters	Values						
Concentration (mg/L)	100	150	200	100	100	100	100
Flow rate (mL/min)	1.4	1.4	1.4	3.5	7.0	1.4	1.4
Bed height (cm)	6	6	6	6	6	4	8
t_b (min)	130.72	64.65	22.65	31.58	65.23	76.68	111.28
$q_{0(exp)}$ (mg/g)	72.09	74.51	84.52	51.15	73.38	63.70	68.03
Thomas model							
k_T ($\times 10^{-4}$mL/min/mg)	2.6	3.0	1.7	4.7	5.6	3.7	1.5
q_0 (mg/g)	56.68	62.54	54.98	40.05	41.76	65.21	60.69
R^2	0.9906	0.9883	0.9863	0.9945	0.9876	0.9868	0.9918
Adams-Bohart model							
K ($\times 10^{-3}$L/mg/min)	1.0	0.6	1.2	1.4	2.1	0.8	0.7
N (mg/L)	11.57	14.63	13.66	11.29	14.28	15.51	13.25
R^2	0.9581	0.9451	0.9150	0.9961	0.9641	0.9094	0.9250
Yoon-Nelson model							
k_{YN} (L/min)	0.025	0.031	0.015	0.052	0.056	0.039	0.016
τ (min)	91.94	100.85	80.56	29.27	12.89	68.95	123.21
R^2	0.9819	0.9874	0.9836	0.9598	0.9876	0.9755	0.9805

CHAPTER 5
CONCLUSION

The results of characterizations (FTIR, BET-method, SEM, XRD), batch adsorptions (effect of initial dye concentration, contact time, pH, temperature, desorption, isotherms, kinetics), and dynamic adsorptions (effect of inlet concentration, flow rate, bed height, modeling) studies of modified montmorillonite clay adsorbed RR120 were concluded as following.

5.1 Conclusion

5.1.1 Characterization

The FTIR spectrum of MMT obviously different from CTS/MMT, CTAB/MMT, TTAB/MMT, and CTS/OMMT. The band at 2,945 and 2,879 cm^{-1} were attributed to aliphatic C-H stretching in CTS structure and the peak at 1,488 cm^{-1} (C-H bending) accompanied with the C-H stretching peaks (2,920-2,933 cm^{-1}) was attributed to alkyl groups of the surfactants. According to BET analysis,all modified adsorbents are mesoporouse and showincreasing in pore sizes from 12.56 nm (MMT) to 15.8 (CTS/MMT), 42.24 (CTAB/MMT), 33.56 (TTAB/MMT), and 34.86 nm (CTS/OMMT). XRD patterns showthe d-spacing of MMT and CTS/MMT are 13.5 and 15.3 Å respectively. For CTAB/MMT, TTAB/MMT, and CTS/OMMT,the XRD patterns were undetermined due to the limitation of the equipment but could be estimated that CTAB/MMT and CTS/OMMT have higher d-spacing than TTAB/MMT, CTS/MMT, and MMT. However, the pore sizes from BET analysis and d-spacing from XRD analysis are similar indicating the porous structure of the clay come from the inter layer space of the aluminosilicate sheets. These results confirmed that the intercalation of CTS, CTAB, and TTAB actually occurred. SEM images show the changing of MMT particle size whichwas larger and separated more from each other for CTS/MMT, CTAB/MMT, and TTAB/MMT lead to cavity structure. In case of CTS/OMMT, the cavity structure was coverage by additional CTS.

5.1.2 Batch adsorption studies

To select the optimal adsorbent, the percent dye removal are tested for four adsorbents (MMT, CTS/MMT, CTS/OMMT, and OMMT) and the results are were 0, 45.62, 47.47, and 100 %, respectively. The experiment conditions are initial RR120 concentration: 200 ppm, adsorbent concentration: 0.1 g/100mL, room temperature and pH 5.5±0.4. According to yielding the highest percent dye removal, OMMT is selected for using in further experiments.

The batch adsorption experiments are investigated in various parameters such as the effect of contact time,initial dye concentration, temperature, pH, isotherms, kinetics, thermodynamics, and desorption. For effect of contact time, the adsorption capacity of RR120 onto OMMTshows increasingwith contact time at all experiment temperatures and the equilibrium time is 360 min.For effect of initial dye concentration, the adsorption capacity of RR120 onto OMMT increaseswith initial concentrations at all experiment temperatures. The highest adsorption capacity is 245.91 mg/g at initial concentration of 300 mg/L,pH 5.5±0.4 and 65 °C. The adsorption capacity of RR120 onto OMMT increases with operating temperatures.For effect of temperature, the adsorption capacities are 148.75, 185.36, 230.45, and 245.91 mg/g at the temperature of 35, 45, 55, and 65 °C, respectively.For effect of pH, the adsorption capacity of RR120 onto OMMTdecreases slightly with initial pH increases. The adsorption capacities are 163.60, 155.77, 148.81, 145.33, and 144.46 mg/g at the initial pH of 2, 4, 6, 8, and 10, respectively. The adsorption isotherm of RR120 adsorbed onto OMMT fits better with Langmuir isotherm with the R^2 of 0.9992, 0.9979, 0.9987, and 0.9991 at the temperature of 35, 45, 55, and 65 °C, respectively. The Langmuir monolayer maximum adsorption capacities (q_m) are 162.60, 199.21, 250.67, and 265.00 mg/g for 35, 45, 55, and 65 °C, respectively.However, high R^2(>0.8942) of Freundlich isotherm is considerable indicating that the adsorption of RR120 onto OMMT is effected by both chemisorption and physisorption. The adsorption isotherm of RR120 adsorbed onto OMMT fitted better with Pseudo-second-order kinetic model with the R^2 of 0.9982, 0.9970, 0.9939, and 0.9960 at the temperature of 35, 45, 55, and 65 °C, respectively. It indicated that the formation rate of adsorbate and adsorbent interaction (chemisorption) on the external surface of adsorbent is the rate of limiting step. The activation energy for the adsorption of RR120 onto OMMT is -14.5216 kJ/mol. Gibbs free energy change ($\Delta G°$), standard

enthalpy ($\Delta H°$), and standard entropy ($\Delta S°$) are -7.06 to -4.28kJ/mol, 33.2469kJ/mol, and 85.50 J/K/mol, respectively. The results indicate that the adsorption is spontaneouse, endothermic, and the randomness increases at the interface during the adsorption.Desorption experiments were carried out in 0.1 M NaOH solution, 100 mL, 0.1 g OMMT, 200 rpm, 35°C, and 24 h desorption time. The % desorption is 38.86, 89.20, and 87.84 % for the first, second, and third cycle, respectively. These results in low reutilization of OMMT for RR120.However, the study shows that the OMMT is useful as a promising adsorbent for the remove of RR120 dye in wastewater treatment.

5.2.1 Fixed bed adsorption study

In order to investigate the feasible of the adsorbent in more practical way, fixed bed column is used for testing the effect of parameters such as inlet dye concentration, flow rate, and bed height. The effect of adsorbate RR120 concentration on the column performance was studied by varying the inlet concentration of 100, 150, and 200 mg/L, bed height of 60 mm and feed flow rate of 1.4 mL/min were used. The breakpoint time was found to decrease with increasing adsorbate inlet concentration which is 111.28, 76.68, 65.23 min for 100, 150, 200 mg/L, respectively. To investigate the effect of flow rate on RR120 adsorption, the influent RR120 concentration the bed height were held constant at 100 mg/L, and 60 mm, and the flow rate was 1.4, 3.5 and 7.0 mL/min, respectively. The breakpoint time was found to decrease with increasing adsorbate flow rate which is 111.28, 31.58, 22.65 min for 1.4, 3.5, 7 mL/min, respectively. To investigate the effect of bed height,the experiments are performedat different bed height (40 to 80 mm) and the same influent concentration (C_0 =100 mg/L) and flow rate (v =1.4 mL/min). The results showed that increasing of the column bed height, the breakpoint time was increasedwhich is 64.65, 111.28, 130.72 min for 1.4, 3.5, 7 mL/min, respectively. Moreover the experimental data are fitted with the dynamic adsorption models such as Thomas, Adams–Bohart, and Yoon–Nelson models. The Thomas rate constant (k_T) is increase with flow rate but decrease with bed height. For maximum solid-phase concentration (q_0) were obtained using linear regression analysis and the results which could describe the experimental data at lower flow rate, 1.4 mL/min, but failed in higher flow rate and high bed height, 80 mm. For Adams–Bohart model, the maximum adsorption capacity, N, and kinetic constant, K, were calculated. Kvalues are increased with flow rate increase. Due to low R^2, another values

of N and K effected by experiment parameter are not increased or decreased as a predictable tend. In case of Yoon–Nelson model, k_{YN} (L/min), the rate velocity constant, and τ (min), the time in required for 50% adsorbate breakthrough were determined. k_{YN} values were increased with flow rate increase, but decreased with bed height. T values were increased with bed height increase, but decreased with flow rate. The study shows that the optimum condition for fixed bed column are 100 mg/L inlet dye concentration, 1.4 mL/min floe rate, and 80 mm bed height.

5.2 Recommendations

This study was attempt to removal reactive dye from waste water so different dyes may result in different way due to molecular sizes and functional groups of the dyes which was recommended for future study. Using real waste water or tap water might be useful due to more realistic scenario than synthesis waste water.

REFERENCES

REFERENCE

Absalan, G., et al. "Removal of reactive red-120 and 4-(2-pyridylazo) resorcinol from aqueous samples by Fe3O4 magnetic nanoparticles using ionic liquid as modifier", **Journal of Hazardous Materials**. 192(2): 476-484; August, 2011.

Ahmad, A. A., and Hameed, B. H. "Fixed-bed adsorption of reactive azo dye onto granular activated carbon prepared from waste", **Journal of Hazardous Materials**. 175(1–3): 298-303; March, 2010.

Akçay, M., and Akçay, G. "The removal of phenolic compounds from aqueous solutions by organophilic bentonite", **Journal of Hazardous Materials**. 113(1–3): 189-193; September, 2004.

Aksu, Z. "Application of biosorption for the removal of organic pollutants: a review", **Process Biochemistry**. 40(3–4): 997-1026; March, 2005.

Al-Anber, M. A. "Thermodynamics approach in the adsorption of heavy metals", **Juan Carlos Moreno-Pirajan, Thermodynamics-Interaction Studies-Solids, Liquids and Gases Book, first ed., In-Tech, Rijeka**. 737-764, 2011.

Al-Degs, Y. S., et al. "Effect of solution pH, ionic strength, and temperature on adsorption behavior of reactive dyes on activated carbon", **Dyes and Pigments**. 77(1): 16-23; January, 2008.

Asok Adak, M. B. a. A. P. "Adsolubilization of Organic Compounds in Surfactant-Modified Alumina", **Surface Science & Technology, India**. 21(1-2): 97-112; January, 2005.

Ausar, S. F., et al. "Growth of milk fermentative bacteria in the presence of chitosan for potential use in cheese making", **International Dairy Journal**. 12(11): 899-906; November, 2002.

Bayramoğlu, G., and Yakup Arıca, M. "Biosorption of benzidine based textile dyes "Direct Blue 1 and Direct Red 128" using native and heat-treated biomass of Trametes versicolor", **Journal of Hazardous Materials**. 143(1): 135-143; May, 2007.

REFERENCES (CONTINUE)

Bhattacharyya, K. G., and Sarma, A. "Adsorption characteristics of the dye, Brilliant Green, on Neem leaf powder", **Dyes and Pigments**. 57(3): 211-222; June, 2003.

Bohart, G., and Adams, E. "Some aspects of the behavior of charcoal with respect to chlorine", **Journal of the Chemical Society**. 42(7); 523-544; March, 1920.

Brown, G., et al. "Crystal structures of clay minerals and their X-ray identification", **Mineralogical Society, London**. 361-410, 1980.

Çelekli, A., et al. "Kinetic and equilibrium studies on the adsorption of reactive red 120 from aqueous solution on Spirogyra majuscula", **Chemical Engineering Journal**. 152(1): 139-145; October, 2009.

Darder, M., et al. "Chitosan–clay nanocomposites: application as electrochemical sensors", **Applied Clay Science**. 28(1): 199-208; January, 2005.

Dolphen, R., et al. "Adsorption of Reactive Red 141 from wastewater onto modified chitin", **Journal of Hazardous Materials**. 145(1): 250-255; June, 2007.

Fathy, N. A., and El-Sherif, I. Y. "Equilibrium removal of Pb (II) Ions from aqueous solution onto oxidized-KOH-activated carbons", **Carbon Lett**. 12(1): 1-7; March 2011.

Guo, B., et al. "Macroporous Poly(calcium acrylate−divinylbenzene) Bead A Selective Orthophosphite Sorbent", **Industrial & Engineering Chemistry Research**. 42(22): 5559-5567; October, 2003.

Gupta, V. K., and Suhas. "Application of low-cost adsorbents for dye removal – A review", **Journal of Environmental Management**. 90(8): 2313-2342; June, 2009.

Ho, Y. S., and McKay, G. "The kinetics of sorption of basic dyes from aqueous solution by sphagnum moss peat", **The Canadian Journal of Chemical Engineering**. 76(4): 822-827; August, 1998.

Hu, Z., et al. "Effects of surfactant concentration on alkyl chain arrangements in dry and swollen organic montmorillonite", **Applied Clay Science**. 75: 134-140; May, 2013.

REFERENCES (CONTINUE)

Huang, F.-C., et al. "Effects of exchange titanium cations on the pore structure and adsorption characteristics of montmorillonite", **Journal of Colloid and Interface Science**. 256(2): 360-366; December, 2002.

Huang, Y.-H., et al. "Thermodynamics and kinetics of adsorption of Cu(II) onto waste iron oxide", **Journal of Hazardous Materials**. 144(1–2): 406-411; June, 2007.

Jocic, D., et al. **Biopolymer-based Stimuli-Responsive Polymeric Systems for Functional Finishing of Textiles**. Netherlands: INTECH Open Access Publisher, 2010.

Kim, S.-K. **Chitin and Chitosan Derivatives: Advances in Drug Discovery and Developments**. U.S.A: CRC Press, 2013.

Kitiyanan, B., et al. "Absolubilization of Styrene and Isoprene in Cetyltrimethylammonium Bromide Admicelle on Precipitated Silica", **Langmuir**. 12(9): 2162-2168; January, 1996.

Langmuir, I. "The adsorption of gases on plane surfaces of glass, mica and platinum", **Journal of the American Chemical society**. 40(9): 1361-1403; September, 1918.

Lertsutthiwong, P., et al. "Influence of chitosan characteristics on the properties of biopolymeric chitosan–montmorillonite", **Progress in Natural Science: Materials International**. 22(5): 502-508; October, 2012.

Mobasherpour, I., et al. "Research on the Batch and Fixed-Bed Column Performance of Red Mud Adsorbents for Lead Removal", **soil and water**. 2(1): 83-96; January, 2014.

Monvisade, P., and Siriphannon, P. "Chitosan intercalated montmorillonite: Preparation, characterization and cationic dye adsorption", **Applied Clay Science**. 42(3–4): 427-431; January, 2009.

Murray, H. H. **Applied Clay Mineralogy: Occurrences, Processing and Applications of Kaolins, Bentonites, Palygorskitesepiolite, and Common Clays**. U.S.A.: Elsevier Science, 2006.

REFERENCES (CONTINUE)

Namasivayam, C., and Kavitha, D. "Removal of Congo Red from water by adsorption onto activated carbon prepared from coir pith, an agricultural solid waste", **Dyes and Pigments**. 54(1): 47-58; July, 2002.

Namasivayam, C., et al. "Removal of dyes from aqueous solutions by cellulosic waste orange peel", **Bioresource Technology**. 57(1): 37-43; July, 1996.

Pereira, F., et al. "Chitosan-montmorillonite biocomposite as an adsorbent for copper (II) cations from aqueous solutions", **International journal of biological macromolecules**. 61(4): 471-478; October, 2013.

Pérez-Marín, A. B., et al. "Removal of cadmium from aqueous solutions by adsorption onto orange waste", **Journal of Hazardous Materials**. 139(1): 122-131; January, 2007.

Piccin, J. S., et al. "Adsorption isotherms and thermochemical data of FD&C Red 40 binding by Chitosan", **Brazilian Journal of Chemical Engineering**. 28: 295-304; June, 2011.

Ralph, E. G., and Necip, G. **Developments in Sedimentology**. U.S.A.: Elsevier, 1978.

Ross, C. S., and Shannon, E. V. "THE MINERALS OF BENTONITE AND RELATED CLAYS AND THEIR PHYSICAL PROPERTIES1", **Journal of the American Ceramic Society**. 9(2): 77-96; February, 1926.

Tabak, A., et al. "Adsorption of Reactive Red 120 from aqueous solutions by cetylpyridinium-bentonite", **Journal of chemical technology and biotechnology**. 85(9): 1199-1207; May, 2010.

Thomas, W. J., and Crittenden, B. **Adsorption Technology & Design**. Oxford: Butterworth-Heinemann, 1998.

Umpuch, C., and Sakaew, S. "Removal of methyl orange from aqueous solutions by adsorption using chitosan intercalated montmorillonite", **Songklanakarin J Sci Technol**. 35(4): 451-459; July, 2013.

Vijayaraghavan, K., and Yun, Y.-S. "Bacterial biosorbents and biosorption", **Biotechnology Advances**. 26(3): 266-291; May, 2008.

REFERENCES (CONTINUE)

Volesky, B. "Biosorption process simulation tools", **Hydrometallurgy**. 71(1–2): 179-190; October, 2003.

Wang, C.-C., et al. "Adsorption of basic dyes onto montmorillonite", **Journal of Colloid and Interface Science**. 273(1): 80-86; May, 2004.

Wang, L., and Wang, A. "Adsorption characteristics of Congo Red onto the chitosan/montmorillonite nanocomposite", **Journal of Hazardous Materials**. 147(3): 979-985; August, 2007.

Wang, Q., et al. "Removal of a Cationic Dye by Adsorption/Photodegradation Using Electrospun PAN/O-MMT Composite Nanofibrous Membranes Coated with", **International Journal of Photoenergy**. 2012(1): 1-8; January, 2012.

Woodmansey, A. " Chitosan Treatment of Sediment Laden Water - Washington State I-90 Issaquah Project", **Federal Highway Administration. U.S. Department of Transportation**. 2002.

Yan, L.-G., et al. "Adsorption of benzoic acid by CTAB exchanged montmorillonite", **Applied Clay Science**. 37(3): 226-230; September, 2007.

Yoon, Y. H., and NELSON, J. H. "Application of gas adsorption kinetics I. A theoretical model for respirator cartridge service life", **The American Industrial Hygiene Association Journal**. 45(8): 509-516; August, 1984.

Yu, W. H., et al. "Clean production of CTAB-montmorillonite: formation mechanism and swelling behavior in xylene", **Applied Clay Science**. 97-98: 222-234; August, 2014.

Yuh-Shan, H. "Citation review of Lagergren kinetic rate equation on adsorption reactions", **Scientometrics**. 59(1): 171-177; January, 2004.

Zhou, Q., et al. "TEM, XRD, and thermal stability of adsorbed paranitrophenol on DDOAB organoclay", **Journal of Colloid and Interface Science**. 311(1): 24-37; July, 2007.

Zhu, L., and Ma, J. "Simultaneous removal of acid dye and cationic surfactant from water by bentonite in one-step process", **Chemical Engineering Journal**. 139(3): 503-509; June, 2008.

APPENDICES

APPENDIX A

Data of effect of some parameters onto OMMT in batch system

Table A.1 Effect of initial dye concentration and temperature on adsorption of RR120 onto OMMT. Adsorbent dose: 0.1 g/ 100 mL.

Temperature (°C)	C_0 (mg/L)	C_e (mg/L)			C_{avg} (mg/L)	STDEV	qe (mg/g)
		1	2	3			
35	50	4.8694	6.6401	5.7548	5.7551	0.8853	42.0567
	100	17.7070	14.1656	14.6082	15.4946	1.9296	89.8685
	150	26.5604	44.2674	48.6941	39.8432	11.7121	115.9879
	200	69.9425	72.1558	71.7132	71.2750	1.1712	131.9251
	250	97.3882	128.3754	106.2417	110.6754	15.9608	141.6646
	300	153.6078	149.6237	150.9517	151.4040	2.02859	148.7478
45	50	1.3055	3.4813	1.7406	2.1755	1.1513	45.2511
	100	7.8329	11.7494	9.1384	9.5724	1.9942	88.7618
	150	4.3516	23.0635	11.7494	13.0532	9.4240	133.1427
	200	30.0261	33.9426	32.6371	32.1979	1.9942	164.9055
	250	68.7554	67.8851	69.6258	68.7469	0.8703	177.5236
	300	95.7354	117.4935	126.1967	113.1278	15.6900	185.3555
55	50	0.4545	1.3636	2.2727	1.3053	0.9091	47.2727
	100	4.0909	5.4545	5.9091	4.9312	0.9462	97.2727
	150	8.6364	11.8182	9.5455	9.5724	1.6389	141.8182
	200	19.5455	24.5455	23.1818	21.4653	2.5847	181.3636
	250	40.4546	41.8182	47.2727	41.3352	3.6078	210.0000
	300	78.1818	73.6364	76.8182	72.9529	2.3325	230.4545
65	50	1.0455	1.0000	0.9091	0.9848	0.0694	48.1364
	100	2.6364	2.3182	2.5455	2.5000	0.1639	96.5910
	150	3.6364	6.8182	4.5455	5.0000	1.6389	142.7273
	200	9.5455	10.9091	13.6364	11.3636	2.0830	184.5455
	250	25.0000	26.8182	28.6364	26.8182	1.8182	219.0909
	300	54.0910	52.2727	50.4546	52.2727	1.8182	245.9091

CURRICULUM VITAE

NAME	Mr. Pariwat Namduang
DATE OF BIRTH	10 August 1989
EDUCATION	B.Eng (Chemical Engineering), Sirindhorn International Institute of Technology, Thammasat University, Pathumthani, Thailand
ACADEMIC CONFERENCE	Pariwat Namduang1 and Chakkrit Umpuch. "Removal of Reactive Red 120 by using Organo-montmorillonite", 4th International Conference on Environmental Engineering, Science and Management. Environmental Engineering Association of Thailand, 2015.

Table A.2 Effect of contact time and temperature on adsorption of RR120 onto OMMT. Adsorbent dose: 0.1 g/ 100 mL at 35°C.

Time	C_t at 35(°C) (mg/L)					
(min)	1	2	3	AVG	STDEV	q_t (mg/g)
0	301.3889	302.3148	306.0185	303.2407	2.44977	0
5	233.3333	236.5741	235.6481	235.1852	1.6692	68.0556
15	215.7407	217.5926	217.1296	216.8210	0.9637	86.5741
30	192.5926	195.8333	194.9074	194.4444	1.6692	108.7963
60	177.7778	175.463	176.8519	176.6975	1.1651	127.3148
90	168.5185	165.2778	167.1296	166.9753	1.6259	136.5741
120	163.4259	160.1852	159.2593	160.9568	2.1879	142.1296
150	154.1667	155.5556	157.4074	155.7099	1.6259	147.6852
180	153.2407	154.6296	151.3889	153.0864	1.6259	150.4630
240	150.463	146.7593	148.1481	148.4568	1.8710	155.0926
360	148.6111	145.3704	146.2963	146.7593	1.6692	156.4815
480	148.1481	145.3704	145.8333	146.4506	1.4882	156.4815
600	148.6111	145.8333	146.2963	146.9136	1.4882	156.4815

Table A.3 Effect of contact time and temperature on adsorption of RR120 onto OMMT. Adsorbent dose: 0.1 g/ 100 mL at 45°C.

Time	C_t at 45(°C) (mg/L)					
(min)	1	2	3	AVG	STDEV	q_t (mg/g)
0	304.6296	302.7778	302.3148	303.2407	1.2249	0.0000
5	217.5926	215.2778	210.6481	214.5062	3.5359	90.2778
15	187.5000	192.1296	189.8148	189.8148	2.3148	113.4259
30	174.0741	177.7778	175.9259	175.9259	1.8519	127.3148
60	153.7037	162.0370	157.4074	157.7160	4.1752	145.8333
90	147.2222	150.4630	148.1481	148.6111	1.6692	154.6296
120	139.8148	142.5926	141.6667	141.3580	1.4144	162.0370
150	133.7963	137.0370	136.1111	135.6481	1.6692	167.5926
180	129.1667	132.4074	130.5556	130.7099	1.6259	172.6852
240	124.0741	126.8519	125.0000	125.3086	1.4144	178.2407
360	119.9074	121.2963	121.2963	120.8333	0.8019	182.4074
480	119.4444	121.7593	120.8333	120.6790	1.1651	182.4074
600	119.9074	121.2963	121.2963	120.8333	0.8019	182.4074

Table A.4 Effect of contact time and temperature on adsorption of RR120 onto OMMT. Adsorbent dose: 0.1 g/ 100 mL at 55°C.

Time (min)	C_t at 55(°C) (mg/L)					
	1	2	3	AVG	STDEV	q_t (mg/g)
0	301.8519	305.0926	303.2407	303.3951	1.6259	0.0000
5	178.7037	181.9444	180.5556	180.4012	1.6259	122.6852
15	161.5741	163.4259	162.037	162.3457	0.9637	141.2037
30	144.9074	146.7593	145.8333	145.8333	0.9259	157.4074
60	126.8519	130.5556	128.7037	128.7037	1.8519	174.5370
90	113.8889	117.1296	115.7407	115.5864	1.6259	187.5000
120	103.7037	105.5556	104.6296	104.6296	0.9259	198.6111
150	96.2963	99.0741	97.22222	97.5309	1.4144	206.0185
180	89.3519	91.6667	90.74074	90.5864	1.1651	212.5000
240	124.0741	126.8519	82.87037	111.2654	24.6300	220.3704
360	77.3148	79.1667	78.24074	78.2407	0.9259	225.0000
480	76.8519	79.6296	77.77778	78.0864	1.4144	225.0000
600	77.3148	79.6296	78.24074	78.3951	1.16510	225.0000

Table A.5 Effect of contact time and temperature on adsorption of RR120 onto OMMT. Adsorbent dose: 0.1 g/ 100 mL at 65°C.

Time (min)	C_t at 65(°C) (mg/L)					
	1	2	3	AVG	STDEV	q_t (mg/g)
0	305.0926	301.8519	302.3148	303.0864	1.7527	0.0000
5	143.5185	157.4074	162.0370	154.3210	9.6373	150.4630
15	152.7778	136.5741	133.3333	140.8951	10.4175	164.3519
30	129.6296	120.8333	131.0185	127.1605	5.5233	175.9259
60	112.9630	107.4074	110.1852	110.1852	2.7778	193.0556
90	96.7593	100.0000	97.6852	98.1482	1.6692	205.0926
120	85.6482	97.2222	78.7037	87.1914	9.3552	215.2778
150	75.4630	78.2407	81.0185	78.2407	2.7778	224.5370
180	74.0741	68.5185	71.7593	71.4506	2.7906	231.9444
240	64.3519	62.0370	59.2593	61.8827	2.5498	240.7407
360	60.1852	64.8148	46.2963	57.0988	9.6373	247.6852
480	51.8519	53.2407	53.7037	52.9321	0.9637	250.4630
600	52.3148	52.7778	53.2407	52.7778	0.4630	250.4630

Table A.6 Effect of initial pH on adsorption of RR120 onto OMMT. Adsorbent dose: 0.1 g/ 100 mL, initial dye concentration: 300 mg/L, temperature: 35 °C.

pH	Ce (mg/L)	q_e (mg/g)
2	127.4863	163.6002
4	134.448	155.7683
6	141.4097	148.8066
8	144.8906	145.3257
10	147.9364	144.4555

Table A.7 Desorption and regeneration data. Adsorbent/desorption dose: 0.1 g/ 100 mL, initial dye concentration: 300 mg/L or NaOH concentration: 0.1 M, temperature: 35 °C.

Cycle	$C_{e\ ad}$ (mg/L)	$q_{e\ ad}$ (mg/g)	$q_{e\ de}$ (mg/g)
1	134.7826	152.1739	59.1304
2	246.5217	41.3044	36.8450
3	266.9565	32.1740	28.2610

APPENDIX B

Data of effect of some parameters onto OMMT in fixed bed column

Table B.1 Fixed bed dynamic adsorption data for 60 cm bed height, 1.4 mL/min flow rate and different inlet dye concentrations.

Time (min)	C_0 = 100 mg/L C_t (mg/L)	Time (min)	C_0 = 150 mg/L C_t (mg/L)	Time (min)	C_0 = 200 mg/L C_t (mg/L)
0	0.0000	0	0.0000	0	0.4630
15	0.0000	15	1.8519	15	0.9259
26	0.0000	25	2.3148	25	0.9259
30	0.0000	30	2.3148	30	1.3889
34	0.0000	35	3.2407	35	1.8519
39	0.9259	40	6.9444	40	23.1482
49	1.3889	45	12.0370	45	59.7222
54	2.3148	50	21.7593	50	85.6482
59	6.0185	55	37.5000	55	104.1667
64	12.9630	60	48.6111	60	116.2037
69	18.5185	65	59.2593	65	129.1667
74	25.0000	70	68.9815	70	134.2593
79	32.4074	75	81.4815	75	143.9815
84	39.3519	80	93.0556	80	148.6111
89	45.8333	85	100.0000	85	150.4630
94	50.9259	90	105.0926	90	155.0926
99	57.8704	95	109.7222	95	161.5741
104	61.5741	100	112.5000	105	168.5185
109	64.8148	105	118.9815	110	171.7593
114	66.6667	110	118.9815	115	174.0741
119	68.5185	115	124.0741	120	178.2407
124	71.2963	120	126.3889	125	179.1667
129	73.6111	125	129.1667	130	177.7778

Table B.1 Fixed bed dynamic adsorption data for 60 cm bed height, 1.4 mL/min flow rate and different inlet dye concentrations. (Continue)

Time (min)	C_0 = 100 mg/L C_t (mg/L)	Time (min)	C_0 = 150 mg/L C_t (mg/L)	Time (min)	C_0 = 200 mg/L C_t (mg/L)
134	76.3889	130	131.0185	140	181.9444
139	77.3148	135	131.4815	150	186.5741
144	79.1667	140	134.2593	160	189.3519
149	81.0185	145	133.7963	170	189.3519
154	82.4074	150	136.5741	200	194.9074
159	84.7222	155	137.0370	210	192.5926
164	85.1852	160	137.5000		
169	85.6482	165	137.5000		
174	87.0370	170	138.8889		
179	87.5000	175	138.4259		
184	88.8889	185	139.3519		
189	89.8148	200	140.7407		
194	91.2037	220	139.8148		
199	91.6667	240	145.8333		
204	92.1296				
209	93.5185				
219	93.9815				
229	94.9074				
239	96.2963				
249	97.2222				
269	97.2222				
289	97.2222				

Table B.2 Fixed bed dynamic adsorption data for 60 cm bed height, 100 mg/L inlet dye concentration and different flow rates.

Time (min)	v = 1.4 mL/min C_t (mg/L)	Time (min)	v = 3.5 mL/min C_t (mg/L)	Time (min)	v = 7.0 mL/min C_t (mg/L)
0	0.0000	0	0.0000	0	0.0000
15	0.0000	5	2.3150	5	3.7037
26	0.0000	10	10.6480	10	3.2407
30	0.0000	15	31.4810	15	6.9444
34	0.0000	20	57.4070	20	14.8148
39	0.9259	25	68.0560	25	27.7778
49	1.3889	30	77.7780	30	49.5370
54	2.3148	35	82.4070	35	58.7963
59	6.0185	40	84.7220	40	63.4259
64	12.9630	45	87.5000	45	69.9074
69	18.5185	55	93.0560	55	77.7778
74	25.0000	65	97.2220	65	82.4074
79	32.4074	75	100.0000	75	85.6482
84	39.3519	85	102.7780	85	89.3519
89	45.8333	100	102.7780	100	91.6667
94	50.9259	115	102.7780	115	94.4444
99	57.8704				
104	61.5741				
109	64.8148				
114	66.6667				
119	68.5185				
124	71.2963				
129	73.6111				

Table B.2 Fixed bed dynamic adsorption data for 60 cm bed height, 100 mg/L inlet dye concentration and different flow rates. (Continue)

Time (min)	v = 1.4 mL/min C_t (mg/L)	Time (min)	v = 3.5 mL/min C_t (mg/L)	Time (min)	v = 7.0 mL/min C_t (mg/L)
139	77.3148				
144	79.1667				
149	81.0185				
154	82.4074				
159	84.7222				
164	85.1852				
169	85.6482				
174	87.0370				
179	87.5000				
184	88.8889				
189	89.8148				
194	91.2037				
199	91.6667				
204	92.1296				
209	93.5185				
219	93.9815				
229	94.9074				
239	96.2963				
249	97.2222				
269	97.2222				
289	97.2222				

Table B.3 Fixed bed dynamic adsorption data for 100 mg/L inlet dye concentration, 1.4 mL/min and different bed heights.

Time (min)	Z = 4 cm C_t (mg/L)	Time (min)	Z = 6 cm C_t (mg/L)	Time (min)	Z = 8 cm C_t (mg/L)
0	1.3890	0	0.0000	0	0.0000
5	2.3150	15	0.0000	5	0.4630
10	2.3150	26	0.0000	10	0.4630
20	2.3150	30	0.0000	15	0.0000
30	2.3150	34	0.0000	20	0.9259
40	2.3150	39	0.9259	25	1.8519
50	6.9440	49	1.3889	30	1.8519
55	14.3520	54	2.3148	40	1.8519
60	29.6300	59	6.0186	50	1.3889
65	40.7410	64	12.9630	60	1.3889
70	48.6110	69	18.5185	90	3.7037
75	58.3330	74	25.0000	105	17.1296
80	62.9630	79	32.4074	110	25.9259
85	68.5190	84	39.3519	115	31.4815
90	71.7590	89	45.8333	120	35.6482
95	75.4630	94	50.9259	125	42.1296
100	78.2410	99	57.8704	130	47.2222
105	81.0190	104	61.5741	135	53.2407
110	84.2590	109	64.8148	140	55.5556
115	84.7220	114	66.6667	145	60.6482
120	87.0370	119	68.5185	150	64.8148
140	92.1300	124	71.2963	155	67.1296

Table B.3 Fixed bed dynamic adsorption data for 100 mg/L inlet dye concentration, 1.4 mL/min and different bed heights. (Continue)

Time (min)	Z = 4 cm C_t (mg/L)	Time (min)	Z = 6 cm C_t (mg/L)	Time (min)	Z = 8 cm C_t (mg/L)
160	95.3700	134	76.3889	165	71.2963
170	98.1480	139	77.3148	170	72.6852
180	98.6110	144	79.1667	175	73.6111
195	98.6110	149	81.0185	180	75.0000
210	98.6110	154	82.4074	190	77.3148
225	98.6110	159	84.7222	205	82.4074
240	98.6110	164	85.1852	220	85.6482
		169	85.6482	235	87.9630
		174	87.0370	250	90.2778
		179	87.5000	265	91.6667
		184	88.8889	280	94.4444
		189	89.8148	295	95.8333
		194	91.2037	310	96.7593
		199	91.6667	330	98.6111
		204	92.1296	350	100.4630
		209	93.5185	370	102.3148
		219	93.9815	390	102.3148
		229	94.9074	410	102.3148
		239	96.2963	420	102.3148
		249	97.2222		
		269	97.2222		
		289	97.2222		

APPENDIX C

Calculations of some valuables

1 Surfactant weight to %CEC Montmorillonite calculation

$W_{surfactant}(g) = 0.8$

$$\left(\frac{meq}{g}\right) \times W_{Clay}(g) \times MW_{surfactant} \left(\frac{g}{mol}\right) \times \left(\frac{mole}{eq}\right) \times \left(\frac{eq}{1000\ meq}\right) \times \%CEC$$

where $W_{surfactant}$ is surfactant weight (g)

W_{Clay} is montmorillonite weight (g)

$MW_{surfactant}$ is surfactant molecular weight (g/mol)

%CEC is mole percent of surfactant to montmorillonite CEC

2 d-spacing calculation

Bragg's law

$$2d\sin\theta = n\lambda$$

where n = 1 for XRD analysis,

$$\lambda = 2d\sin\theta$$

$$d = \frac{\lambda}{2\sin\theta}$$

where d is d-spacing or inter layer space of MMT

n is a positive integer

λ is the wavelength of incident wave. For this work, it equal to the wavelength of CuKα = 1.54 Å.

θ is the scattering angle (see figure below).

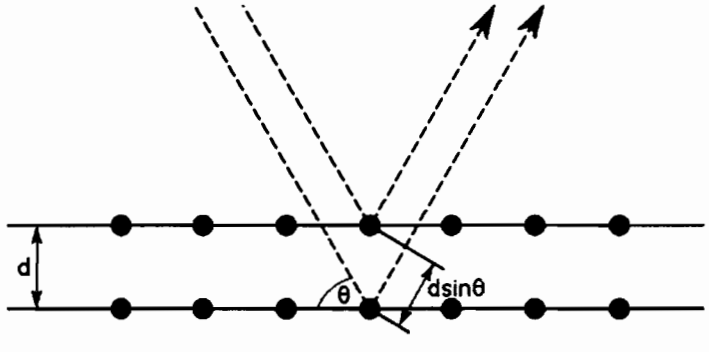

APPENDIX D

Conference article

Removal of Reactive Red 120 by using Organo-montmorillonite

Pariwat Namduang[1] and Chakkrit Umpuch[2]

[1] Graduate student, Environment Engineering Program, Department of Chemical Engineering, Faculty of Engineering, Ubon Ratchathani University, Ubon Ratchathani, Thailand ; [2] Assistance Professor, Department of Chemical Engineering, Faculty of Engineering, Ubon Ratchathani University, Ubon Ratchathani 34190, Thailand.*

**Phone : + 66 45 35 33 59, Fax : +66 45 35 3333, E-mail : Chakkrit.u@ubu.ac.th*

ABSTRACT

In this present work, batch adsorption of reactive red 120 (RR120) onto organo-montmorillonite (OMMT) was investigated. The effects of operation parameters such as contact time, initial dye concentration, initial pH and temperature were studied. The result revealed that adsorption of RR120 was initially rapid and reached equilibrium at 150 min. The adsorption capacity increased with the initial dye concentration and temperature but decreased slightly with initial pH. The highest adsorption capacity of 224.96 mg/g was obtained at 300 mg/l dye solution and 55°C. Kinetics data were best described by the pseudo-second order model. The equilibrium data were better fitted by Langmuir isotherm which provides monolayer adsorption capacity (q_m) of 142.86 mg/g. The adsorption of RR120 increased with operating temperatures indicating an endothermic process. These results suggested that the OMMT can be used as an effective adsorbent for removing RR120 from aqueous solutions.

Keywords : Intercalation; Cationic surfactant; Adsorption; Reactive Red 120; Organo-Montmorillonite

INTRODUCTION

Reactive dyes are most commonly used in textile industry because of their good fastness properties and ease applications. However, by using conventional dyeing method, 10-50 % of the dye left into water body. The release of colored water into the natural stream causes harmful to the aquatic lives. For example, reduction of photosynthetic activity due to reducing light penetration and also being toxic due to the presence of aromatics, metals, chlorides, etc., in the dyes [1].

Among the several separation methods for dyes removal from wastewater, adsorption has been found to be an effective and economical method. Activated carbon is a well-known natural materials based adsorbent which is widely used in many applications. However, the preparation of activated carbon consumes a lot of heat and it has low reutilization. This results in high cost of activated carbon. Hence, development of new low cost adsorbents becomes more interested. These low-cost alternative adsorbents could be classified into (a) natural materials such as wood, peat, coal, clay etc. (b) industrial/agricultural wastes or by-products such as slag, sludge, fly ash, bagasse fly ash, red mud etc. and (c) synthesized products [2].

Recently, natural clay such as montmorillonite (MMT) has been accepted as one of the low-cost adsorbents for the removal of dyes from wastewater. In Thailand, MMT is very cheap and is commercially produced. MMT, a member of the smectite group, is a 2:1 clay, meaning that it has 2 tetrahedral sheets sandwiching a central octahedral sheet. MMT swells with the addition of water due to water penetrating the interlayer molecular spaces and concomitant adsorption. Expandable layered silicate is an important characteristic to enhance adsorption. MMT has high cation exchange capacity (CEC) meaning that it has highly negative charge on the surface providing good property for cationic surfactant modification. From our preliminary study, the adsorption capacity of MMT to RR120 is very low (<5%) due to the repulsive interaction between the negatively fixed charge on the MMT surface and the RR120 anions. After the modification, organo-MMT(OMMT) has much higher the RR120 uptake than that of precursor. Hence, the surface property of MMT was altered from negatively charge to positively charge and/or hydrophobic and only the OMMT was used in this study. Several studies have been reported that the organo-clays were successfully in dyes removal such as cetyltrimethylammonium modified montmorillonite which had high adsorption capacity for congo red dye (229 mg/g) [3]. Also another cetyltrimethylammonium modified bentonite using for the adsorption of Orange II dye with very high adsorption capacity (868.1 mg/g) had been observed [4]. Hence, OMMT could have high affinity for reactive dye such as Reactive Red 120 (RR120) due to electrostatic interactions and hydrophobic interaction. The electrostatic interactions occur between dye anions and the positive charges on the external surface of admicelle coating on the MMT. The hydrophobic interaction takes place between hydrophobic part of the dye and long chain inside admicelle of surfactant coating on the MMT surface.

In the present study, MMT was modified by cetyltrimethylammonium bromide (CTAB) for adsorption of Reactive Red 120 (RR120). Batch adsorption tests were investigated to study adsorption isotherm, kinetic, effect of initial pH and influence of temperature.

METHODOLOGY

Materials

Sodium MMT was purchased from Thai Nippon Chemical Industry Cp., Ltd.. The cation exchange capacity (CEC) of the MMT providing from supplier is 80 meq/100 g. The RR120 ($C_{44}H_{24}C_{l2}N_{14}O_{20}S_6Na_6$) with the molecular weight of 1469.98 g/mole was purchased from Sigma–Aldrich Chemical Co., St. Louis, USA and its chemical structure was shown in Fig. 1. Other agents used were analytical grade and all solutions were prepared by dissolving in distilled water.

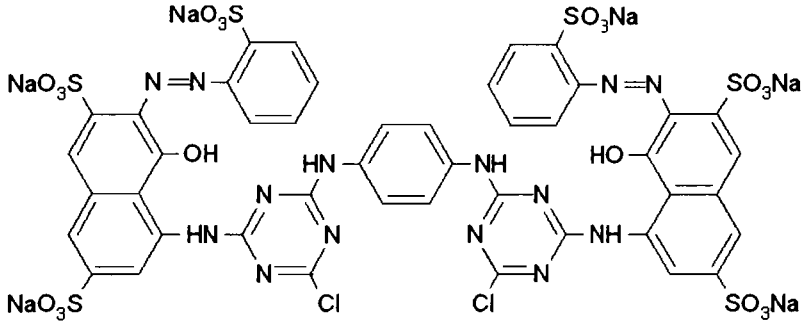

Fig. 1 Chemical structure of RR120 dye

Preparation of OMMT

The OMMT was prepared by reacting MMT with CTAB (Amresco, 99%). Amount of CTAB equivalent to 1.5 of the CEC of MMT was firstly dissolved in 100 mL distilled water and then 1.0 g MMT was added. The reaction mixtures were stirred at room temperature for 12 h. The mixture was washed several times by distilled water until the constant conductivity of supernatant obtained. The OMMT was dried in a hot air oven at 105°C until weight constant and ground to 200 mesh sieve to obtain the particle size below 74 μm. The schematic diagram of MMT and OMMT structure was shown in Fig. 2.

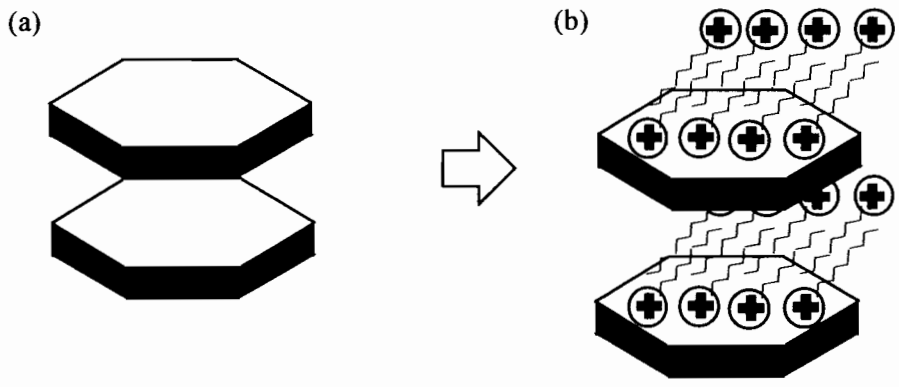

Fig. 2 Structures of (a) MMT and (b) organo MMT

Adsorption experiments

The adsorption of RR120 on the OMMT was investigated in batch system. A stock solution (1000 mg/l) of dye was prepared by dissolving in distilled water. The batch tests were divided into 4 parts. First, the effect of contact time on dye removal was carried out in the 100 ml dye solutions (200 mg/l) by adding 0.1 g OMMT and stirring for predetermined intervals of time. Second, the effect of initial concentrations of the dye, the initial concentration was studied. A series of 250 mL Erlenmeyer flasks were added with 100 mL dye solutions having initial concentration between 50 and 300 mg/l. 0.1 g of OMMT was then added and those flasks were stirred at 35°C and pH 5.9. Preliminary adsorption experiments indicated that 6 h was sufficient to attain equilibrium. To test the influence of temperature, the adsorption was performed with 0.1 g OMMT in 300 mg/l dye solution (100 ml) over the temperature range 25°C to 55°C. Finally, to study the effect of pH, the adsorption was performed with aqueous solutions over the pH range 2–10, adjusted by diluted HCl or NaOH solutions. The suspensions were centrifuged at 8,000 rpm and the equilibrium dye concentration in the supernatant was determined at 534 nm using a UV-VIS spectrophotometer.

The equilibrium amounts of adsorbed dye (q_e: mg/g) by OMMT samples were calculated by the following equation:

$$q_e = (C_0 - C_e)V/M \quad (1)$$

where C_0 and C_e represent the initial and equilibrium concentrations of adsorbate (mg/l), respectively, V is the volume of the dye solution (l) and M is the mass (g) of the adsorbent.

RESULTS AND DISCUSSIONS

Effect of contact time

The effect of contact time on the adsorption capacities of RR120 is shown in Fig. 3. The adsorption capacity increased rapidly at first 50 min and then kept slower increase until reached constant, which was assigned as equilibrium stage. Under experimental conditions mentioned earlier, the equilibrium time for the adsorption of RR120 on OMMT is 150 min. The results showing that at the initial stage, the large amount of dye molecules were adsorbed onto available active site at the external surface of admicelle which was rapidly and then slowly diffused into the internal spaces of the adsorbent. Finally, the available sites were fully occupied causing constant adsorption capacity at the equilibrium time.

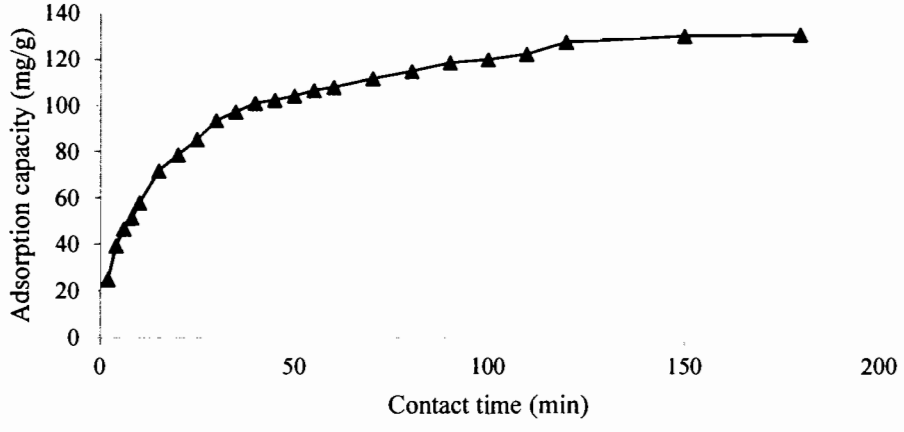

Fig. 3 Effect of contact time on the adsorption capacities of OMMT. Initial RR120 concentration: 50-300 mg/l, adsorbent concentration: 0.1 g/100ml, temperature: 35°C and pH 5.9.

Effect of initial dye concentration

In general, the removal of dye was dependent on the initial concentration of the dye [5, 6]. The relationship between the initial dye concentration and adsorption capacity of RR120 on OMMT is presented in Fig. 4. It can be seen that the RR120 uptake increases from 50 to 127.31 mg/g with increasing in initial dye concentrations from 50 to 150 mg/l and then increased slightly from 127.31 to 143.98 mg/g with increasing in initial concentrations from 150 to 300 mg/l. At low initial dye concentration, the adsorption capacity was low because the dye molecules could not diffuse deeply into the internal active sites of the adsorbent. At higher

initial dye concentrations, the dye molecules could diffuse deeper and the internal active sites could be more saturated. The saturation of the dye in the adsorbent may occur when the curve reach plateau. This result shown that initial dye concentrations provide an important driving force for RR120 uptake onto OMMT which in agreement with the study of adsorption of RR120 onto *S. majuscula* alga [7].

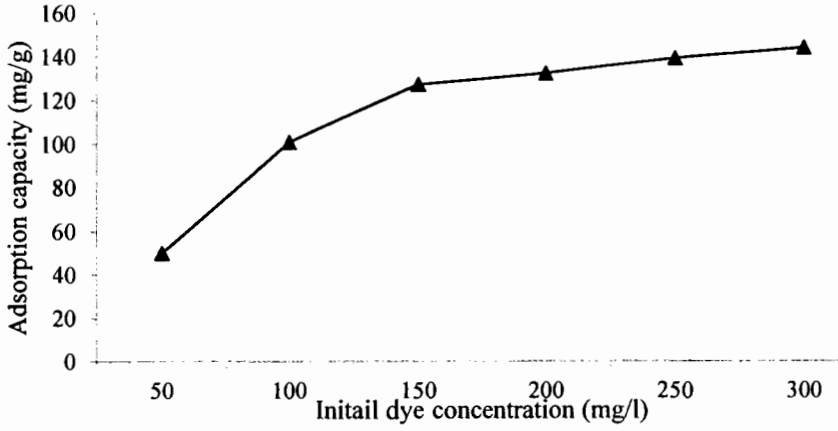

Fig. 4 Effect of initial dye concentration on the adsorption capacities of OMMT. Initial RR120 concentration: 50-300 mg/l, adsorbent concentration: 0.1 g/100ml, temperature: 35°C and pH 5.9.

Effect of temperature

The effect of temperature on adsorption was studied by varying temperatures in a range of 25 - 55°C, and the results are shown in Fig. 5. The amount of RR120 adsorbed on OMMT increases from 100.93 to 224.69 mg/g when increasing in operating temperatures from 25 to 55°C. It was found that the increase of temperature facilitated to the adsorption. It has been well documented that increase of temperature may cause swelling effect which denotes as an expansion of basal spacing inside the internal structure of adsorbent [8]. This swelling effect allows higher amount of dye molecules penetrating into the wider intercalated space. The similar trend has been observed for the adsorption of reactive dyes on activated carbon [9] and RR120 on Fe_3O_4 magnetic nanoparticles [10].

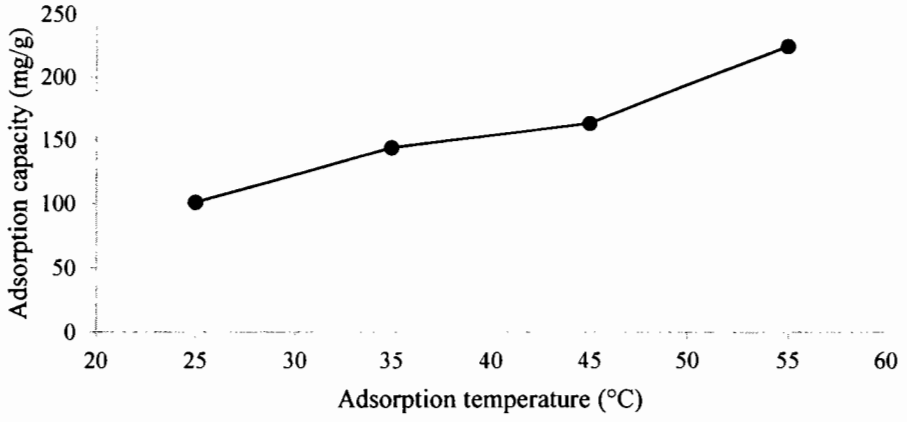

Fig. 5 Effect of adsorption temperature on the adsorption capacities of OMMT. Initial RR120 concentration: 300 mg/l, adsorbent concentration: 0.1 g/100ml. Temperature: 25-55°C and pH 5.9.

Effect of initial pH

The effect of the pH value of the original solution on the adsorption capacity of RR120 dye is shown in Fig. 6. It can be seen that the effect of the pH on the adsorption capacity is weak. When the pH value of the dye solution was raised from 2 to 10, the adsorption capacity reduced slightly from 163.60 to 144.46 mg/g. At low pH values, the net positive charge increase as a result of the penetration of cationic species into the interlayer which allowed dye molecules reach the external surface of OMMT more easily due to electrostatic attraction [11]. The slight decrease in adsorption may be attributed to the competition between anionic dye molecules and the excessive hydroxyl ions to the positive active site in alkaline pH values. The dyes also could be adsorbed into interior bilayer space by hydrophobic-hydrophobic interaction. The hydrophobicity of the dye and its conjugated base are different and has lower value at higher solution pH [12]. However, comparatively high adsorption capacity of the anionic dye on the adsorbent still occurred at pH 10 due to the fact that hydrophobic interactions between RR120 dye and OMMT taken place [3].

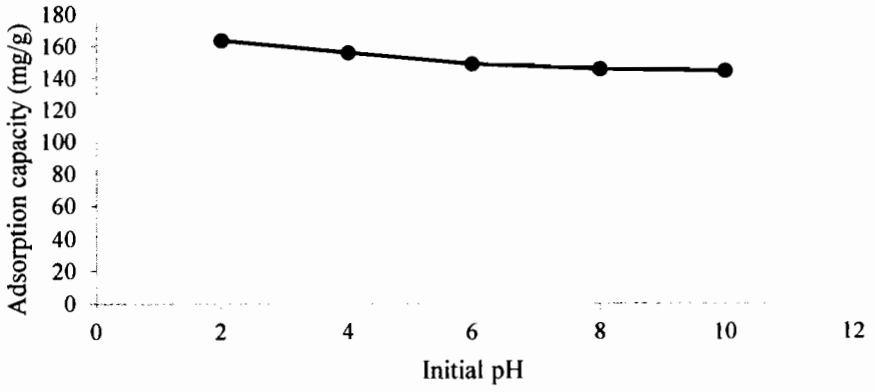

Fig. 6 Effect of initial pH on the adsorption capacities of OMMT. Initial RR120 concentration: 300 mg/l, adsorbent concentration: 0.1 g/100ml. Temperature: 35°C.

Adsorption isotherms

Fig. 7 shows adsorption isotherm which is a plot of adsorption capacity versus equilibrium dye concentration for the adsorption. It can be seen that adsorption capacity rises sharply at low equilibrium dye concentration and then increases gradually with increasing in equilibrium dye concentration.

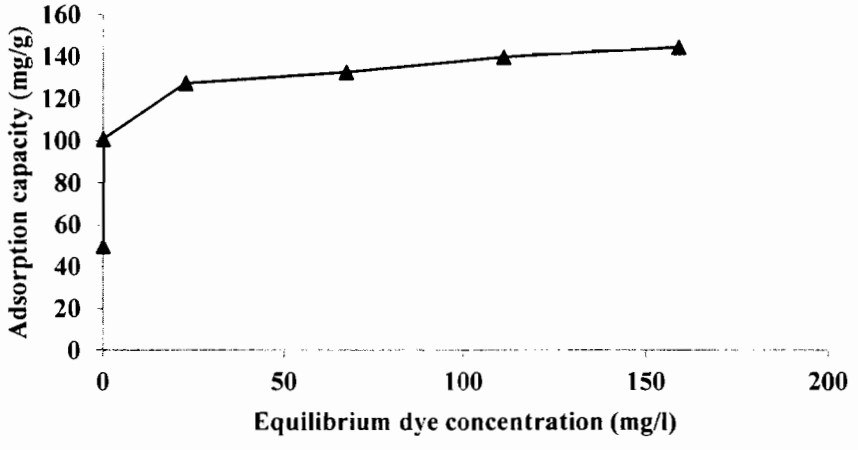

Fig. 7 Adsorption isotherm for the adsorption of RR120 on OMMT. Adsorbent concentration: 0.1 g/100ml, temperature: 35°C and pH 5.9.

The equilibrium data were interpreted using Langmuir and Freundlich models [13]. They assume monolayer coverage for Langmuir isotherm and multilayer adsorption for Freundlich isotherm and are presented by following equation, respectively:

$$\frac{C_e}{q_e} = \frac{1}{bq_m} + \frac{C_e}{q_m} \quad (2)$$

$$\ln q_e = \ln K_f + \frac{1}{n} \ln C_e \quad (3)$$

where q_m (mg/g) and b (l/mg) are the Langmuir isotherm coefficients. The value of q_m stand for the maximum adsorption capacity. K_f (mg/g) and n are the Freundlich constants. Two adsorption isotherms were constructed by plotting the C_e/q_e versus C_e, ln q_e versus ln C_e, respectively

Two adsorption isotherms were constructed by plotting the C_e/q_e versus C_e for Langmuir isotherm, ln q_e versus ln C_e for Freundlich isotherm, respectively, as shown in Fig. 8. The values of R^2 of Langmuir and Freundlich models are 0.9986 and 0.6774, respectively, as listed in Table 1. In addition, the q_m value for the adsorption of RR120 by OMMT was 142.86 mg/g. The equilibrium data was better fitted to the Langmuir isotherm model indicating that the surface of OMMT was covered by the monolayer of RR120 molecules.

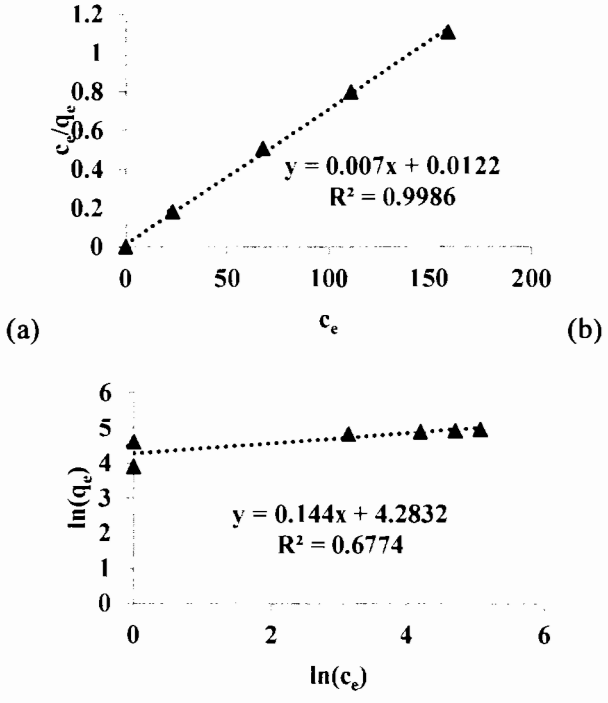

Fig. 8 Isotherms models of OMMT: (a) Langmuir isotherm model and (b) Freundlich isotherm model. Conditions: Adsorbent concentration: 0.1 g/100ml, temperature: 35°C.

Table 1 The isotherm constants and the correlation coefficients of the two isotherm models

Langmuir isotherm model			Freundlich isotherm model		
q_m (mg/g)	b (l/mg)	R^2	K_f (mg/g)	n	R^2
142.86	1.7429	0.9986	29.744	6.9444	0.6774

Adsorption kinetics

In order to investigate the adsorption mechanisms of RR120 on the adsorbents, pseudo-first-order and pseudo-second-order models were used. The pseudo-first-order equation [14] can be expressed as Eq.(4):

$$\ln(q_e-q_t)=\ln q_e-k_1 t \tag{4}$$

The pseudo-second-order model is based on the assumption of chemisorption of the adsorbate on the adsorbents [15]. This model is given as Eq.(5):

$$\frac{t}{q_t}=\frac{1}{k_2 q_e^2}+\frac{t}{q_e} \tag{5}$$

where q_t is the amount of adsorption dye (mg/g) at time t (min) and k_1 (min^{-1}), k_2 (g/mg/min) are the adsorption rate constant of pseudo-first-order, pseudo-second-order adsorption, respectively. The validity of the two models can be interpreted by the linear plots of $\ln(q_e - q_t)$ versus t and (t/q_t) versus t, respectively. The rate constants k_1 and k_2 can be obtained from the plot of experimental data.

The validity of the two models can be interpreted by the linear plots of $\ln(q_e - q_t)$ versus t for the pseudo-first order equation and (t/q_t) versus t for pseudo-second order equation, respectively, as shown in Fig. 9. The rate constants k_1 and k_2 can be obtained from the plot of experimental data.

The rate constants and the correlation coefficients of the pseudo-first-order and pseudo-second-order kinetic models are 0.0451 min^{-1}, 0.7403 and 0.0006 g/mg/min, 0.9975 respectively, as listed in Table 2. It is clearly seen that the kinetic data conform to the pseudo second order model indicating that the formation rate of adsorbate and adsorbent interaction on the external surface of adsorbent is the rate of limiting step.

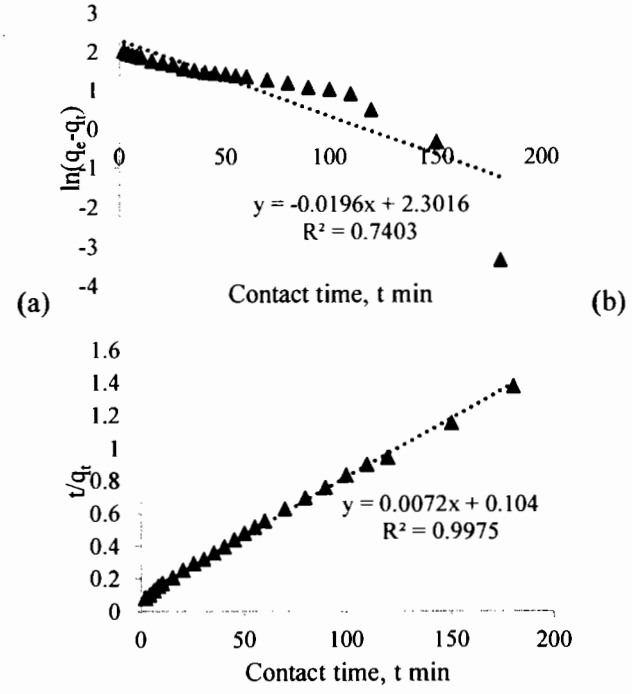

Fig. 9 Kinetics models of OMMT: (a) Pseudo-first-order kinetic model and (b) Pseudo-second-order kinetic model. Conditions: Adsorbent concentration: 0.1 g/100ml, temperature: 35°C and pH 5.9.

Table 2 The rate constant and the correlation coefficients of the two kinetic models

q_{exp} (mg/g)	Pseudo-first-order model			Pseudo-second-order model		
	k_1 (min^{-1})	q_{cal} (mg/g)	R^2	$k_2 \times 10^3$ (g/mg/min)	q_{cal} (mg/g)	R^2
130.10	0.0451	142.719	0.7403	0.564	137.124	0.9975

CONCLUSION

OMMT was synthesized by intercalation of CTAB into MMT. In this investigation, the effect of temperature, initial pH, initial dye concentration and contact time were investigated. The highest adsorption capacity was found to be 224.69 mg/g which was obtain under a certain condition such as adsorbent concentration 0.1 g/100ml, 300 mg/l initial dye concentration, 55°C, pH 5.9 and equilibrium time 150 min. The adsorption process followed the pseudo-second order and the Langmuir isotherm, respectively. The Langmuir monolayer adsorption

capacity was 142.86 mg/. This study showed that the OMMT is useful as a promising adsorbent for the remove of RR120 dye in wastewater treatment

ACKNOWLEDGEMENT

This work was financially supported with Environmental Engineering graduate program, Department of Chemical Engineering, Ubon Ratchathani University.

REFERENCE

[1] Bayramoğlu, G. and Yakup Arıca, M., Biosorption of benzidine based textile dyes "Direct Blue 1 and Direct Red 128" using native and heat-treated biomass of Trametes versicolor. Journal of Hazardous Materials, 2007. 143(1): p. 135-143.

[2] Gupta, V. K. and Suhas, Application of low-cost adsorbents for dye removal – A review. Journal of Environmental Management, 2009. 90(8): p. 2313-2342.

[3] Wang, L. and Wang, A., Adsorption properties of Congo Red from aqueous solution onto surfactant-modified montmorillonite. Journal of Hazardous Materials, 2008. 160(1): p. 173-180.

[4] Zhu, L. and Ma, J., Simultaneous removal of acid dye and cationic surfactant from water by bentonite in one-step process. Chemical Engineering Journal, 2008. 139(3): p. 503-509.

[5] Namasivayam, C., Muniasamy, N., Gayatri, K., Rani, M., and Ranganathan, K., Removal of dyes from aqueous solutions by cellulosic waste orange peel. Bioresource Technology, 1996. 57(1): p. 37-43.

[6] Namasivayam, C. and Kavitha, D., Removal of Congo Red from water by adsorption onto activated carbon prepared from coir pith, an agricultural solid waste. Dyes and pigments, 2002. 54(1): p. 47-58.

[7] Çelekli, A., Yavuzatmaca, M., and Bozkurt, H., Kinetic and equilibrium studies on the adsorption of reactive red 120 from aqueous solution on Spirogyra majuscula. Chemical Engineering Journal, 2009. 152(1): p. 139-145.

[8] Bhattacharyya, K. G. and Sarma, A., Adsorption characteristics of the dye, Brilliant Green, on Neem leaf powder. Dyes and Pigments, 2003. 57(3): p. 211-222.

[9] Al-Degs, Y. S., El-Barghouthi, M. I., El-Sheikh, A. H., and Walker, G. M., Effect of solution pH, ionic strength, and temperature on adsorption behavior of reactive dyes on activated carbon. Dyes and Pigments, 2008. 77(1): p. 16-23.

[10] Absalan, G., Asadi, M., Kamran, S., Sheikhian, L., and Goltz, D. M., Removal of reactive red-120 and 4-(2-pyridylazo) resorcinol from aqueous samples by Fe3O4 magnetic nanoparticles using ionic liquid as modifier. Journal of Hazardous Materials, 2011. 192(2): p. 476-484.

[11] Tabak, A., Baltas, N., Afsin, B., Emirik, M., Caglar, B., and Eren, E., Adsorption of Reactive Red 120 from aqueous solutions by cetylpyridinium-bentonite. Journal of chemical technology and biotechnology, 2010. 85(9): p. 1199-1207.

[12] Yan, L.-G., Wang, J., Yu, H.-Q., Wei, Q., Du, B., and Shan, X.-Q., Adsorption of benzoic acid by CTAB exchanged montmorillonite. Applied Clay Science, 2007. 37(3): p. 226-230.

[13] Periasamy, K. and Namasivayam, C., Removal of nickel(II) from aqueous solution and nickel plating industry wastewater using an agricultural waste: Peanut hulls. Waste Management, 1995. 15(1): p. 63-68.

[14] Lagergren, S., About the theory of so-called adsorption of soluble substances. Kungliga Svenska Vetenskapsakademiens Handlingar, 1898. 24(4): p. 1-39.

[15] Srivastava, V. C., Mall, I. D., and Mishra, I. M., Adsorption of toxic metal ions onto activated carbon: Study of sorption behaviour through characterization and kinetics. Chemical Engineering and Processing: Process Intensification, 2008. 47(8): p. 1269-1280.